수의학박사 학위논문

Study for the mechanism underlying spinal astrocyte sigma-1 receptor-mediated GluN1 phosphorylation in the development of neuropathic pain

척수 별아교세포 sigma-1 수용체를 통한 GluN1 인산화 조절이 신경병증성 통증 형성에 미치는 영향

2016년 8월

서울대학교 대학원

수의학과 수의생명과학(수의생리학) 전공

최 스 란

Doctoral Thesis

Study for the mechanism underlying spinal astrocyte sigma-1 receptor-mediated GluN1 phosphorylation in the development of neuropathic pain

Sheu-Ran Choi

Advisor: Jang-Hern Lee, D.V.M. Ph.D.

Major in Veterinary Biomedical Sciences
(Veterinary Physiology)
Department of Veterinary Medicine
The Graduate School
Seoul National University

August 2016

ABSTRACT

Study for the mechanism underlying spinal astrocyte sigma-1 receptor-mediated GluN1 phosphorylation in the development of neuropathic pain

Sheu-Ran Choi
Major in Veterinary Biomedical Sciences
Department of Veterinary Medicine
The Graduate School
Seoul National University

Damage to the peripheral nerves can lead to the development of neuropathic pain, which causes considerable suffering and distress to these patients and is associated with several diagnostic symptoms including mechanical allodynia (MA, sensation of pain to non-noxious mechanical stimuli) and thermal hyperalgesia (TH, increased pain response to noxious thermal stimuli). The development of peripheral neuropathic pain involves a variety of pathophysiological mechanisms in both the peripheral and central nervous systems. In this regard, spinal *N*-methyl-D-aspartate (NMDA) receptors have been shown to play a key role in the development of 'central sensitization', a phenomenon in which nociceptive inputs to the dorsal horn increase the excitability and synaptic efficacy of neurons in spinal pain pathways. In our previous study, activation of spinal sigma-1 receptors (Sig-1Rs) contributes to the

functional potentiation of NMDA receptors via increases in phosphorylation of GluN1 subunit (pGluN1). However, the precise cellular mechanisms underlying Sig-1Rs-related neuropathic pain are not investigated.

The present study was designed to investigate whether: (1) neuronal nitric oxide synthase (nNOS)-induced nitric oxide (NO) mediates Sig-1R-induced increase in spinal pGluN1 expression in pain hypersensitivity and activation of Sig-1R results in a time-dependent modification of nNOS activity in the dorsal horn; (2) Sig-1R modulation of astrocytic D-serine plays an important role in increasing pGluN1 expression via nNOS activation and that this pathway contributes to the development of persistent neuropathic pain induced by peripheral nerve injury; and finally (3) spinal Sig-1Rs modulate the production of reactive oxygen species (ROS) via activation of NADPH oxidase 2 (Nox2) as a downstream of nNOS/NO signaling, ultimately leading to the development of chronic neuropathic pain.

All experiments were performed on Male ICR mice and Sprague-Dawley rats. Neuropathic pain was produced by chronic constriction injury (CCI) of the common sciatic nerve according to the method described by Bennett and Xie with a minor modification. Sensitization to innocuous mechanical stimulation (mechanical allodynia, MA) was examined using the 0.16 g or 2.0 g von Frey filament, and sensitization to noxious heat stimulation (thermal hyperalgesia, TH) was examined with the hot-plate apparatus or plantar analgesia meter. In the present study, the following drugs were used: PRE084 (a Sig-1R agonist), BD1047 (a Sig-1R antagonist), L-NAME (a non-specific NOS inhibitor), 7-nitroindazole (a specific nNOS inhibitor), ODQ (a sGC inhibitor), cyclosporin A (a calcineurin inhibitor), NMDA (a NMDA receptor agonist), D-serine, LSOS (a Srr inhibitor), DAAO (an endogenous D-serine degrading enzyme), fluorocitrate (an astrocyte metabolic

inhibitor), chelerythrine (a PKC inhibitor), PKI (a PKA inhibitor), NAC (a ROS scavenger) and apocynin (a NADPH oxidase inhibitor). All drugs were administrated intrathecally. Immunohistochemistry, DHE staining, NADPH-diaphorase staining, NO detection, Western blot assay and co-immunoprecipitation were performed according to each experiment procedure. The image analysis and statistical analysis were performed using a computer-assisted image analysis system (Metamorph) and a Prism 5.0 (Graph Pad Software), respectively.

Intrathecal (i.t.) injection of Sig-1R agonist, PRE084 significantly evoked mechanical and thermal hypersensitivity, and increased the number of PKC-dependent pGluN1-ir cells in spinal cord. The PRE084-induced hypersensitivity and increase in PKC-dependent pGluN1 expression were significantly blocked by pretreatment with L-NAME or 7-nitroindazole. I.t. administration with PRE084 time-dependently decreased the ratio of phosphorylated nNOS (pnNOS) to nNOS expression and the number of spinal pnNOS-ir cells. This decrease in the pnNOS form was prevented by BD1047, a Sig-1R antagonist and cyclosporin A, a calcineurin inhibitor, but not by a sGC inhibitor.

I.t. administration with the D-serine degrading enzyme, DAAO attenuated the facilitation of NMDA-induced pain behaviors induced by PRE084. Exogenous D-serine facilitates NMDA-induced nociception and increases PKC-dependent pGluN1 expression, which was attenuated by preteatment with the nNOS inhibitor, 7-nitroindazole. In CCI mice, i.t. administration with exogenous D-serine during the induction phase of neuropathic pain restored MA and PKC-dependent pGluN1 suppressed by BD1047. Furthermore, administration with the serine racemase inhibitor, LSOS or DAAO suppressed CCI-induced MA, pGluN1, nNOS activation and NO production. I.t. administration with 7-nitroindazole or the sGC inhibitor, ODQ

also attenuated CCI-induced MA and pGluN1. By contrast, D-serine and nNOS signaling had no effect on CCI-induced TH or GluN1 expression.

Sig-1R-induced pain hypersensitivity was dose-dependently attenuated by pretreatment with the ROS scavenger, NAC or the Nox inhibitor, apocynin. PRE084 also induced an increase in Nox2 activation and ROS production, which were attenuated by pretreatment with BD1047, apocynin, or 7-nitroindazole. CCI-induced nerve injury produced an increase in Nox2 activation and ROS production in the spinal cord, all of which were attenuated by i.t. administration with BD1047 during the induction phase of neuropathic pain. Furthermore, administration with BD1047 or apocynin reversed CCI-induced increase in pGluN1 expression and MA during the induction phase, but not the maintenance phase.

The present study demonstrates that Sig-1R modulation of astrocytic D-serine plays an important role in potentiating NMDA receptor function via increase in PKC-dependent phosphorylation of GluN1 subunit and that this pathway contributes to the development of persistent neuropathic pain. In addition, nNOS activation mediates the role of D-serine and has pro-oxidant effects in the CNS via modulation of Nox2 activity and concomitant ROS production, leading to modulate persistent pain. Collectively, these findings demonstrate that spinal Sig-1R activation plays a key role in the development of neuropathic pain induced by peripheral nerve injury, and Sig-1Rs could be a useful therapeutic target for alleviating mechanical allodynia under the neuropathic pain conditions.

Key words: sigma-1 receptor, nNOS, Nox2, D-serine, neuropathic pain, astrocyte, GluN1

Student number: 2009-21641

CONTENTS

LIST OF FIGURES

ABBREVIATIONS

Apocynin	4′-Hydroxy-3′-methoxyacetophenone
BD1047	*N*-[2-(3,4-dichlorophenyl)ethyl]-N-methyl-2-(dimethylamino) ethylamine dihydrobromide
Ca^{2+}/CAM	Ca^{2+}/calmodulin
CaMKII	Ca^{2+}/CAM-dependent protein kinase II
CCI	Chronic constriction injury
Chelerythrine	1,2-Dimethoxy-12-methyl[1,3]benzodioxolo[5,6-c]phenanthridinium chloride
CNS	Central nervous system
CREB	cAMP response element binding protein
CsA	Cyclosporin A
DAAO	D-amino acid oxidase
DAG	Diacyl glycerol
DHE	Dihydroethidium
DHEAS	Dehydroepiandrosterone sulfate
DMSO	Dimethyl sulfoxide
eNOS	Endothelial nitric oxide synthase
ER	Endoplasmic reticulum
GluN1	NMDA receptor GluN1 subunit
iNOS	Inducible nitric oxide synthase
IP_3	Inositol triphosphate
ir	Immunoreactive

i.t.	Intrathecal
L-NAME	N(G)-L-nitro-arginine methyl ester
LSOS	L-serine O-sulfate potassium salt
MA	Mechanical allodynia
NAC	*N*-Acetyl-L-cysteine
NADPH	Nicotinamide adenine dinucleotide phosphate
NMDA	*N*-Methyl-D-aspartate
Nox2	NADPH oxidase 2
nNOS	Neuronal nitric oxide synthase
NO	Nitric oxide
NOS	Nitric oxide synthase
ODQ	1H-[1,2,4]oxadiazolo[4,3-a]Quinoxalin-1-one
P450scc	P450 side-chain cleavage
pGluN1	Phosphorylated GluN1 subunit
PIP_2	Phosphatidylinositol 4,5-bisphosphate
PKA	Protein kinase A
PKC	Protein kinase C
PKG	Protein kinase G
PKI	PKA inhibitor 14-22 amide
PLC	Phospholipase C
pnNOS	Phosphorylated nNOS
PRE084	2-(4-Morpholinethyl) 1-phenylcyclohexanecarboxylate hydrochloride
PSD-95	Postsynaptic density protein-95
PWF	Paw withdrawal frequency

PWL	Paw withdrawal latency
ROS	Reactive oxygen species
7-NI	7-Nitroindazole
Sig-1R	Sigma-1 receptor
sGC	Soluble guanylyl cyclase
Srr	Serine racemase
TH	Thermal hyperalgesia
TRPV1	Transient receptor potential vanilloid 1

BACKGROUND

Neuropathic pain

The development of neuropathic pain can be induced by damage to the spinal cord or peripheral nerves, which causes several diagnostic symptoms including mechanical allodynia (sensation of pain to non-noxious mechanical stimuli) and thermal hyperalgesia (increased pain response to noxious thermal stimuli) (Woolf and Mannion, 1999). Neuropathic pain is clinically important because the pain is often refractory to treatment. This is due in part to the significant convergence of the pathological, physiological and inflammatory processes that maintain the neuropathic pain state. A better understanding of the mechanisms that contribute to the neuropathic pain is required in order to develop proper therapeutic targets to treat neuropathic pain.

Central sensitization

It has been demonstrated that diverse pathophysiological mechanisms in both the peripheral and central nervous systems are involved in the development of peripheral neuropathic pain (Baron, 2006). Especially, abnormal activation of spinal *N*-methyl-D-aspartate (NMDA) receptors has been known to play a key role in the development of 'central sensitization', a phenomenon in which nociceptive inputs to the dorsal horn increase the excitability and synaptic efficacy of neurons in spinal nociceptive pathways (Woolf, 1983; Woolf and Mannion, 1999). Chen et al. suggested that phosphorylation of the NMDA receptor GluN1 subunit (pGluN1) at serine and threonine residues can increase neuronal excitability by reducing the Mg^{2+} block and by increasing the probability of channel openings (Chen et al., 1992). Regarding our previous studies showing that peripheral nerve injury not only induces the

development of pain but also increases spinal pGluN1 expression, the functional potentiation of NMDA receptor activity via the increased pGluN1 expression in spinal cord can be a critical mechanism underlying the development of neuropathic pain. However, the precise cellular mechanisms by which pGluN1 expression increases under the neuropathic pain condition are not clearly investigated.

Sigma-1 receptor

The sigma-1 receptor (Sig-1R) has recently been identified as a unique ligand-regulated molecular chaperone in the endoplasmic reticulum (ER) of cells, and has been implicated in diverse pathophysiological diseases including pain (Alonso et al., 2000; Collier et al., 2007; Maurice and Su, 2009; Su and Hayashi, 2003). Previous studies from our laboratories have demonstrated that the spinal Sig-1R activation plays an important role in formalin-induced pain and chronic constriction injury (CCI)-induced neuropathic pain (Kim et al., 2006; Roh et al., 2008b). Furthermore, intrathecal (i.t.) injection of Sig-1R agonists induces pain hypersensitivity, which is closely associated with calcium-dependent second messenger cascades including protein kinase C (PKC) and PKC-dependent pGluN1 expression in spinal cord (Roh et al., 2011; Roh et al., 2008a; Roh et al., 2010). Despite this work, the precise mechanisms underlying Sig-1R-related pain induction and its alteration of cellular activity including pGluN1 remains to be fully examined.

Neuronal NOS

Nitric oxide (NO) is generated from L-arginine and molecular oxygen by the activity of three distinct nitric oxide synthase (NOS) isoforms: neuronal NOS (nNOS), inducible NOS (iNOS), and endothelial NOS (eNOS) (Palmer et al., 1988).

Importantly NO plays a critical role in modulating synaptic transmission in both the central and peripheral nervous system (Meller and Gebhart, 1993). It has been well demonstrated that NO produced by nNOS in spinal cord participates in the early induction (Levy and Zochodne, 2004) and/or the maintenance of neuropathic pain (Xu et al., 2007). In addition, the physical association of nNOS and the NMDA receptor with postsynaptic density protein-95 (PSD-95) through their specialized PDZ domains helps to explain the preferential link between NMDA receptors and NO production (Brenman et al., 1996; Garthwaite, 2008). These findings raised the possibility that the action of spinal Sig-1R on NMDA receptor function (pGluN1 modulation) could be closely associated with nNOS activation in spinal cord leading to increased production of NO.

D-serine

D-serine is an endogenous ligand for the glycine site of the NMDA receptors, which can closely modulate functional activity of NMDA receptors (Mothet et al., 2000). D-serine is generated from L-serine by the activity of serine racemase (Srr) and this biosynthesizing enzyme is expressed exclusively in astrocytes (Wolosker et al., 1999). Recent reports suggest that D-serine plays an important role as a gliotransmitter, which upon release from astrocytes activates NMDA receptors on postsynaptic neurons contributing to the processing of nociceptive transmission in the spinal cord dorsal horn (Lefèvre et al., 2015; Miraucourt et al., 2011). This is consistent with our previous results showing that i.t. administration of the Srr inhibitor, LSOS or the D-serine degrading enzyme, DAAO significantly suppresses the development of mechanical allodynia (MA) in CCI mice (Moon et al., 2015). Although it has been documented that spinal D-serine activates NMDA receptor, there is limited

understanding of the cellular mechanisms involved in the induction of persistent pain by endogenous D-serine. Since Sig-1R activation can increase the production of D-serine via modulation of the Srr expression (Moon et al., 2005), there is a possibility that the Sig-1R-induced increase in D-serine may be involved in the functional potentiation of NMDA receptors, which underlies the development of MA in CCI mice.

NADPH oxidase

Reactive oxygen species (ROS) are molecules and ions of oxygen that have an unpaired electron, rendering them extremely reactive. Thus, they interact with a large number of molecules leading to alterations in the function of the target molecules (Bedard and Krause, 2007). ROS have been suggested as important modulators of persistent pain, including neuropathic and capsaicin-induced inflammatory pain, and they have also been implicated in NMDA receptor activation via enhancement of spinal pGluN1s, which is an essential step in central sensitization (Gao et al., 2007; Kim et al., 2004; Schwartz et al., 2008). Recent studies suggest that NADPH oxidase (Nox) is the first identified enzyme system that generates ROS as its primary function and is also important during pain sensitization (Bedard and Krause, 2007; Kallenborn-Gerhardt et al., 2012). Among several homologs of Nox identified so far, Nox2 activation can be induced by elevated intracellular Ca^{2+} concentration and the activation of Ca^{2+}-activated protein kinases, particularly PKC, which plays a critical role in Nox2 activation (Raad et al., 2009). As previously described, spinal Sig-1R activation modulates intracellular Ca^{2+} signaling by promoting the efflux of Ca^{2+} into the cytoplasm, leading to an increase in PKC activity, which results in potentiation of NMDA receptor function (Monnet, 2005; Roh et al., 2008). Although it has been

documented that Sig-1R activation in the spinal cord mediates induction of the chronic neuropathic pain after peripheral nerve injury, there is limited understanding of the cellular mechanisms relating to Sig-1R-mediated pain facilitation. Moreover, it has been suggested that Nox2 activation is related to pain sensitization, but the receptor or upstream signaling involved in the modulation of spinal Nox2 activation is poorly understood, particularly in the case of nociceptive signaling.

OBJECTIVES

This study is aimed to

1. examine whether: (1) intrathecal nNOS inhibitor injection reduced Sig-1R-induced mechanical and thermal hypersensitivity and the increase in spinal pGluN1-immunoreactive (ir) cells; (2) activation of Sig-1R results in a time-dependent modification of nNOS activity in the dorsal horn; and (3) this change in nNOS activity is blocked by Sig-1R, calcineurin or soluble guanylyl cyclase (sGC) inhibitor, respectively.

2. examine whether: (1) the Sig-1R-induced facilitative effect on NMDA-induced nociception is mediated by D-serine; (2) D-serine modulates spinal PKC-dependent (Ser896) pGluN1 expression, which accounts for the potentiation of NMDA receptor function; and (3) the nNOS/NO signaling cascade mediates the effect of D-serine on the increase in pGluN1 expression and development of peripheral neuropathic pain.

3. examine whether: (1) direct activation of the spinal Sig-1R using the agonist, PRE084 in naïve mice induces Nox2 activation and ROS production; (2) pretreatment with the ROS scavenger, NAC or with the Nox inhibitor, apocynin reduces Sig-1R-induced pain hypersensitivity; (3) CCI in sciatic nerve induces spinal cord Nox2 activation and accompanying ROS production, which contributes to the CCI-induced increase in pGluN1 expression and induction of the neuropathic pain in rats; and (4) these CCI-induced changes are inhibited by time-dependent administration of BD1047.

CHAPTER 1

The role of nNOS on sigma-1 receptor-induced GluN1 phosphorylation in pain hypersensitivity

Manuscript published in Br J Pharmacol. 2011 Aug;163(8):1707-20.

ABSTRACT

It has been demonstrated that activation of the spinal sigma-1 receptor (Sig-1R) induced mechanical and thermal hypersensitivity via calcium-dependent second messenger cascades and phosphorylation of the spinal NMDA receptor GluN1 subunit (pGluN1). Here, the role of NO in this process is examined, since it plays a critical role in PKC-mediated calcium signaling and the potentiation of NMDA receptor function. The present study was designed to determine whether (1) intrathecal nNOS inhibitor injection reduced Sig-1R-induced mechanical and thermal hypersensitivity and the increase in spinal pGluN1-immunoreactive (ir) cells, (2) activation of Sig-1R results in a time-dependent modification of nNOS activity in the dorsal horn, and (3) this change in nNOS activity is blocked by Sig-1R, calcineurin or a soluble guanylyl cyclase (sGC) inhibitors, respectively. Intrathecal injection of Sig-1R agonist, PRE084 significantly evoked mechanical and thermal hypersensitivity, and increased the number of PKC and PKA-dependent pGluN1-ir cells in spinal cord. The PRE084-induced hypersensitivity and increase in PKC-dependent pGluN1 expression were significantly blocked by pretreatment with L-NAME or 7-NI. Intrathecal PRE084 time-dependently decreased the ratio of phosphorylated nNOS (pnNOS) to nNOS expression and the number of spinal pnNOS-ir cells. This decrease in the pnNOS form was prevented by BD1047, a Sig-1R antagonist and cyclosporin A, a calcineurin inhibitor, but not by a sGC inhibitor. These findings demonstrate that spinal Sig-1R-induced sensitization is mediated by an increase in nNOS activity, which is associated with an NO-induced increase in PKC-dependent pGluN1 expression.

INTRODUCTION

The sigma-1 receptor (Sig-1R) has recently been identified as a unique ligand-regulated molecular chaperone in the endoplasmic reticulum of cells, and has been implicated in a myriad of cellular functions and biological processes (Collier et al., 2007; Maurice and Su, 2009). Previous studies from our laboratories have demonstrated that the spinal Sig-1R plays a pro-nociceptive role in formalin-induced pain (Kim et al., 2006), and that the direct activation of spinal Sig-1R using intrathecal (i.t.) injection of agonists enhances the response to peripheral mechanical stimuli, which is closely associated with calcium-dependent second messenger cascades including protein kinase C (PKC) (Roh et al., 2008a; Roh et al., 2010). In addition, it has been shown that the activation of Sig-1R increases PKC- and PKA-dependent phosphorylation of the NMDA receptor GluN1 subunit (pGluN1) in the spinal cord dorsal horn, which results in the potentiation of i.t. NMDA injection-evoked spontaneous pain behavior (Kim et al., 2008). Moreover, several studies including a previous investigation from our laboratories have shown that the blockade of spinal Sig-1R using i.t. injection of the Sig-1R antagonist, BD1047 or using Sig-1R knockout mice reduces the development of neuropathic pain and blocks the nerve injury-induced increase of phosphorylation of extracellular signal-regulated kinase as well as pGluN1 in the spinal dorsal horn (de la Puente et al., 2009; Roh et al., 2008b). Despite this work, the precise mechanisms underlying Sig-1R-mediated pain induction and its alteration of cellular activity including pGluN1 remains to be fully examined.

Nitric oxide (NO) is generated from L-arginine and molecular oxygen by the activity of three distinct nitric oxide synthase (NOS) isoforms: neuronal NOS (nNOS),

inducible NOS (iNOS), and endothelial NOS (eNOS) (Palmer et al., 1988). Importantly NO plays a critical role in modulating synaptic transmission in both the central and peripheral nervous system (Meller and Gebhart, 1993). It has been well demonstrated that NO produced by nNOS in spinal cord participates in the early induction (Levy and Zochodne, 2004) and/or the maintenance of neuropathic pain (Xu et al., 2007). In addition, the physical association of nNOS and the NMDA receptor with postsynaptic density protein-95 (PSD-95) through their specialized PDZ domains helps to explain the preferential link between NMDA receptors and NO production (Brenman et al., 1996; Garthwaite, 2008). These findings raised the possibility that the action of spinal Sig-1R on NMDA receptor function (pGluN1 modulation) could be closely associated with nNOS activation in spinal cord leading to increased production of NO.

In terms of potential mechanisms by which Sig-1R might potentiate NO, it is known that nNOS possesses several putative sites for phosphorylation in relation to the regulation by Ca^{2+}/calmodulin (Ca^{2+}/CAM). This phosphorylation is regulated by some kinases and phosphatases, for example, PKA, PKC, PKG, Ca^{2+}/CAM-dependent protein kinase II (CaMKII), phosphatase I, which can affect nNOS activity differently by phosphorylation at separate sites on the nNOS isoform or by differential effects on phosphorylation at the same site (Garthwaite, 2008; Zhou and Zhu, 2009). In this regard, CaMKII phosphorylates nNOS at Ser847, which reduces nNOS activity by inhibiting Ca^{2+}/CaM binding. In contrast, protein phosphatase 1 decreases the level of phosphorylation of nNOS (pnNOS) at Ser847, leading to an increase of nNOS activity (Rameau et al., 2004; Zhou and Zhu, 2009). These results imply that the decrease in pnNOS possibly represents an increase in nNOS activity, which subsequently induces up-regulation of NO production. Although it was well documented that the increase of

pnNOS at Ser847 results in a neuroprotective effect during cerebral ischemia (Osuka et al., 2002; Zhou et al., 2008), the potential effect of changes in pnNOS on pain modulation in the spinal cord, particularly in relation to Sig-1R-induced mechanical and thermal hypersensitivity, has not been examined.

In this regard, the present study was designed to investigate the potential relationship between Sig-1R-induced mechanical and thermal hypersensitivity and NO signaling via nNOS activation in spinal cord. Thus, it was examined whether (1) i.t. pretreatment with an nNOS inhibitor could reduce Sig-1R-mediated pain induction by affecting the Sig-1R produced PKC- and PKA-dependent increase in spinal pGluN1-ir cells, (2) the activation of Sig-1R results in a time-dependent modification of nNOS activity (i.e. a decrease in pnNOS or a reduction of nNOS linked to PSD-95) in the spinal cord dorsal horn, and (3) this change in nNOS activity could be blocked by i.t. preadministration of a Sig-1R antagonist, a calcineurin inhibitor or a soluble guanylyl cyclase (sGC) inhibitor, respectively.

MATERIALS AND METHODS

Experimental animals

Male ICR mice (20-25g) were purchased from the Laboratory Animal Center of Seoul National University (Seoul, Republic of Korea). They had free access to food and water and were maintained in temperature and light controlled rooms (23±2℃, 12/12h light/dark cycle with lights on at 08:00) for at least 1 week prior to beginning an experiment. The experimental protocols for animal usage were reviewed and approved by the SNU Animal Care and Use Committee and were consistent with the *Guide for the Care and Use of Laboratory Animals* published by the US National Institutes of Health (NIH publication No. 96-01, revised 1996).

Drugs and intrathecal (i.t.) administration

The following drugs were used: 2-(4-morpholinethyl)1-phenylcyclohexanecarboxylate (PRE084; PRE, 3 nmol), a sigma-1 receptor agonist; N-[2-(3,4-dichlorophenyl)ethyl]-N-methyl-2-(dimethylamino) ethylamine dihydro-bromide (BD1047; BD, 100 nmol), a sigma-1 receptor antagonist; N(G)-nitro-L-arginine methyl ester (L-NAME, 3, 10 and 100 nmol), a non-specific NOS inhibitor; 7-Nitroindazole (7-NI, 10, 100 and 200 nmol), a specific nNOS inhibitor; Cyclosporin A (CsA, 20 nmol), a calcineurin inhibitor; 1H-[1,2,4]-oxadiazolo [4,3-a] quinoxalin-1-one (ODQ, 300 pmol), a sGC inhibitor. L-NAME, 7-NI, CsA and ODQ were supplied by Sigma–Aldrich (St. Louis, MO). PRE and BD were supplied by Tocris Cookson Ltd. (Bristol, UK). The doses of PRE and BD used were based on our previous study showing that these doses produce maximal effects with no detectable side-effects (Roh et al., 2008a). The doses of L-NAME, 7-NI, CsA and ODQ were selected based

on doses previously used in the literature including our previous study (Chu et al., 2005; Karlsson et al., 2004; Tanabe et al., 2009; Yoon et al., 2008). PRE, BD, L-NAME, and ODQ were dissolved in physiological saline, and 7-NI and CsA were dissolved in 5% DMSO, then, diluted in Corn oil. All drugs were administered 10 minutes before PRE. Paw withdrawal responses to von Frey stimulation and heat stimuli (see below) were measured before and 30, 60, and 120 min after treatment with PRE (or saline) in all groups of mice. Drugs were dissolved in 5 μl of vehicle and administrated intrathecally.

Intrathecal (i.t.) drug administration was performed using a 50 μl Hamilton syringe connected to a 30-gauge needle based on the technique previously described by Hylden and Wilcox (1980). Briefly, the mouse was held tightly between the thumb and middle finger at the level of the both iliac crests, and the fifth lumbar spinous process was palpated with the index finger. The needle was inserted through the vertebral column into the L_{5-6} intervertebral space and successful insertion of the needle into the intrathecal space was determined by a tail flick response. Each drug was slowly injected over a 10 second period. Then, the needle was carefully removed from the spinal cord. The drug control groups received an identical injection of vehicle without drug.

Behavioral assessments

Sensitization to innocuous mechanical stimulation (mechanical allodynia) was examined with von Frey filaments (North Coast Medical, Morgan Hill, CA) as described in our previous study (Roh et al., 2008a). Based on this study, the 0.16 g von Frey filament was selected for testing. This von Frey filament was applied from underneath the metal mesh flooring to each hind paw. The filament was applied 10

times to each paw with each application separated by 10 sec intervals. The number of paw withdrawal responses following each von Frey stimulus was then counted. The results of mechanical response testing in each experimental animal were expressed as a percent withdrawal response frequency (PWF, %), which represented the percentage of paw withdrawals out of a maximum of 20 (right hind paw-10 and left hind paw-10).

Sensitization to noxious heat stimulation (thermal hyperalgesia) was examined with a hot-plate apparatus (Model-35100, Ugo Basile, Comerio, Italy) (Duman et al., 2006; Milano et al., 2008). The temperature of plate was maintained at 55 ± 0.5 ℃. Animals were placed into an acrylic cylinder (20 cm in diameter, 25 cm high) on the heated surface, and the time (in seconds) between placement and shaking or licking or lifting of their hind paws or jumping (whichever occurred first), was recorded as the paw withdrawal latency (PWL, sec). Baseline withdrawal latency (8-12 sec) was determined before experimental treatment. The withdrawal latency was then measured 30, 60, and 120 min after treatment with PRE (or saline) in each experimental animal. The test was duplicated in each animal, and the mean latency was calculated. Cutoff time in the absence of a response was set at 20 sec to minimize tissue damage.

Paw pinch-induced spinal Fos expression

In another set of experiments, it was quantified the number of Fos-ir cells in the spinal cord dorsal horn induced by a paw pinch stimulus and examined the effect of i.t. injection of drugs on this expression. Mice were anesthetized with 3% isoflurane in a mixture of N_2O/O_2 gas before application of the paw pinch to avoid any potential stress response or escape response. The right hind paw was pinched with a hemostatic forceps for 10 min (Lee et al., 1992; Roh et al., 2008a). Eight experimental groups

were as follows: 1) anesthesia only, 2) PRE only (no pinch stimulation), 3) paw pinch, 4) PRE (3 nmol) + pinch, 5) L-NAME (100 nmol) + PRE + pinch, 6) L-NAME (100 nmol) + pinch, 7) 7-NI (100 nmol) + PRE + pinch, and 8) 7-NI (100 nmol) + pinch. The PRE was administered 30 min before pinch stimulation (Roh et al., 2008a), and L-NAME and 7-NI were administered 10 min before i.t. PRE injection.

Two hours after paw-pinch stimulation, the mice were humanely killed and perfused with fixative, and Fos immunohistochemical staining was subsequently performed on spinal cord sections according to the method detailed in our previous reports (Kwon et al., 2001; Roh et al., 2008a). After postfixation and cryoprotection, a series of frozen sections (40 μm thickness) were cut through the L_{4-6} segments of the spinal cord and processed for Fos immunohistochemistry as previously described (Roh et al., 2008a).

Western blot assay

Mice were deeply anesthetized with 3% isoflurane in a mixture of N_2O/O_2 gas at one time point before and at several time points (30, 60 and 120 min) after i.t. injection of PRE (3 nmol) to determine the time-dependent effect of Sig-1R activation on the change in pnNOS to nNOS expression using immunoblot analysis (n = 5 mice / group). Animals were perfused transcardially with calcium-free Tyrode's solution and then the spinal cords were collected into an ice-cooled, saline-filled glass dish. Spinal segments were separated into left and right halves under a neuro-surgical microscope. The spinal cord was subsequently further subdivided into dorsal and ventral halves by cutting straight across from the central canal laterally to a midpoint in the white matter. The right and left spinal cord dorsal horns were subsequently used for Western blot

analysis. The L_{4-6} spinal cord dorsal segments were homogenized in lysis buffer (20 mM Tris-HCl, 10 mM EGTA, 2 mM EDTA, pH 7.4 and proteinase inhibitors) containing 1% Triton X-100. Homogenates were subsequently centrifuged at 15,000 rpm for 40 minutes at 4℃ and, then, the supernatant was used for Western blot analysis. The protein concentration was estimated by the Bradford dye assay (Bio-Rad Laboratories). Spinal cord homogenates (20 μg protein) were separated using 10% SDS-polyacrylamide gel electrophoresis and transferred to nitrocellulose membrane. After the blots had been washed with TBST (10 mM Tris-HCl, pH 7.6, 150 mM NaCl and 0.05% Tween-20), the membranes were blocked with 5% skimmed milk for 1 h at RT and incubated at 4℃ overnight with a primary antibody specific for β-actin (1:1k, loading control, Sigma), nNOS (1:1k, cat# 610311, BD Biosciences, San Jose, CA) or for pnNOS (1:1k, cat# ab16650, Abcam Inc., Cambridge, MA; this antibody is specific for mouse nNOS phosphorylated on serine 847). The membranes were washed and primary antibodies were detected using goat anti-rabbit IgG conjugated to horseradish peroxidase. The bands were visualized with enhanced chemiluminescence (Amersham Pharmacia Biotech, England, UK). The positive pixel area of specific bands was measured with a computer-assisted image analysis system and normalized against the corresponding β-actin loading control bands. Then the ratio of pnNOS (Ser847) to nNOS expression was calculated. The mean value of the ratio of pnNOS to nNOS expression in animals prior to PRE injection (0 min) was set at 100%. Thus, the % change in pnNOS to nNOS expression in each time-point group was examined.

Co-immunoprecipitation

Interaction of nNOS with PSD-95 in spinal dorsal horn was analyzed by

immunoprecipitation and Western blotting (n = 3 mice / group). Tissue homogenates were lysed with lysis buffer (1% Triton X-100 in 50 mM Tris-HCl [pH 7.4] that contained 150 mM NaCl, 5 mM EDTA, 2 mM Na_3VO_4, 2.5 mM Na_4PO_7, 100 mM NaF, 200 nM microcystin-lysine-arginine, and protease inhibitors) and the tissue lysates (300 μg) were mixed with 10 μg of rabbit anti-nNOS antibody (BD Biosciences). The samples were incubated for 4 h, mixed with Protein A/G PLUS-agarose immunoprecipitation reagent (Pierce, Rockford, IL), and then incubated for an additional 12 h. The beads were washed four times, and the bound proteins were released from the beads by boiling in SDS-PAGE sample buffer for 5 min. The samples were analyzed by Western blotting with mouse anti-PSD95 monoclonal antibody (1:1k, cat# P246, Sigma, St. Louis, MO).

Immunohistochemistry

In a separate set of experiments, mice were anesthetized with 3% isoflurane in a mixture of N_2O/O_2 gas at one time point before and at several time points (30, 60 and 120 min) after i.t. injection of PRE (3 nmol) and perfused transcardially with calcium-free Tyrode's solution followed by a fixative containing 4% paraformaldehyde and 0.2% picric acid in 0.1 M phosphate buffer (pH 7.4). The spinal cords were removed immediately after perfusion, post-fixed in the identical fixative for 12 h and then placed in 30% sucrose in PBS (pH 7.4) overnight at 4℃. Serial transverse sections (40 μm) of the spinal cord were cut using a cryostat (Microm, Germany). Spinal L_{4-6} tissue sections were processed for pnNOS (rabbit polyclonal anti-pnNOS-Ser847 antibody, 1:3k; Abcam Inc.), protein kinase C (PKC)-dependent pGluN1 (Ser896, 1:1k, cat# 06–640, Upstate Biotechnology, Lake Placid, NY, USA; this antibody is

specific for GluN1 phosphorylated on serine 896) or protein kinase A (PKA)-dependent pGluN1 (Ser897, 1:1k, cat# 06–641, Upstate Biotechnology; this antibody is specific for GluN1 phosphorylated on serine 897) immunohistochemistry using the avidin-biotin-peroxidase complex (ABC) procedure as previously described (Osuka et al., 2007). Visualization of the ABC complex was performed using 3,3-diaminobenzidine (Sigma) and the 3,3-diaminobenzidine reaction was intensified with 0.2% nickel chloride.

Image analysis

Tissue sections were examined under a brightfield microscope (Zeiss Axioscope, Hallbergmoos, Germany) and three to five spinal cord sections from the L_{4-6} lumbar spinal cord segments were randomly selected from each animal, and subsequently scanned. Individual sections were digitized with 4096 grey levels using a cooled CCD camera (Micromax Kodak 1317; Princeton Instruments, AZ, USA) connected to a computer-assisted image analysis system (Metamorph version 6.3r2; Molecular Devices Corporation, PA). To maintain a constant threshold for each image and to compensate for subtle variability of the immunostaining, the neurons that were at least 70% darker than the average gray level of each image were only counted after background subtraction and shading correction. The average number of Fos-ir, pGluN1-ir and pnNOS-ir cells per section from each animal was obtained and these values were averaged across each group and presented as group data. The expression of Fos, pGluN1 and pnNOS was quantified in the following three dorsal horn regions: 1) the superficial dorsal horn (SDH, laminae I and II); 2) the nucleus proprius (NP, laminae III and IV); and 3) the neck region (NECK, laminae V and VI). All analytical

procedures described above were performed without the knowledge of the experimental conditions.

Statistical analysis

All values are expressed as the mean ± SEM. Statistical analysis was performed using Prism 5.0 (Graph Pad Software, San Diego, USA). Repeated measures two-way ANOVA was performed to determine overall differences between experimental groups in all nociceptive behavioral tests. *Post-hoc* analysis was performed using the Bonferroni's multiple comparison test in order to determine the *P* value among experimental groups. One-way ANOVA followed by the Bonferroni's comparison test was used to determine differences between experimental groups in immunohistochemistry and Western blot assay. A $P < 0.05$ was considered statistically significant.

RESULTS

1. Effect of i.t. pretreatment with NOS inhibitors on PRE-induced pain hypersensitivity

The i.t. administration of PRE (3 nmol, VEH+PRE) significantly increased PWF to innocuous mechanical stimuli (mechanical allodynia) for the entire 120 min post-injection testing period as compared to those of VEH+VEH treated group (Fig. 1-1A and B; $^{**}P < 0.01$, $^{***}P < 0.001$ v.s. VEH+VEH treated group). I.t. pretreatment with L-NAME (3, 10 and 100 nmol, Fig. 1-1A), a non-selective NOS inhibitor or with 7-NI (10, 100 and 200 nmol, Fig. 1-1B), a selective nNOS inhibitor dose-dependently suppressed this PRE-induced increase in PWF ($\#P < 0.05$, $\#\#P < 0.01$, $\#\#\#P < 0.001$ v.s. VEH+PRE injected group). The i.t. injection of these inhibitors alone (L-NAME+VEH or 7-NI+VEH), in the absence of PRE, did not affect PWF in comparison to the VEH+VEH group (Fig. 1-1A and B).

The i.t. injection of PRE (3 nmol, VEH+PRE) also decreased PWL to noxious heat stimuli (thermal hyperalgesia) for the entire 60 min post-injection testing period as compared to that of the VEH+VEH treated group (Fig. 1-1C and D; $^{**}P < 0.01$, $^{***}P < 0.001$ v.s. VEH+VEH treated group). I.t. pretreatment with L-NAME (100 nmol, Fig. 1-1C) or with 7-NI (200 nmol, Fig. 1-1D) blocked the PRE-induced decrease in PWL ($\#\#\#P < 0.001$ v.s. VEH+PRE injected group). The injection of these inhibitors alone (L-NAME+VEH or 7-NI+VEH) did not evoke a significant change in PWL in comparison to the VEH+VEH group (Fig. 1-1C and D).

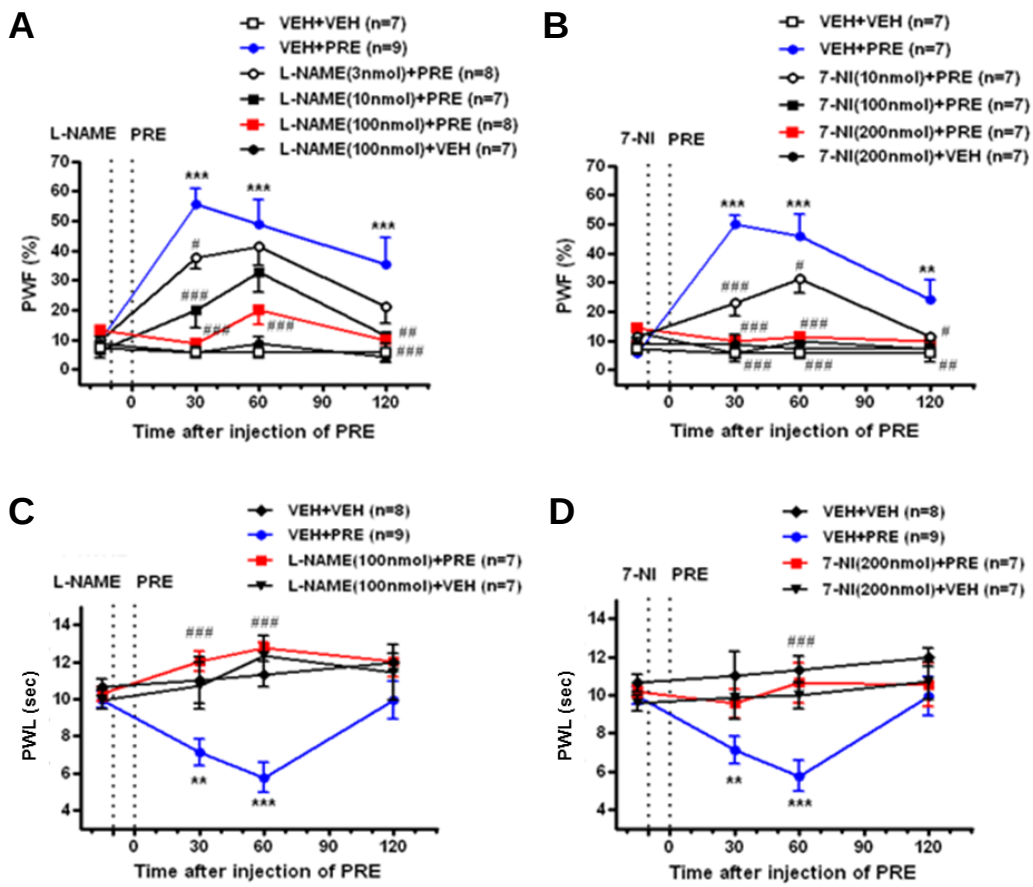

Figure 1-1. The effect of i.t. administration of L-NAME (a non-selective NOS inhibitor) or 7-NI (a selective nNOS inhibitor) on the PRE084 (PRE)-induced changes in the paw withdrawal frequency (PWF, %) and the paw withdrawal latency (PWL, sec) over time. Either L-NAME (A and C) or 7-NI (B and D) was applied 10 min before PRE injection, respectively. The PWF (A and B) and the PWL (C and D) were examined at 30, 60, 120 min after PRE injection using a von-Frey filament (0.16 g), and hot plate test (55 ± 0.5 ℃), respectively. ***P* < 0.01, ****P* < 0.001 v.s. VEH+VEH group; #*P* < 0.05, ##*P* < 0.01, ###*P* < 0.001 v.s. VEH+PRE group. n = 7–9 mice / group.

2. Effect of i.t. pretreatment with NOS inhibitors on the PRE-induced enhancement of Fos expression caused by a paw pinch stimulus

The normal control animals that merely received isoflurane treatment showed only a few Fos-ir neurons that were scattered in the SDH, NP, and NECK regions of the dorsal horn of the spinal cord (Fig. 1-2A and B). A diagram depicting the location of each of these three regions in the spinal dorsal horn is superimposed on the photomicrograph of the spinal cord illustrated in the first plate of figure 1-2B. Right paw-pinch stimulation for 10 min significantly increased the number of Fos-ir cells in all regions of the ipsilateral spinal cord dorsal horn (Fig. 1-2A and B), but had no effect on Fos expression in the contralateral dorsal horn (data not shown). Intrathecal treatment with the PRE (3 nmol) significantly enhanced paw pinch-induced Fos expression in the dorsal horn compared with that observed in the paw pinch only group (Fig. 1-2A and B; $^{**}P < 0.01$, $^{***}P < 0.001$ v.s. Pinch group). Intrathecal pretreatment with L-NAME (100 nmol) or 7-NI (100 nmol) before the injection of PRE completely blocked this PRE–induced facilitatory effect on spinal Fos expression (Fig. 1-2A and B; $^{###}P < 0.001$ v.s. PRE+Pinch group). In contrast, NAME or 7-NI alone in the absence of PRE did not modify paw pinch-evoked Fos expression in the dorsal horn. Similarly, i.t. injection of PRE without paw pinch stimulation had no effect on the number of Fos-ir neurons in the dorsal horn compared with those present in normal animals (Fig. 1-2A and B).

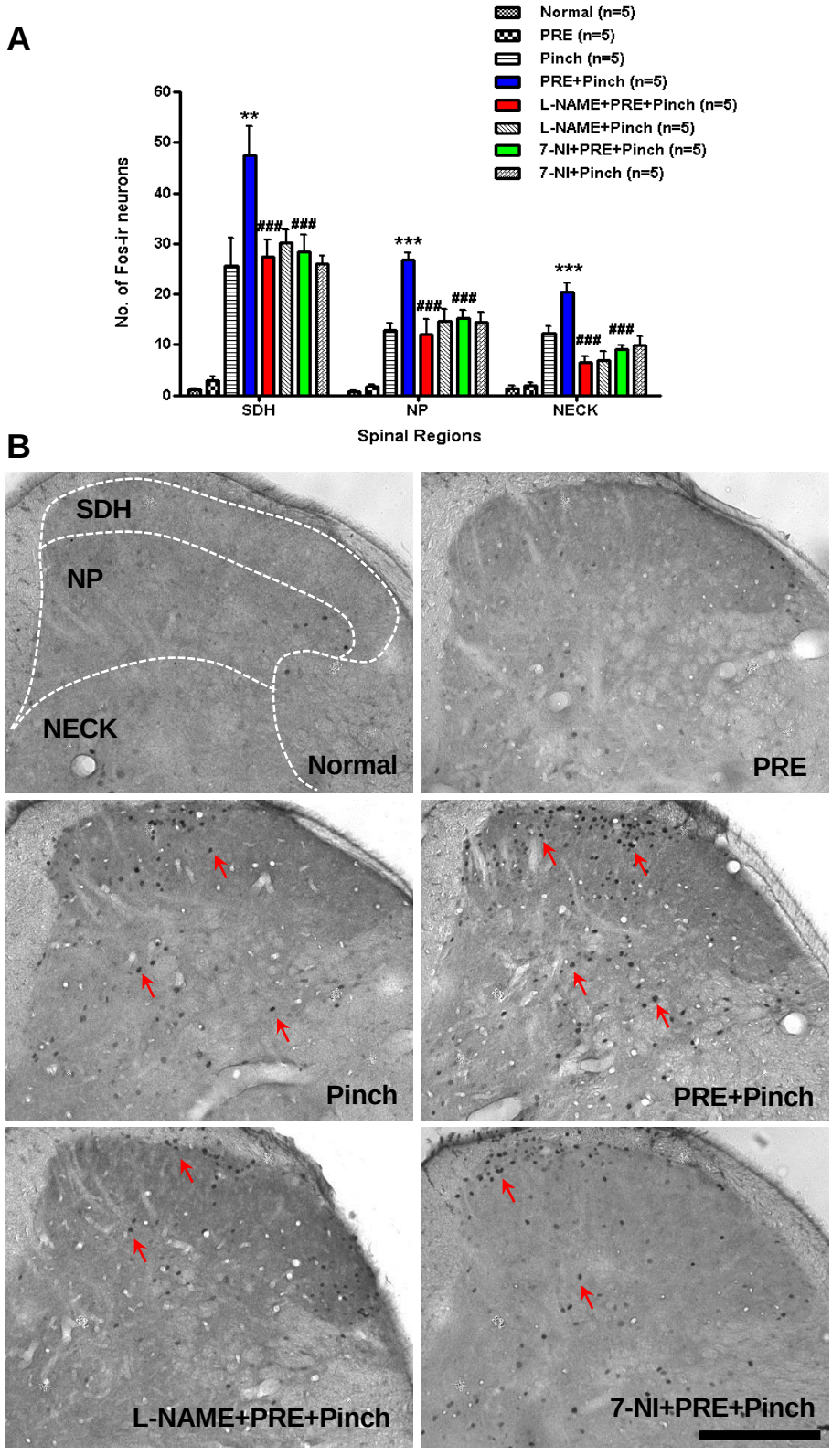
A
Normal (n=5)
PRE (n=5)
Pinch (n=5)
PRE+Pinch (n=5)
L-NAME+PRE+Pinch (n=5)
L-NAME+Pinch (n=5)
7-NI+PRE+Pinch (n=5)
7-NI+Pinch (n=5)
No. of Fos-ir neurons
Spinal Regions
SDH
NP
NECK
B
SDH
NP
NECK
Normal
PRE
Pinch
PRE+Pinch
L-NAME+PRE+Pinch
7-NI+PRE+Pinch

Figure 1-2. The effect of i.t. administration of L-NAME (a non-selective NOS inhibitor) or 7-NI (a selective nNOS inhibitor) on PRE084 (PRE)-induced enhancement of paw pinch-evoked spinal cord Fos expression. (A) The number of Fos-immunoreactive (ir) neurons in the superficial dorsal horn (SDH, lamina I–II), in the nucleus proprius (NP, lamina III–IV) and in the neck region (NECK, lamina V–VI) of the spinal cord dorsal horn are depicted graphically in panel A. $^{**}P < 0.01$, $^{***}P < 0.001$ v.s. Pinch group; $^{###}P < 0.001$ v.s. PRE+Pinch group. n = 5 mice / group. (B) Photomicrographs of representative spinal cord sections are illustrated in B. The white dotted lines in the first panel depict the location of each of the three regions analyzed in the spinal cord dorsal horn. Normal control group (Normal), i.t. PRE alone-treatment group (PRE, 3nmol), paw pinch-stimulated group (Pinch), i.t. PRE treatment + paw pinch group (PRE+Pinch), i.t. L-NAME (100 nmol) + PRE treatment + paw pinch group (L-NAME+PRE+Pinch), and i.t. 7-NI (100 nmol) + PRE treatment + paw pinch group (7-NI+PRE+Pinch). The PRE was administered 30 min before pinch stimulation, and L-NAME and 7-NI were administered 10 min before PRE injection. Arrows indicate representative Fos-ir cells. Scale bar = 200 μm.

3. Effect of i.t. pretreatment with NOS inhibitors on the PRE-induced increase in the number of pGluN1-ir cells in the spinal dorsal horn

The i.t. administration of PRE (3 nmol) significantly increased the number of PKC-dependent (Ser896) pGluN1-ir cells in the NP (laminae III-IV) and NECK regions (laminae V-VI) and PKA-dependent (Ser897) pGluN1-ir cells in the SDH (laminae I-II), NP and NECK regions of the spinal cord dorsal horn at the 30 min post-injection time point (Fig. 1-3; $*P < 0.05$, $**P < 0.01$, $***P < 0.001$ v.s. VEH+VEH group). I.t. pretreatment with L-NAME (100 nmol) or 7-NI (100 nmol) potently suppressed this PRE-induced increase in the number of PKC-dependent (Ser896) pGluN1-ir neurons in the spinal cord dorsal horn, particularly in the NP and NECK regions (Fig. 1-3A and B; $\#P < 0.05$, $\#\#P < 0.01$ v.s. VEH+PRE group). By contrast, the PRE-induced increased number of PKA-dependent (Ser897) pGluN1-ir neurons was not reduced by either L-NAME (100 nmol) or 7-NI (100 nmol) injection (Fig. 1-3A and B). The i.t. injection of these inhibitors alone, in the absence of PRE, did not affect spinal pGluN1 expression in comparison to the VEH+VEH group (Fig. 1-3A and B).

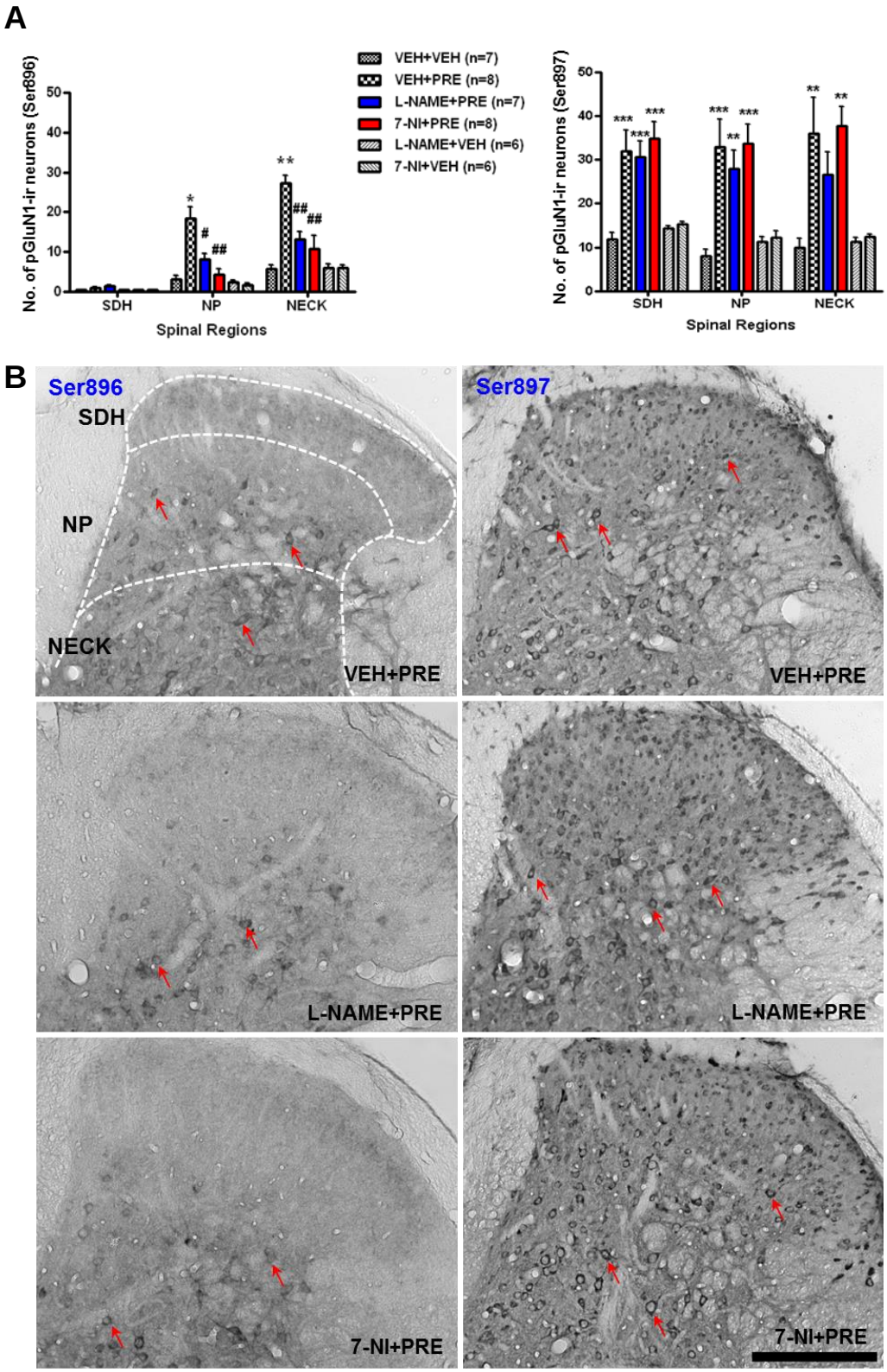
A
No. of pGluN1-ir neurons (Ser896)
VEH+VEH (n=7)
VEH+PRE (n=8)
L-NAME+PRE (n=7)
7-NI+PRE (n=8)
L-NAME+VEH (n=6)
7-NI+VEH (n=6)
SDH
NP
NECK
Spinal Regions
No. of pGluN1-ir neurons (Ser897)
B
Ser896
SDH
NP
NECK
VEH+PRE
Ser897
VEH+PRE
L-NAME+PRE
L-NAME+PRE
7-NI+PRE
7-NI+PRE

Figure 1-3. The effect of i.t. administration of L-NAME (a non-selective NOS inhibitor) or 7-NI (a selective nNOS inhibitor) on the i.t. PRE084 (PRE)-induced increase in the number of PKC (Ser896)- and PKA (Ser897)-dependent GluN1 subunit phosphorylation (pGluN1)-immunoreactive (ir) cells in the spinal cord dorsal horn. Graphs (A) and photomicrographs (B) of representative L_{4-5} spinal cord sections illustrating PKC-dependent (Ser896) and PKA-dependent (Ser897) pGluN1-ir cells in the spinal cord dorsal horn induced by i.t. administration of PRE084 (PRE, 3 nmol) alone, or following pretreatment with L-NAME (100 nmol) or 7-NI (100 nmol). **P* < 0.05, ***P* < 0.01, ****P* < 0.001 v.s. VEH+VEH group; #*P* < 0.05, ##*P* < 0.01 v.s. VEH+PRE group. n = 6–8 mice / group. SDH, superficial dorsal horn; NP, nucleus proprius; NECK, neck of dorsal horn. The white dotted lines depict the location of each of these three regions in the spinal cord dorsal horn. Arrows indicate representative pGluN1-ir cells. Scale bar = 200 μm.

4. Effect of i.t. PRE injection on the PSD-95 binding to nNOS in the spinal cord

I.t. injection of PRE (3 nmol) significantly decreased the ratio of pnNOS (Ser847) to nNOS expression at both the 30 and 60 min time points after PRE injection, (Fig. 1-4A; $*P < 0.05$ v.s. non-treated value of normal mice). In addition, i.t. injection of PRE also reduced the amount of nNOS and PSD-95 binding forms in the spinal cord dorsal horn at 30 and 60 min post-injection (Fig. 1-4B).

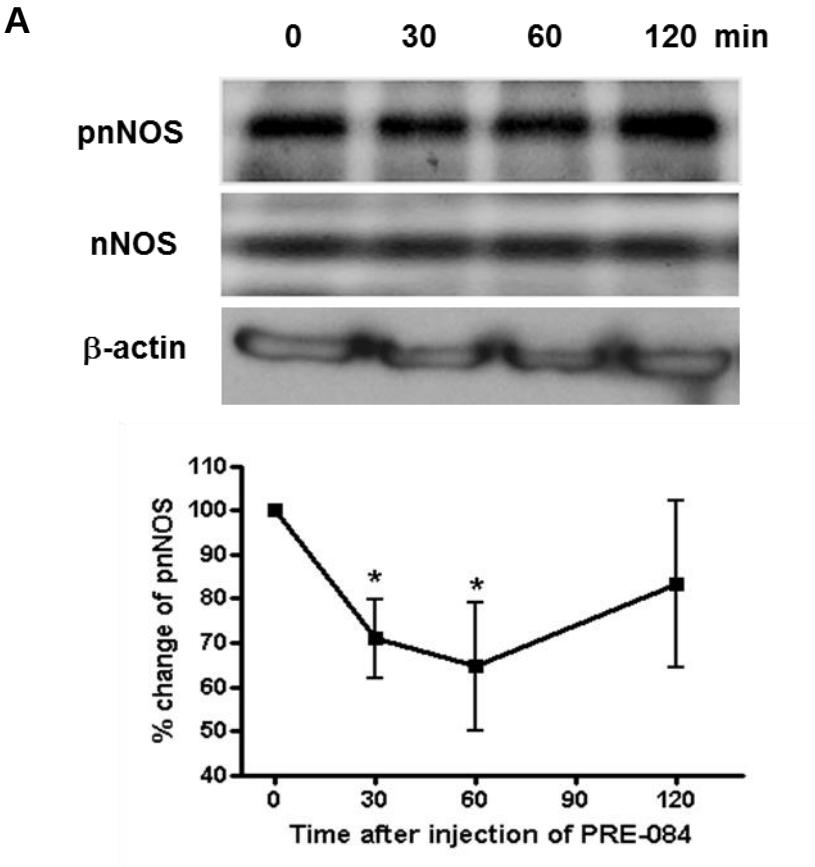
A
0
30
60
120 min
pnNOS
nNOS
β-actin
% change of pnNOS
110
100
90
80
70
60
50
40
*
*
0
30
60
90
120
Time after injection of PRE-084
B
0
30
60 (min)
Input: PSD-95
IP: nNOS
IB: PSD-95

Figure 1-4. Changes in the PSD-95 binding of nNOS in spinal cord over time following i.t. administration of PRE084 (PRE). (A) Western blots illustrating the effect of i.t. injection of PRE on the ratio of pnNOS (Ser847) to nNOS expression in the spinal cord dorsal horn. The representative bands of pnNOS, nNOS and β-actin expression are presented in the upper portion of panel A, and a graph depicting the change of the ratio of pnNOS (Ser847) to nNOS expression is shown in the lower portion of panel A. $*P < 0.05$ v.s. non-treated value of normal mice. n = 3 mice / group. (B) A co-immunoprecipitation method was also used to determine the interaction of nNOS with PSD-95 in spinal dorsal horn. Homogenates were immunoprecipitated (IP) with anti-nNOS, then blotted (IB) with anti-PSD95 antibody. Homogenates sampled at 0 (normal), 30, 60 min after PRE injection were examined. Input, 300 μg of tissue lysates at each time point.

5. Effect of i.t. PRE injection on the phosphorylation (Ser847) of nNOS in the spinal cord

The number of pnNOS-ir cells in SDH (laminae I-II) region was dramatically decreased after i.t. PRE (3 nmol) injection, especially 30 and 60 min post-injection (Fig. 1-5A). Image analysis confirmed that a significant decrease in the number of pnNOS (Ser847)-ir neurons occurred 30 and 60 min after PRE injection as compared with that of non-treatment group (0 min) (Fig. 1-5B; $***P < 0.001$).

A

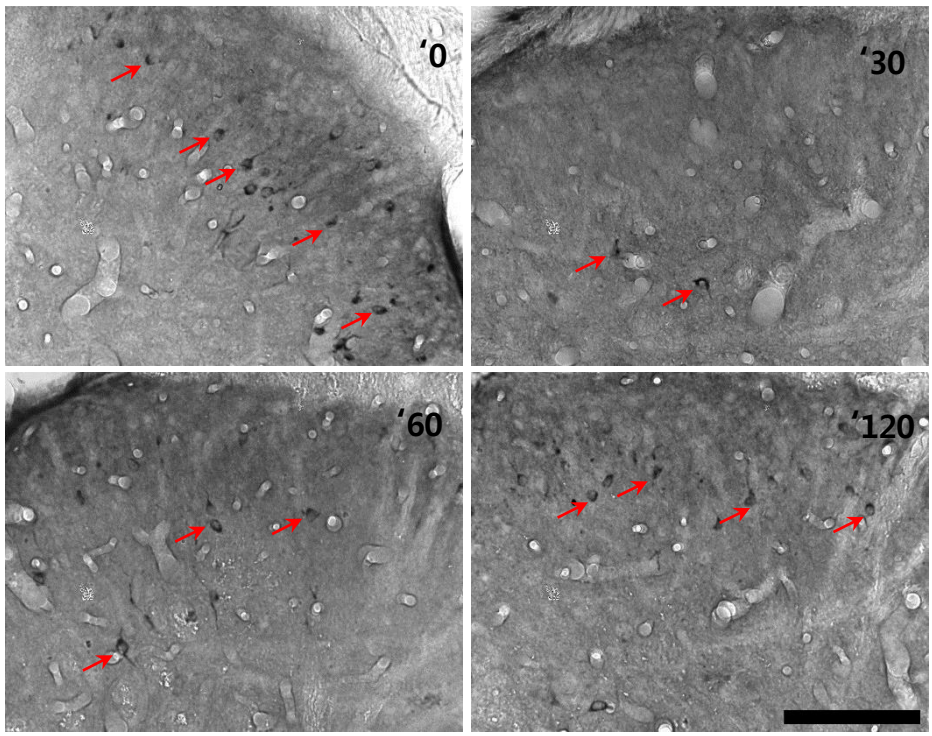
'0
'30
'60
'120

B

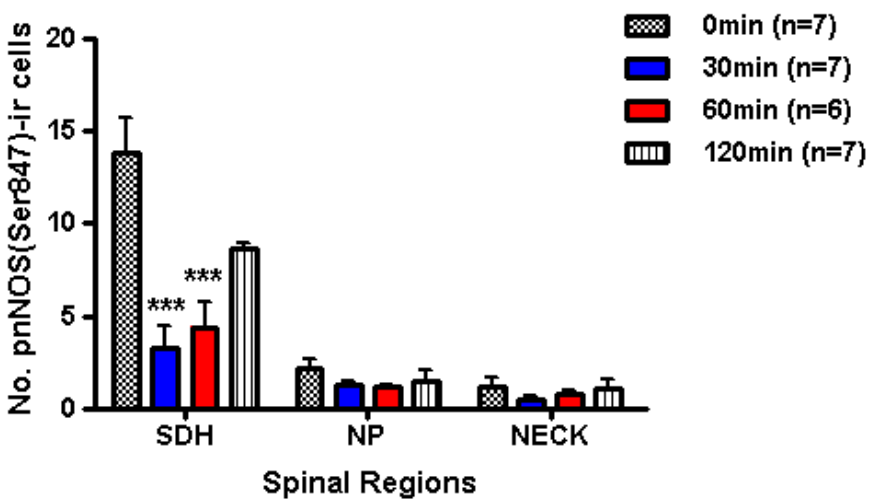
0min (n=7)
30min (n=7)
60min (n=6)
120min (n=7)
No. pnNOS(Ser847)-ir cells
20
15
10
5
0
***
***
SDH
NP
NECK
Spinal Regions

Figure 1-5. Representative photomicrographs (A) and graph (B) illustrating the effect of i.t. injection of PRE084 (PRE) on the number of pnNOS (Ser847)-immunoreative (ir) cells in the spinal cord dorsal horn. (A) Arrows indicate representative pnNOS-ir cells. Scale bar = 100 μm. (B) The graph shows the changes in the number of pnNOS-ir cells in the superficial dorsal horn (SDH, lamina I–II), in the nucleus proprius (NP, lamina III–IV) and in the neck region (NECK, lamina V–VI) of the spinal cord dorsal horn. ***$P < 0.001$ v.s. non-treated value of normal mice. n = 6–7 mice / group.

6. Effect of pretreatment with a Sig-1R antagonist on PRE-induced mechanical and thermal hypersensitivity and decrease in pnNOS expression

I.t. pretreatment with Sig-1R antagonist, BD1047 (BD, 100 nmol), completely abolished PRE084 (PRE, 3 nmol)-induced mechanical and thermal hypersensitivity at both the 30 and 60 min time points after PRE injection (Fig. 1-6A and B; $^{**}P < 0.01$, $^{***}P < 0.001$ v.s. VEH+VEH group, $^{\#}P < 0.05$, $^{\#\#\#}P < 0.001$ v.s. VEH+PRE group). Pretreatment with BD alone (BD+VEH) did not alter the PWF and the PWL. In addition, the PRE-induced decrease in the number of pnNOS-ir neurons in the SDH (laminae I-II) region was prevented by pretreatment with BD (Fig. 1-6C; ***P < 0.001 v.s. VEH+VEH group, ###P < 0.001 v.s. VEH+PRE group). Pretreatment with BD alone did not affect the number of pnNOS-ir cells in the spinal cord (Fig. 1-6C).

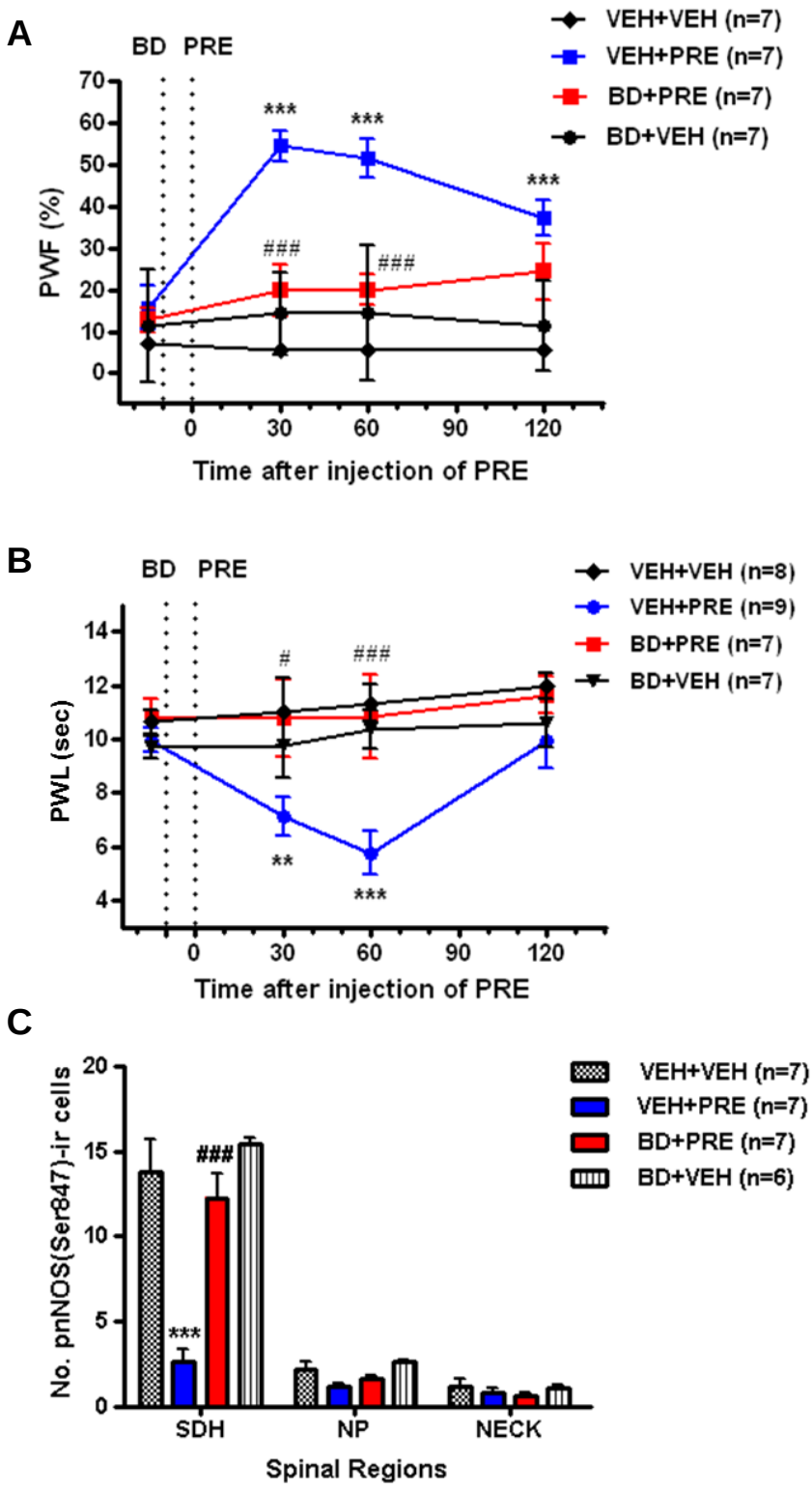
A
BD PRE
VEH+VEH (n=7)
VEH+PRE (n=7)
BD+PRE (n=7)
BD+VEH (n=7)
PWF (%)
Time after injection of PRE
B
BD PRE
VEH+VEH (n=8)
VEH+PRE (n=9)
BD+PRE (n=7)
BD+VEH (n=7)
PWL (sec)
Time after injection of PRE
C
VEH+VEH (n=7)
VEH+PRE (n=7)
BD+PRE (n=7)
BD+VEH (n=6)
No. pnNOS(Ser847)-ir cells
SDH
NP
NECK
Spinal Regions

Figure 1-6. Effects of i.t. administration of BD1047 (BD), a sigma-1 receptor antagonist, on PRE084 (PRE)-induced changes in the paw withdrawal frequency (PWF, %, A), in the paw withdrawal latency (PWL, sec, B) and in the number of pnNOS (Ser847)-immunoreactive (ir) cells in the spinal cord dorsal horn (C). BD was applied 10 min before PRE injection. $^{**}P < 0.01$, $^{***}P < 0.001$ v.s. VEH+VEH group; $^{\#}P < 0.05$, $^{\#\#\#}P < 0.001$ v.s. VEH+PRE group. n = 6–9 mice / group. SDH, superficial dorsal horn; NP, nucleus proprius; NECK, neck of dorsal horn.

7. Effect of pretreatment with a calcineurin inhibitor on PRE-induced mechanical and thermal hypersensitivity and decrease in pnNOS expression

I.t. pretreatment with calcineurin inhibitor, CsA (20 nmol), significantly attenuated PRE-induced mechanical and thermal hypersensitivity at all time points (Fig. 1-7A and B; $^{**}P < 0.01$, $^{***}P < 0.001$ v.s. VEH+VEH group, $^{\#}P < 0.05$, $^{\#\#}P < 0.01$, $^{\#\#\#}P < 0.001$ vs. VEH+PRE group). Pretreatment with CsA alone did not alter the PWF and the PWL. The PRE-induced decrease in the number of pnNOS-ir neurons in the SDH region was blocked by pretreatment with CsA (Fig. 1-7C; $^{**}P < 0.01$ v.s. VEH+VEH group, $^{\#\#}P < 0.01$ v.s. VEH+PRE group). Pretreatment with CsA alone did not affect the number of pnNOS-ir cells in the spinal cord (Fig. 1-7C).

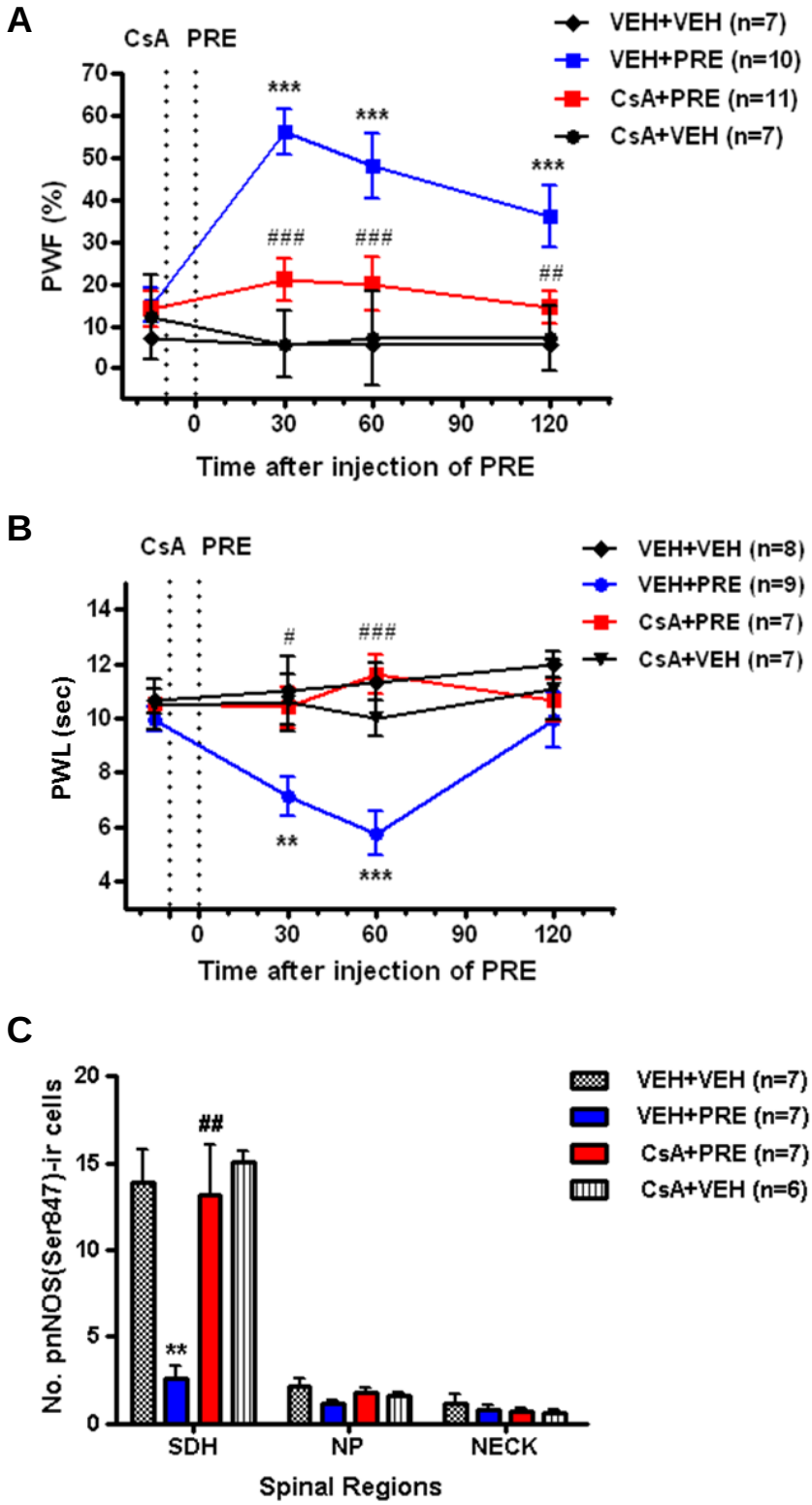
A
CsA PRE
VEH+VEH (n=7)
VEH+PRE (n=10)
CsA+PRE (n=11)
CsA+VEH (n=7)
PWF (%)
Time after injection of PRE
B
CsA PRE
VEH+VEH (n=8)
VEH+PRE (n=9)
CsA+PRE (n=7)
CsA+VEH (n=7)
PWL (sec)
Time after injection of PRE
C
VEH+VEH (n=7)
VEH+PRE (n=7)
CsA+PRE (n=7)
CsA+VEH (n=6)
No. pnNOS(Ser847)-ir cells
SDH
NP
NECK
Spinal Regions

Figure 1-7. Effects of i.t. administration of cyclosporin A (CsA), a calcineurin inhibitor, on PRE084 (PRE)-induced changes in the paw withdrawal frequency (PWF, %, A), in the paw withdrawal latency (PWL, sec, B) and in the number of pnNOS (Ser847)-immunoreactive (ir) cells (C). CsA was applied 10 min before PRE injection. $^{**}P < 0.01$, $^{***}P < 0.001$ v.s. VEH+VEH group; $\#P < 0.05$, $\#\#P < 0.01$, $\#\#\#P < 0.001$ v.s. VEH+PRE group. n = 6–11 mice / group. SDH, superficial dorsal horn; NP, nucleus proprius; NECK, neck of dorsal horn.

8. Effect of i.t. pretreatment with a sGC inhibitor on PRE-induced mechanical and thermal hypersensitivity and decrease in pnNOS expression

I.t. pretreatment with the soluble guanylyl cyclase inhibitor, ODQ (300 pmol) significantly decreased PRE-induced mechanical and thermal hypersensitivity (Fig. 1-8A and B; $^{**}P < 0.01$, $^{***}P < 0.001$ v.s. VEH+VEH group, $\#\#P < 0.01$, $\#\#\#P < 0.001$ v.s. VEH+PRE group). Pretreatment with ODQ alone did not alter either PWF or PWL or pnNOS expression. In contrast, the PRE-induced decrease in the number of pnNOS-ir neurons was notably not modified by pretreatment with ODQ (Fig. 1-8C; $^{***}P < 0.001$ v.s. VEH+VEH group).

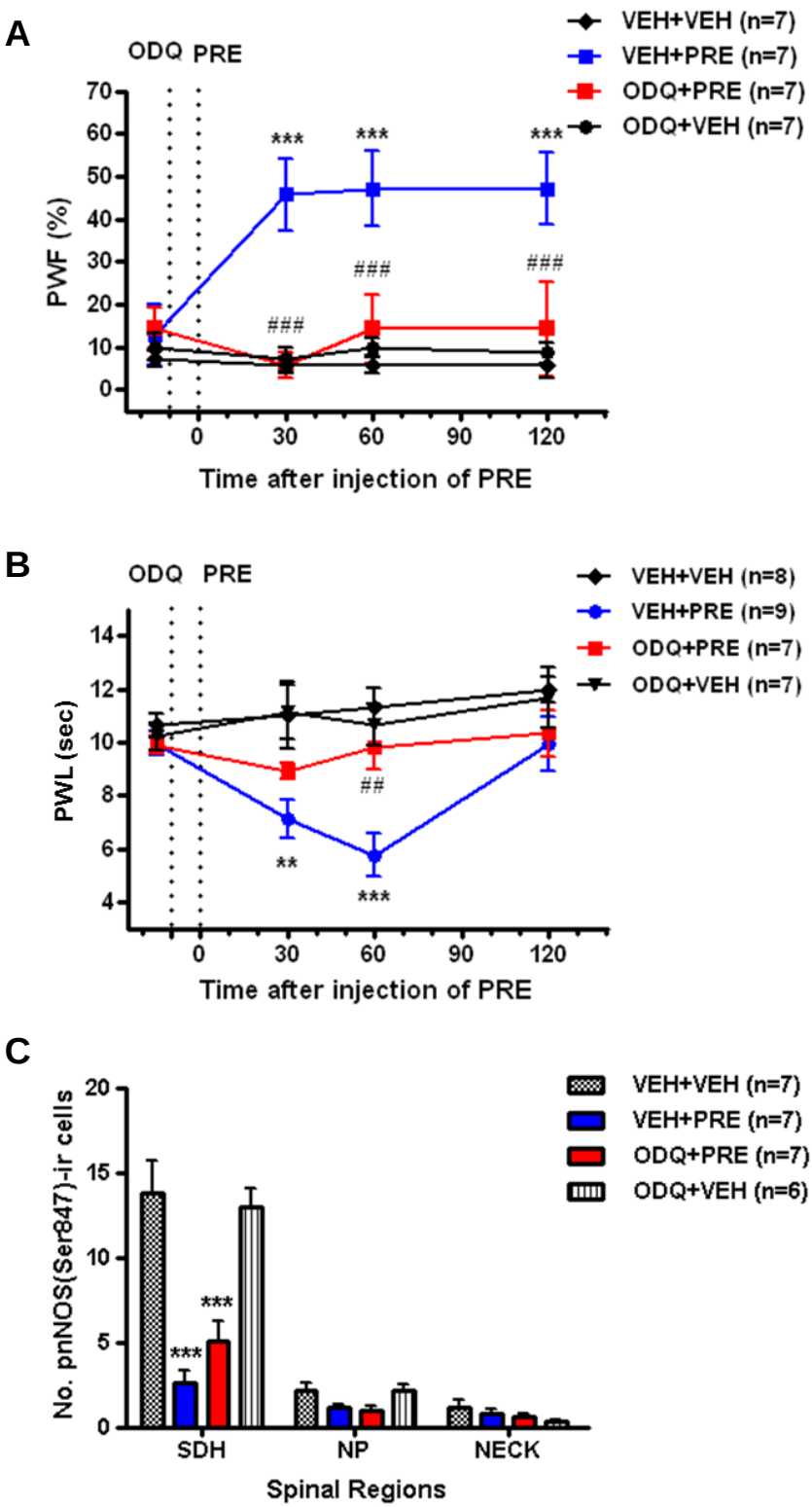
A
ODQ PRE
VEH+VEH (n=7)
VEH+PRE (n=7)
ODQ+PRE (n=7)
ODQ+VEH (n=7)
PWF (%)
70
60
50
40
30
20
10
0
***
***
***
###
###
###
0
30
60
90
120
Time after injection of PRE
B
ODQ PRE
VEH+VEH (n=8)
VEH+PRE (n=9)
ODQ+PRE (n=7)
ODQ+VEH (n=7)
PWL (sec)
14
12
10
8
6
4
##
**
***
0
30
60
90
120
Time after injection of PRE
C
VEH+VEH (n=7)
VEH+PRE (n=7)
ODQ+PRE (n=7)
ODQ+VEH (n=6)
No. pnNOS(Ser847)-ir cells
20
15
10
5
0
***
***
SDH
NP
NECK
Spinal Regions

Figure 1-8. Effects of i.t. administration of ODQ, a soluble guanylate cyclase inhibitor, on PRE084 (PRE)-induced changes in the paw withdrawal frequency (PWF, %, A), in the paw withdrawal latency (PWL, sec, B) and in the number of pnNOS (Ser847)-immunoreactive (ir) cells in the spinal cord dorsal horn (C). ODQ was applied 10 min before PRE injection. ***P* < 0.01, ****P* < 0.001 v.s. VEH+VEH group; ##*P* < 0.01, ###*P* < 0.001 v.s. VEH+PRE group. n = 6–9 mice / group. SDH, superficial dorsal horn; NP, nucleus proprius; NECK, neck of dorsal horn.

DISCUSSION

Recent studies from our laboratories have demonstrated that i.t. administration of a Sig-1R agonist (PRE) significantly induced mechanical and thermal hypersensitivity to peripheral stimuli (Roh et al., 2008b; Roh et al., 2010). These PRE-mediated effects were associated with an increase in intracellular Ca^{2+} concentration through a PLC-IP_3-PKC signaling pathway, which is also known to be closely linked to NO signaling via nNOS activation. The present study is the first to demonstrate that i.t. pretreatment with either the non-selective NOS inhibitor, L-NAME or the selective nNOS inhibitor, 7-NI reduced PRE-mediated mechanical allodynic and thermal hyperalgesic behaviors as well as the PRE-induced increase in paw pinch-evoked spinal cord Fos expression (i.e. this increased Fos expression reflects the PRE-induced induction in mechanical hyperalgesia). These results indicated that NO signaling via nNOS activation could also serve as an intrinsic mechanism leading to the initiation of the central sensitization related to Sig-1R activity.

It is well recognized that NO is synthesized by nNOS in the nervous system, which links to NMDA receptors through a postsynaptic density protein, PSD-95 (Xu et al., 2007). Extracellular Ca^{2+} influx into neuronal cells via NMDA receptor activation increases nNOS activity effectively through binding of Ca^{2+}/calmodulin to the nNOS and dephosphorylation occurs by Ca^{2+}/calmodulin dependent nNOS phosphatase, a calcineurin (Zhou and Zhu, 2009). In this regard, it was determined that i.t. PRE injection modified the ratio of pnNOS (phosphorylated form of nNOS) to nNOS expression and decreased the number of pnNOS-ir cells in the spinal cord dorsal horn. Moreover, the Sig-1R-induced reduction in the PSD-95 binding form of nNOS was confirmed using a co-immunoprecipitation method. These results

demonstrate that NO signaling activation stimulated by i.t. PRE is closely linked to decreases in the phosphorylated form of nNOS and its separation from the PSD-95 protein. That is, PRE-induced Sig-1R activation leads to time-dependent NO signaling activation, which ultimately induces mechanical allodynia and thermal hyperalgesia.

The present study also found that the activation of nNOS in the spinal cord contributes to the increase in PKC-dependent, but not PKA-dependent, pGluN1 expression in the spinal cord dorsal horn. NO has been reported to activate PKC in the heart (Ping et al., 1999). Following an ischemic stimulus (endogenous increase of NO) or after treatment with NO-releasing agents (exogenous increase of NO), NO caused an isoform-selective activation of PKCε in rabbit (Ping et al., 1999). Our recent study also demonstrated that the PRE-induced increase in spinal pGluN1 expression is mediated by the PKCα and PKCε isoforms, but not the PKCζ isoform. The PKCα and PKCε isoforms in turn contribute to mechanical allodynia (Roh et al., 2010). PKCα is a classical subtype which is both calcium and diacylglycerol (DAG)-dependent, while PKCε is an atypical subtype that is calcium-independent and DAG-dependent (Yonezawa et al., 2009). Because NO signaling could be associated with DAG as well as calcium, the activation of PKCα and PKCε by NO signaling could have a strong influence on the Sig-1R-induced increase in the PKC-dependent pGluN1 expression.

The precise mechanism by which increased NO induces PKC-dependent pGluN1 modification is a complex problem that will require extensive investigation. NO signaling is carried out by at least two separate pathways. First, NO stimulates soluble guanylyl cyclase (sGC) to increase cyclic guanosine monophosphate (cGMP), which in turn modulates a variety of downstream signaling targets (Koesling et al., 2004).

Second, NO can directly modulate the functions of many proteins by reacting with heme groups, sulfur-iron clusters and thiol moieties (Hess et al., 2005; Miyamoto et al., 2009). Thus, NO can affect PKC activity directly or indirectly by binding to proteins involved in PKC modulation. Furthermore, cGMP is known to be a particularly important second messenger for NO-dependent signaling, (Schmidtko et al., 2008; Schmidtko et al., 2009). In the present study, the result shows that the Sig-1R-induced increase in NO signaling is mediated by a cGMP signal pathway, but not by a direct action of NO on PKC activity, since the soluble guanylyl cyclase (sGC) inhibitor, ODQ, totally attenuated the PRE-induced mechanical and thermal hypersensitivity. Moreover, while Ca^{2+} signaling is also essential for activation of nNOS and catalytic activation of Ca^{2+}-dependent PKC, the activity of PKA is dependent on the concentration of cyclic AMP (cAMP), but not the concentration of Ca^{2+} within the cell. Therefore, the Sig-1R-induced increase in intracellular Ca^{2+} concentration activates a NO-sGC signaling pathway originating from nNOS, which in turn affects PKC-dependent, but not PKA-dependent, pGluN1 expression in the spinal cord dorsal horn.

The immunohistochemical data also showed that the PRE-induced expression pattern of pnNOS differed from that of PKC-dependent pGluN1 (Ser896) based on the differential distribution of these two proteins among the spinal cord laminae (regions). Thus the pnNOS-ir cells were mainly located in superficial dorsal horn (laminae I-II), which is also rich in Sig-1Rs. However, most of the PKC-dependent pGluN1-ir cells were mainly detected in the deeper dorsal horn (laminae III-IV and V-VI) in the present study. The most obvious explanation for this discrepancy is that NO, being a diffusible gas, readily permeates cell membranes and thus it can diffuse from

its site of production in laminae I and II to act on glia and/or other neurons in deeper laminae (Meller and Gebhart, 1993; Schmidtko et al., 2009). Thus even though NO is mainly produced in the superficial dorsal horn by Sig-1R activation, it is reasonable that NMDA receptors (pGluN1) located on deep dorsal horn cells can be affected either directly or indirectly by NO produced more superficially. However, these concepts need to be confirmed by further investigation.

Finally, it was also evaluated whether pretreatment with the Sig-1R antagonist, BD1047, or the phosphatase calcineurin inhibitor, CsA, attenuates PRE-induced mechanical and thermal hypersensitivity and prevents the Sig-1R-induced decrease in the number of pnNOS-ir cells. The results obtained with BD1047 pretreatment confirmed that the PRE injection-mediated pain induction was directly related to Sig-1R activation, which in turn caused activation of an NO signaling cascade. In addition, the blocking effect of BD1047 pretreatment on the PRE-induced increase in pGluN1 expression and PKC activity has also been reported in our previous studies (Kim et al., 2008; Roh et al., 2008a; Roh et al., 2010). Calcineurin (CN) is the Ca^{2+}/calmodulin-dependent phosphatase of pnNOS, and activation of CN plays a critical role in nNOS activation (Zhou and Zhu, 2009). In this study, blocking CN activation by CsA prevented both NO signaling activation and PRE-induced mechanical and thermal hypersensitivity. These results demonstrate that the NO signaling pathway via CN plays a key role in Sig-1R-mediated pain induction. By contrast, the sGC inhibitor, ODQ, attenuated PRE-mediated pain induction, but did not affect the Sig-1R-induced decrease in the number of pnNOS-ir cells. As mentioned above one of the major NO signaling mechanisms in the spinal nociceptive process involves the activation of sGC and subsequent cGMP production (Tao and Johns, 2002). Because sGC inhibition by

ODQ blocked the NO downstream pathway following pnNOS dephosphorylation, it is our contention that ODQ could not modify the Sig-1R-induced decrease in pnNOS-ir cells.

The present study demonstrated that spinal Sig-1R-induced mechanical and thermal hypersensitivity are mediated by an increase in activated nNOS (i.e. as evidenced by a significant decrease in pnNOS and/or by the decrease in the PSD95-PDZ domain binding form), which in turn causes an increase in NO-induced PKC-dependent, PKA-independent, pGluN1 expression. Collectively these findings suggest that the increase in NO signaling that occurs via a Sig-1R-mediated decrease in pnNOS plays an important role in spinal Sig-1R-mediated sensitization.

CHAPTER 2

Modulatory effect of D-serine via nNOS/sGC signaling on sigma-1 receptor-induced GluN1 phosphorylation in neuropathic pain

ABSTRACT

It has been demonstrated that spinal sigma-1 receptor (Sig-1R) activation mediates nociception via an increase in phosphorylation of the NMDA receptor GluN1 subunit (pGluN1). Here the role of D-serine in this process was examined, by which NMDA receptor function is potentiated via neuronal NOS (nNOS) activation. The present study was designed to examine whether the Sig-1R-induced facilitative effect on NMDA-induced nociception is mediated by D-serine, D-serine modulates spinal pGluN1 expression, and nNOS/NO signaling mediates the effect of D-serine on the increase in pGluN1 and the development of neuropathic pain following chronic constriction injury (CCI) of the sciatic nerve. Intrathecal administration of the D-serine degrading enzyme, DAAO attenuated the facilitation of NMDA-induced nociception induced by the Sig-1R agonist, PRE084. Exogenous D-serine facilitates NMDA-induced nociception and increases in both total NO levels and PKC-dependent (Ser896) pGluN1 expression, which were attenuated by preteatment with the nNOS inhibitor, 7-nitroindazole. In CCI mice, intrathecal administration of exogenous D-serine restored mechanical allodynia (MA) and PKC-dependent pGluN1 that were suppressed by the Sig-1R antagonist, BD1047. Furthermore, administration of the serine racemase inhibitor, LSOS or DAAO suppressed CCI-induced MA, pGluN1 and nNOS activation. Intrathecal administration of 7-nitroindazole, the soluble guanylyl cyclase (sGC) inhibitor, ODQ attenuated CCI-induced MA and pGluN1. By contrast, D-serine and nNOS signaling had no effect on CCI-induced thermal hyperalgesia or GluN1 expression. Spinal D-serine is a downstream effector of CCI-induced Sig-1R activation and modulates PKC-dependent pGluN1 expression via nNOS/sGC signaling, and ultimately contributes to the induction of MA following peripheral nerve injury.

INTRODUCTION

Damage to the spinal cord or peripheral nerves can lead to the development of neuropathic pain, which causes considerable suffering and distress to these patients and is associated with several diagnostic symptoms including mechanical allodynia (MA, sensation of pain to non-noxious mechanical stimuli) and thermal hyperalgesia (TH, increased pain response to noxious thermal stimuli) (Woolf and Mannion, 1999). The development of peripheral neuropathic pain involves a variety of pathophysiological mechanisms in both the peripheral and central nervous systems (Baron, 2006). In this regard spinal *N*-methyl-D-aspartate receptors (NMDARs) have been shown to play a key role in the development of 'central sensitization', a phenomenon in which nociceptive inputs to the dorsal horn increase the excitability and synaptic efficacy of neurons in spinal pain pathways (Woolf, 1983; Woolf and Mannion, 1999). Phosphorylation of the NMDAR GluN1 subunit (pGluN1) at serine and threonine residues increases neuronal excitability by reducing the Mg^{2+} block and by increasing the probability of channel openings (Chen and Huang, 1992). This is consistent with our previous results showing that activation of spinal sigma-1 receptors (Sig-1Rs) contributes to Ca^{2+}-dependent second messenger cascades and functional potentiation of NMDARs via increases in PKC-dependent and PKA-dependent phosphorylation at serine 896 and serine 897, respectively, leading to formalin-induced nociceptive behaviors in an animal model of formalin-induced pain and to the development of MA in a neuropathy model involving chronic constriction injury (CCI) of the sciatic nerve (Kim et al., 2006; Roh et al., 2008a; Roh et al., 2008b).

D-serine is an endogenous ligand for the glycine site of the NMDARs, which can

closely modulate functional activity of NMDARs (Mothet et al., 2000). D-serine is generated from L-serine by the activity of serine racemase (Srr) and this biosynthesizing enzyme is expressed exclusively in astrocytes (Wolosker et al., 1999). Recent reports suggest that D-serine plays an important role as a gliotransmitter, which upon release from astrocytes activates NMDARs on postsynaptic neurons contributing to the processing of nociceptive transmission in the spinal cord dorsal horn (Lefèvre et al., 2015; Miraucourt et al., 2011). This is consistent with our previous results showing that reduction of D-serine levels in the spinal cord following intrathecal (i.t.) administration of the Srr inhibitor, LSOS or the D-serine degrading enzyme, DAAO significantly attenuates the development of MA in CCI mice (Moon et al., 2015). Although it has been documented that spinal D-serine activates NMDAR, there is limited understanding of the cellular mechanisms involved in the induction of persistent pain by endogenous D-serine. Since it has been suggested that Sig-1R activation increases the production of D-serine via modulation of Srr expression, it could be possible that the Sig-1R-induced increase in D-serine in astrocytes is involved in the functional potentiation of NMDARs, which underlies the development of MA in CCI mice.

Nitric oxide (NO) is synthesized from L-arginine, NADPH and oxygen by three isoforms of nitric oxide synthase (NOS): neuronal NOS (nNOS), inducible NOS (iNOS) and endothelial NOS (eNOS) (Alderton et al., 2001). It has been well demonstrated that NO plays an important, but complex role as a neuromessenger in nociceptive processes in the spinal cord dorsal horn and induces the development of central sensitization (Cury et al., 2011). Importantly, nNOS co-localizes with NMDARs and the scaffolding protein postsynaptic density protein-95 (PSD-95) links nNOS to the NMDAR, which contributes to the functional coupling of nNOS to

NMDARs (Christopherson et al., 1999). The literature also indicates that activation of NMDARs modulates spinal nociceptive transmission via nNOS/NO signaling cascades (Ferreira et al., 1999; Kawamata and Omote, 1999). In addition, NMDA augments nNOS activity in a concentration-dependent manner and selective D-amino acids degradation has been shown to diminish NMDA-evoked nNOS activity in cerebellar slices (Mothet et al., 2000). These findings raise the possibility that the action of D-serine on NMDAR function and nociceptive transmission at spinal glutamatergic synapses could be closely linked to nNOS activation.

In this regard, a major hypothesis of this study is that Sig-1R modulation of astrocytic D-serine plays an important role in increasing pGluN1 expression via nNOS activation and that this pathway contributes to the development of persistent neuropathic pain. This hypothesis was first examined using an animal model of NMDA-induced nociception to determine the potential interaction of D-serine and nNOS activation that ultimately contributes to the Sig-1R-induced potentiation of nociception induced by the increased phosphorylation of NMDAR. Then, an animal model of peripheral nerve injury was used in order to determine the potential for using NMDAR, D-serine and/or nNOS as therapeutic targets for alleviating MA under conditions of neuropathic pain. Thus, the present study was designed to examine whether: (1) the Sig-1R-induced facilitative effect on NMDA-induced nociception is mediated by D-serine; (2) D-serine modulates spinal PKC-dependent (Ser896) or PKA-dependent (Ser897) pGluN1 expression, which accounts for the potentiation of NMDAR function; and finally (3) the nNOS/NO signaling cascade mediates the effect of D-serine on the increase in pGluN1 expression and development of peripheral neuropathic pain.

MATERIALS AND METHODS

Experimental animals

Experimental animals and maintaining condition are identical with those of Chapter 1.

Peripheral nerve injury model

A chronic constriction injury (CCI) of the common sciatic nerve was performed according to the method described by Bennett and Xie with a minor modification (Bennett and Xie, 1988). Briefly, mice were anesthetized with 3% isoflurane in a mixture of N_2O/O_2 gas. The left sciatic nerve was exposed and 3 loose ligatures of 6-0 silk were placed around the nerve. Sham surgery was performed by exposing the sciatic nerve in the same manner, but without ligating the nerve.

Drugs and i.t. administration

The following drugs were used: *N*-Methyl-D-aspartic acid (NMDA, a NMDA receptor agonist; 0.4 nmol); 2-(4-morpholinethyl)1-phenylcyclohexane carboxylate (PRE084, a Sig-1R agonist; 3 nmol); N-[2-(3,4-dichlorophenyl)ethyl]-N-methyl-2-(dimethylamino)ethylamine dihydrobromide (BD1047, a Sig-1R antagonist; 100 nmol); D-serine (5, 50, 500 nmol); L-serine O-sulfate potassium salt (LSOS, a Srr inhibitor; 10 nmol); D-amino acid oxidase (DAAO, an endogenous D-serine degrading enzyme; 0.001, 0.01, 0.1 U); fluorocitrate (FC, an astrocyte metabolic inhibitor; 0.003, 0.03 nmol); 7-nitroindazole (7-NI, a nNOS inhibitor; 200 nmol); 1H-[1,2,4]oxadiazolo[4,3-a]Quinoxalin-1-one (ODQ, a soluble guanylyl cyclase inhibitor; 300 pmol); chelerythrine (CHE, a PKC inhibitor; 1 nmol); PKA inhibitor 14-22 amide

(PKI, a PKA inhibitor; 2 nmol). NMDA, PRE084, BD1047 and CHE were purchased from Tocris Cookson Ltd. (Bristol, UK), LSOS from Santa Cruz Biotechnology Inc. (CA, USA), D-serine, DAAO, FC, 7-NI and ODQ from Sigma–Aldrich (St. Louis, MO, USA) and PKI from Calbiochem. The doses of all drugs used in the present study were selected based on doses previously used in the literature including those used in previous studies from our laboratories showing that these doses produce maximal effects with no detectable side effects (Gabra *et al.*, 2007; Moon *et al.*, 2015; Morita *et al.*, 2008; Roh *et al.*, 2011; Yoon *et al.*, 2010). FC was dissolved in 0.05% 1N HCl in physiological saline, 7-NI was dissolved in 5% DMSO in Corn oil, and ODQ and CHE were dissolved in 5% DMSO in physiological saline. The remaining drugs were dissolved in physiological saline. The injection volume was 5 μl and all drugs were administrated intrathecally. In CCI mice, drugs were administrated twice a day on postoperative days 0-3, during the induction phase of pain development.

The procedure of i.t. drug administration was performed in unanesthetized naïve mice and CCI mice that were anesthetized with 3% isoflurane in a mixture of N_2O/O_2 gas according to the method described in Chapter 1.

NMDA-induced nociceptive behaviors

Each mouse was acclimated to an acrylic observation chamber for at least 30 min before the first drug injection. NMDA (0.4 nmol in 5 μl sterile saline) was injected intrathecally in order to produce spinally mediated NMDA-induced nociceptive behaviors (Yajima Y *et al.*, 2000; Yoon *et al.*, 2010). Following injection, animals were immediately placed in an observation chamber and nociceptive behaviors including caudally directed licking, scratching and biting were recorded for a 10-min period. The cumulative response time (sec) of these behaviors was measured. To

evaluate the possible role of Sig-1Rs and/or D-serine in NMDA-induced nociception, PRE084 (3 nmol) or D-serine (5, 50, 500 nmol) was intrathecally injected 30 min prior to NMDA injection. Separate groups of animals were pretreated with DAAO (0.001, 0.01 U), FC (0.003, 0.03 nmol), 7-NI (200 nmol), CHE (1 nmol) or PKI (2 nmol) 10 min prior to i.t. injection of PRE084 (3 nmol) or D-serine (500 nmol).

Behavioral assessments in CCI mice

Nociceptive behavioral tests were performed on the ipsilateral hind paw 1 day before surgery on all animals to obtain normal baseline values of paw withdrawal responses to mechanical and thermal stimuli. Then, animals were randomly assigned to experimental and control groups. Postoperative behavioral tests were performed 3 days post-surgery. All behavioral analyses were performed blindly.

To assess nociceptive responses to noxious heat stimuli (thermal hyperalgesia), paw withdrawal latency (PWL, sec) was measured using a plantar analgesia meter (Model 390, IITC Life Science Inc., Woodland Hills, CA) as previously described by Hargreaves et al. with minor modifications (Hargreaves et al., 1988). Mice were placed in acrylic cylinders on a glass floor and allowed to habituate before testing. A radiant heat source was positioned under the floor beneath the hind paw. The test was duplicated in the hind paw of each mouse, and the mean withdrawal latency was calculated. A cutoff latency in the absence of a response was set at 20 sec to prevent tissue damage. Experimental method for mechanical allodynia assay was identical with that of Chapter 1.

Measurement of nitric oxide in the spinal cord

Nitric oxide was determined in the spinal cord dorsal horns from the lumbar

enlargement using a nitric oxide detection kit (cat# ADI-917-020, Enzo Life sciences Inc.). This nitric oxide (total), detection kit is based on the enzymatic conversion of nitrate to nitrite by the enzyme nitrate reductase, followed by the Griess reaction to form a colored azo dye product. Animals (n = 4–5 mice / group) were euthanized 30 min after D-serine injection and on day 3 post-CCI surgery. Mice were deeply anesthetized with 3% isoflurane in a mixture of N_2O/O_2 gas and perfused transcardially with calcium-free Tyrode's solution. The isolated spinal cords were homogenized in PBS by sonication. Homogenates were subsequently centrifuged at 400 g for 10 min at 4℃ and, then, the supernatant was used for nitric oxide detection following the manufacturer's recommendation.

Western blot assay

For Western blot analysis separate groups of animals (n = 5–8 mice / group) were deeply anesthetized with 3% isoflurane in a mixture of N_2O/O_2 gas and mice were euthanized 30 min after D-serine injection and on day 3 post-CCI surgery. Experimental procedures are identical with those of Chapter 1. Spinal cord homogenates (25 - 30 μg protein) were separated using 10% SDS-polyacrylamide gel electrophoresis and transferred to nitrocellulose membrane. The membranes were blocked with 5% skimmed milk for 1 h at RT and incubated at 4℃ overnight with a primary antibody specific for pGluN1 Ser896 (rabbit polyclonal anti-pGluN1 Ser896 antibody, 1:1k, cat# ABN88, Millipore Co.; this antibody is specific for rabbit GluN1 phosphorylated on serine 896), pGluN1 Ser897 (rabbit polyclonal anti-pGluN1 Ser897 antibody, 1:1k, cat# ABN99, Millipore Co.; this antibody is specific for rabbit GluN1 phosphorylated on serine 897), GluN1 (rabbit polyclonal anti-GluN1 antibody, 1:1k, cat# 07-362, Upstate Biotechnology), pnNOS (rabbit polyclonal anti-pnNOS

Ser847 antibody, 1:1k, cat# ab16650, Abcam plc.; this antibody is specific for rabbit nNOS phosphorylated on serine 847), nNOS (mouse monoclonal anti-nNOS antibody, 1:3k, cat# 610308, BD Biosciences) or β-actin (mouse monoclonal anti-β-actin antibody, 1:5k, cat# sc-47778, Santa Cruz Biotechnology Inc.). After washing with TBST, membranes were incubated for 4 h at 4℃ with horseradish peroxidase (HRP)-conjugated anti-rabbit or anti-mouse antibody (1:10k, Santa Cruz Biotechnology Inc.). For analysis of pGluN1 or GluN1 expression, the value of the control groups was set at 100% and, then, the percent change relative to the control groups was calculated for each group. To analyse activation of nNOS, the ratio of pnNOS (Ser847) to nNOS expression was calculated. The value of the ratio of pnNOS to nNOS expression in the control groups was set at 100%. Thus, the percent change in pnNOS to nNOS expression was examined for each group.

NADPH-diaphorase staining and image analysis

NADPH-diaphorase staining was performed to demonstrate the presence of functional NOS enzyme as described previously with minor modifications (Guggilam et al., 2008). A separate group of mice were used for this experiment (n = 6 mice / group) and spinal cord sections were obtained according to the method of immunohistochemistry detailed in Chapter 1. Spinal tissue sections were washed in 0.1 M Tris buffer (pH 7.4) and incubated in β-NADPH (1 mg/ml, Sigma–Aldrich Co.), Nitro blue tetrazolium (NBT, 0.25 mg/ml, Sigma–Aldrich Co.) and 0.5% Triton X-100 for 1 h at 37℃ in the dark. Tissue sections were mounted on slides and examined under a brightfield microscope (Zeiss Axioscope, Germany). Image analysis methods for NADPH-diaphorase staining are identical with those of Chapter 1.

After NADPH-diaphorase staining, several sections were blocked with 3% normal goat serum for 1 h at RT and incubated overnight at RT with a primary antibody specific for c-Fos (rabbit polyclonal anti-c-Fos antibody, 1:10k, cat# PC38, Calbiochem), NeuN (mouse monoclonal anti-NeuN antibody, 1:1k, cat# MAB377, Millipore Co.), GFAP (mouse monoclonal anti-GFAP antibody, 1:1k, cat# MAB360, Millipore Co.) or Iba-1 (rabbit anti-Iba1 antibody, 1:1k, cat# 019-19741, Wako). After washing with PBS, the sections were incubated in biotinylated anti-mouse IgG (1:200, Vector Laboratories) or anti-rabbit IgG (1:200, Vector Laboratories) for 1 h at RT and then incubated with avidin-biotin-peroxidase complex (ABC). The immunoreactivity was visualized by incubating with PBS containing 3,3-diaminobenzidine and H_2O_2. Tissue sections were mounted on slides and examined under a Leica DM500 microscope (Leica Biosystems, Germany).

Statistical analysis

Data are expressed as the mean ± SEM. Statistical analysis was performed using a Prism 5.0 (Graph Pad Software, San Diego, USA). Comparison between all experimental groups, except the data in figure 2-7C, was analyzed by a one-way ANOVA, followed by the Newman-Keuls multiple comparison test for *post-hoc* analysis. Repeated measures two-way ANOVA was performed to determine differences in the data from the time course changes in MA shown in figure 2-7C followed by a Bonferroni's multiple comparison test for *post-hoc* analysis. *P*-values of < 0.05 were considered statistically significant.

RESULTS

1. Effect of i.t. administration of DAAO or fluorocitrate on the Sig-1R-mediated facilitation of NMDA-induced nociceptive behaviors

Intrathecal (i.t.) administration of NMDA (0.4 nmol) elicited nociceptive behaviors including caudally directed licking, scratching and biting, that lasted for the entire 10-min observation period. The most significant NMDA-induced change occurred in licking behavior, which was significantly increased following NMDA administration as compared to that of the vehicle-treated group (Fig. 2-1A; ***P < 0.001 v.s. VEH+VEH). Next, pretreatment with the Sig-1R agonist, PRE084 (3 nmol) significantly facilitated both licking and scratching behaviors induced by administration of NMDA (Fig. 2-1A; #P < 0.05, ##P < 0.01 v.s. VEH+NMDA). The final set of experiments involved measuring the cumulative response time (sec) of nociceptive behaviors for the entire 10-min observation period. I.t. administration of NMDA elicited significant nociceptive behaviors and pretreatment with PRE084 increased these NMDA-induced nociceptive behaviors (Fig. 2-1B and C; **P < 0.01, ***P < 0.001 v.s. VEH+VEH, #P < 0.05, ##P < 0.01 v.s. VEH+NMDA). This facilitatory effect of PRE084 on NMDA-induced nociceptive behaviors was significantly attenuated by pretreatment with the D-serine degrading enzyme, DAAO (0.01 U) or with the astrocyte metabolic inhibitor, fluorocitrate (FC, 0.03 nmol) (Fig. 2-1B and C; ‡P < 0.05 v.s. PRE+NMDA). On the other hand, pretreatment with either DAAO or FC had no effect on NMDA-induced nociceptive behaviors. These results strongly suggest that the Sig-1R-induced facilitation of NMDA-induced nociceptive behaviors is mediated at least partially by D-serine released from astrocytes.

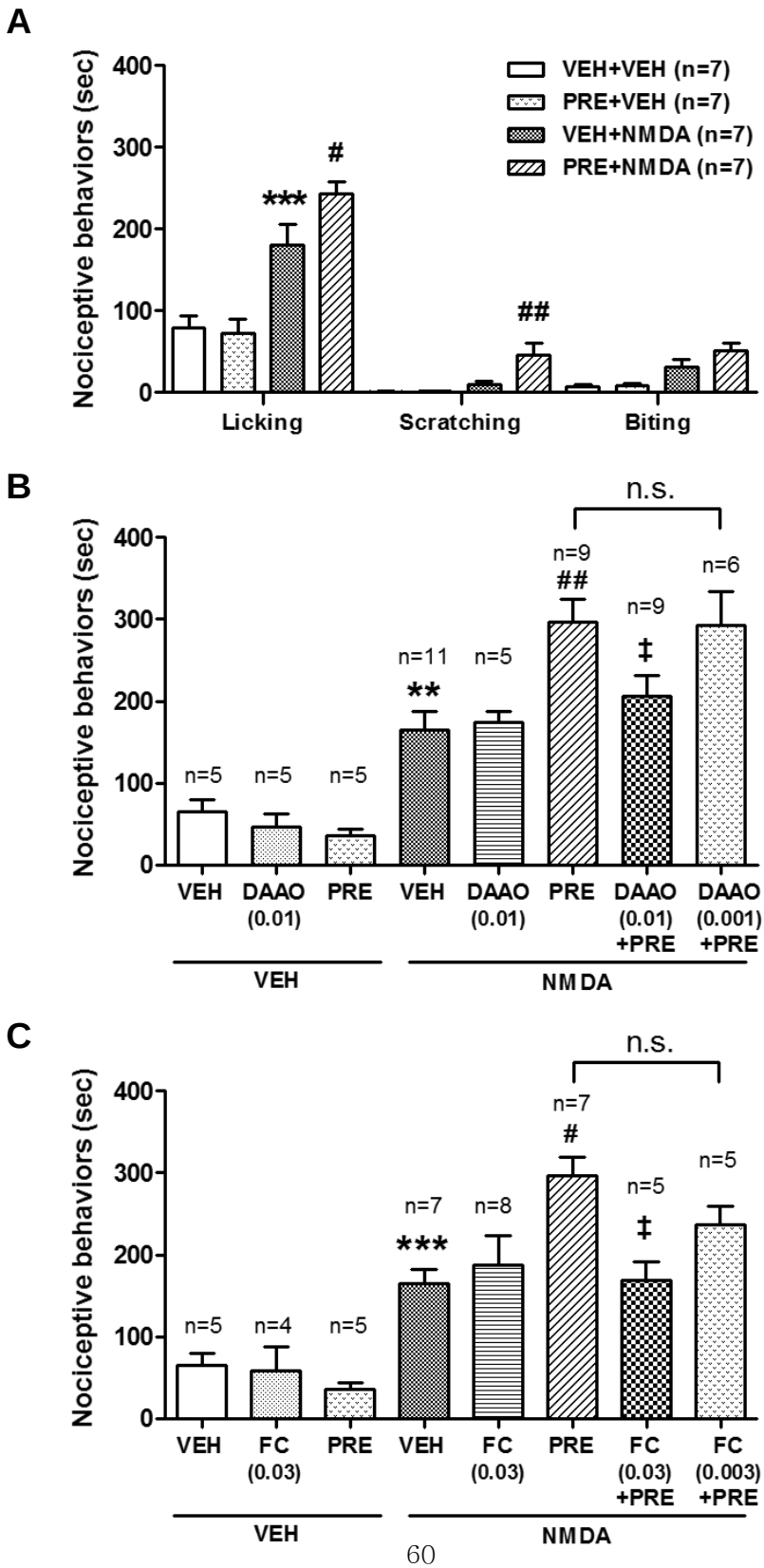
A
Nociceptive behaviors (sec)
400
300
200
100
0
VEH+VEH (n=7)
PRE+VEH (n=7)
VEH+NMDA (n=7)
PRE+NMDA (n=7)
***
#
##
Licking
Scratching
Biting
B
n.s.
n=9
##
n=6
n=9
‡
n=11
**
n=5
n=5
n=5
n=5
VEH
DAAO (0.01)
PRE
VEH
DAAO (0.01)
PRE
DAAO (0.01) +PRE
DAAO (0.001) +PRE
VEH
NMDA
C
n.s.
n=7
#
n=5
n=5
‡
n=7
***
n=8
n=5
n=4
n=5
VEH
FC (0.03)
PRE
VEH
FC (0.03)
PRE
FC (0.03) +PRE
FC (0.003) +PRE
VEH
NMDA

Figure 2-1. Graphs illustrating the effect of i.t. administration of the D-serine degrading enzyme, DAAO (0.01 and 0.001 U) or the astrocyte metabolic inhibitor, fluorocitrate (FC, 0.03 and 0.003 nmol) on the Sig-1R agonist, PRE084-(PRE, 3 nmol) induced increase in NMDA-induced nociceptive behaviors (which included caudally directed licking, scratching and biting). (A) Intrathecal administration of NMDA significantly increased licking behavior. Pretreatment with PRE084 potentiated both licking and scratching behaviors induced by administration of NMDA. ***P < 0.001 v.s. VEH+VEH treated group; #P < 0.05, ##P < 0.01 v.s. VEH+NMDA treated group. n = 7 mice / group. (B and C) DAAO (0.01 U) or FC (0.03 nmol) significantly reduced the PRE084-induced increase in NMDA-induced nociceptive behaviors. **P < 0.01, ***P < 0.001 v.s. VEH+VEH treated group; #P < 0.05, ##P < 0.01 v.s. VEH+NMDA treated group; ‡P < 0.05 v.s. PRE+NMDA treated group; n.s., no significance. n = 4–11 mice / group.

2. Effect of i.t. administration of 7-NI on D-serine-mediated facilitation of NMDA-induced nociceptive behaviors

To confirm the potential role of D-serine in NMDA-induced nociceptive behaviors, exogenous D-serine (at three different doses: 5, 50 and 500 nmol) was intrathecally injected 30 min prior to NMDA injection. As shown in figure 2-2A, D-serine (500 nmol) significantly facilitated NMDA-induced nociceptive behaviors as compared with that of the vehicle-treated group (Fig. 2-2A; **P* < 0.05 v.s. VEH+VEH treated group, #*P* < 0.05 v.s. VEH+NMDA treated group).

To determine whether nNOS activation mediates this facilitation of NMDA-induced nociceptive behaviors by exogenous D-serine, the selective nNOS inhibitor, 7-nitroindazole (7-NI, 200 nmol) was administrated before D-serine (500 nmol). The facilitation of NMDA-induced nociceptive behaviors by D-serine was significantly reduced by pretreatment with 7-NI as compared with that of the vehicle-treated group (Fig. 2-2B; **P* < 0.05 v.s. VEH+VEH treated group, #*P* < 0.05 v.s. VEH+NMDA treated group, ‡*P* < 0.05 v.s. D-ser+NMDA treated group). The quantification of nitric oxide (NO) metabolites in biological samples provides valuable information with regards to *in vivo* NO production, bioavailability and metabolism. Here total NO levels were measured using a nitric oxide detection kit that measures nitrate in the spinal cord dorsal horn and the results are illustrated in figure 2-2C. D-serine (500 nmol) significantly increased total NO levels as compared with that of the vehicle-treated group, and this increase was suppressed by pretreatment with 7-NI (Fig. 2-2C; **P* < 0.05 v.s. VEH+VEH treated group, #*P* < 0.05 v.s. VEH+D-ser treated group). These results demonstrate D-serine's facilitation of NMDA-induced nociceptive behaviors is mediated in large part by nNOS activation.

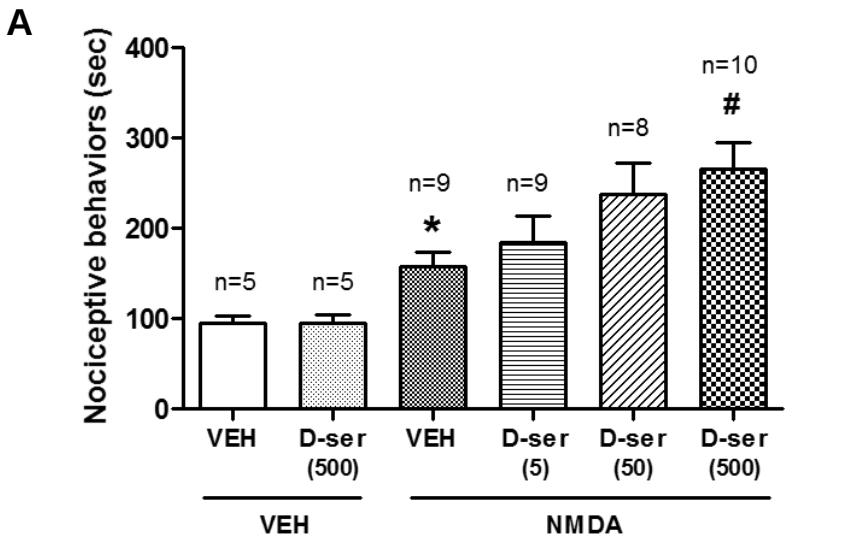
A
Nociceptive behaviors (sec)
400
300
200
100
0
n=5
n=5
n=9
*
n=9
n=8
n=10
#
VEH
D-ser (500)
VEH
D-ser (5)
D-ser (50)
D-ser (500)
VEH
NMDA

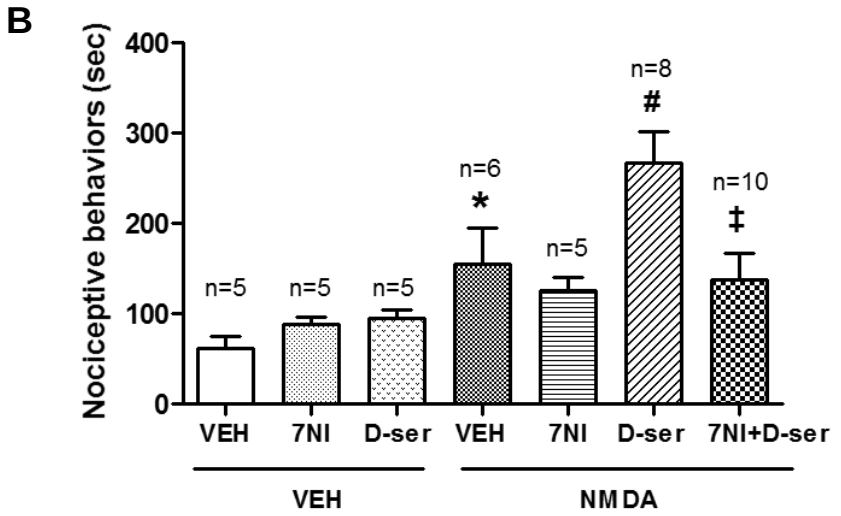
B
Nociceptive behaviors (sec)
400
300
200
100
0
n=5
n=5
n=5
n=6
*
n=5
n=8
#
n=10
‡
VEH
7NI
D-ser
VEH
7NI
D-ser
7NI+D-ser
VEH
NMDA

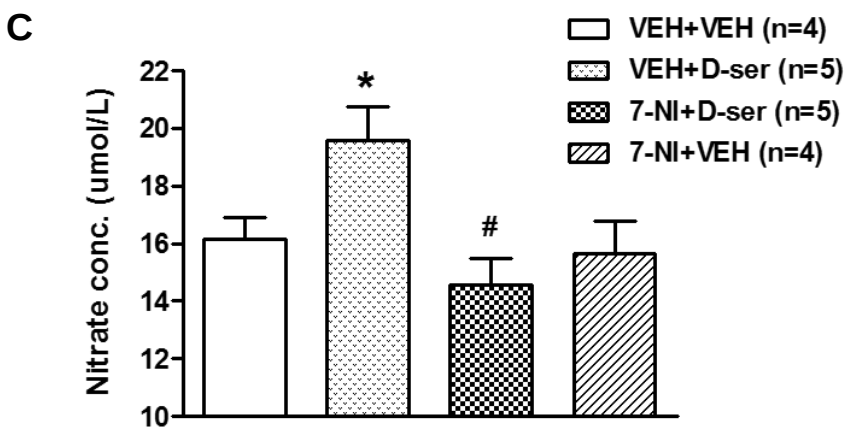
C
Nitrate conc. (umol/L)
22
20
18
16
14
12
10
*
#
VEH+VEH (n=4)
VEH+D-ser (n=5)
7-NI+D-ser (n=5)
7-NI+VEH (n=4)

Figure 2-2. Graphs illustrating the effects of i.t. administration of exogenous D-serine (D-ser, at three different doses: 5, 50 and 500 nmol) on NMDA-induced nociceptive behaviors in naïve mice (A) and in mice pretreated with the selective nNOS inhibitor, 7-nitroindazole (7-NI, 200 nmol) 10 min before i.t. treatment with exogenous D-serine (D-ser, 500 nmol) (B) and the effect of D-serine (D-ser, 500 nmol) on the concentration of NO (measured as nitrate) in the spinal cord dorsal horns (C). (A and B) Note that the 500 nmol dose of exogenous D-serine significantly increased NMDA-induced nociceptive behaviors. Pretreatment with 7-NI reduced the D-serine-induced increase in NMDA-induced nociceptive behaviors. **P* < 0.05 v.s. VEH+VEH treated group; #*P* < 0.05 v.s. VEH+NMDA treated group; ‡*P* < 0.05 v.s. D-ser+NMDA treated group. n = 5–10 mice / group. (C) The D-serine-induced increase in total NO concentration in the dorsal horns was significantly suppressed by pretreatment with 7-NI. **P* < 0.05 v.s. VEH+VEH treated group; #*P* < 0.05 v.s. VEH+D-ser treated group. n = 4–5 mice / group.

3. Effect of i.t. pretreatment with 7-NI on the D-serine-induced increase in pGluN1 expression in the spinal cord dorsal horn

To investigate whether the exogenous D-serine potentiates NMDA receptors activity, the expression of the PKC-dependent (Ser896) and PKA-dependent (Ser897) pGluN1 as well as the total protein expression of GluN1 was examined using a Western blot analysis. Intrathecal administration of D-serine (500 nmol) significantly increased PKC-dependent pGluN1 expression in the spinal cord dorsal horn at the 30 min post-injection time point (Fig. 2-3A; $*P < 0.05$ v.s. VEH+VEH treated group). Pretreatment with the selective nNOS inhibitor, 7-nitroindazole (7-NI, 200 nmol) completely suppressed this D-serine-induced increase in PKC-dependent pGluN1 expression ($\#\#P < 0.01$ v.s. VEH+D-ser treated group). By contrast, neither D-serine nor 7-NI pretreatment had an effect on PKA-dependent pGluN1 or total GluN1 expression (Fig. 2-3A). The i.t. administration of 7-NI alone (7-NI+VEH), in the absence of D-serine, did not affect pGluN1 nor total GluN1 expression in comparison to the vehicle-treated group (VEH+VEH).

In addition, i.t. pretreatment with the PKC inhibitor, chelerythrine (CHE, 1 nmol) significantly reduced D-serine's increase in NMDA-induced nociceptive behaviors (Fig. 2-3B; $**P < 0.01$ v.s. VEH+NMDA treated group, $\#\#P < 0.01$ v.s. D-ser+NMDA treated group). However, i.t. pretreatment with the PKA inhibitor, PKI 14-22 amide (PKI, 2 nmol) had no effect on D-serine's enhancing effect on NMDA-induced nociceptive behaviors. These results suggest that D-serine increases the PKC-dependent phosphorylation of GluN1, which contributes to the potentiation of NMDA receptor function leading to facilitation of nociceptive behaviors following i.t. NMDA administration.

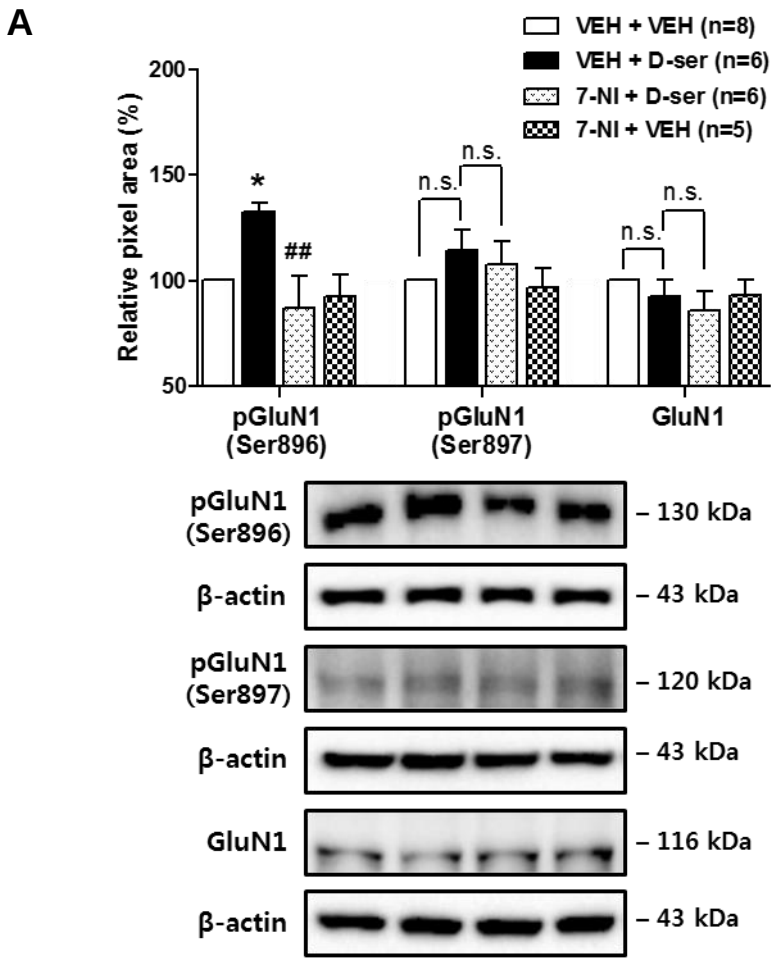
A
VEH + VEH (n=8)
VEH + D-ser (n=6)
7-NI + D-ser (n=6)
7-NI + VEH (n=5)
Relative pixel area (%)
200
150
100
50
*
##
n.s.
n.s.
n.s.
n.s.
pGluN1 (Ser896)
pGluN1 (Ser897)
GluN1
pGluN1 (Ser896)
– 130 kDa
β-actin
– 43 kDa
pGluN1 (Ser897)
– 120 kDa
β-actin
– 43 kDa
GluN1
– 116 kDa
β-actin
– 43 kDa

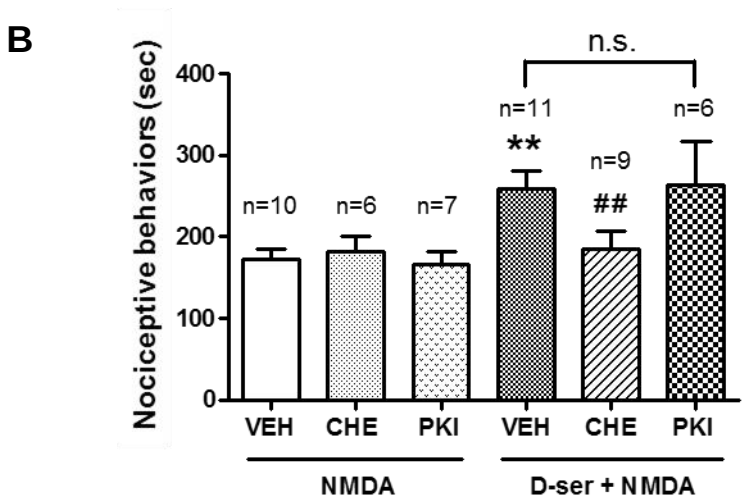
B
Nociceptive behaviors (sec)
400
300
200
100
0
n.s.
n=11
n=6
**
n=9
##
n=10
n=6
n=7
VEH
CHE
PKI
VEH
CHE
PKI
NMDA
D-ser + NMDA

Figure 2-3. Western blot analysis illustrating the effect of i.t. administration with the selective nNOS inhibitor, 7-nitroindazole (7-NI, 200 nmol) administered 10 min before i.t. treatment with D-serine (D-ser, 500 nmol) on the expression of PKC- and PKA-dependent pGluN1 and on the total protein expression of GluN1 in the lumbar spinal cord dorsal horn (A) and a graph illustrating the effect of i.t. administration of the PKC inhibitor, chelerythrine (CHE, 1 nmol) or the PKA inhibitor, PKI 14-22 amide (PKI, 2 nmol) administered 10 min before i.t. treatment with D-serine (D-ser, 500 nmol) on NMDA-induced nociceptive behaviors (B). (A) A graph depicting the changes in the pGluN1 and GluN1 is shown in the upper portion, and representative Western blot bands for pGluN1 and GluN1 expression are presented in the lower portion. Exogenous D-serine (VEH+D-ser) increased PKC-dependent pGluN1 expression at the Ser896 site and this increase was significantly attenuated by 7-NI pretreatment (7-NI+D-ser). However, i.t. exogenous D-serine had no effect on PKA-dependent pGluN1 at the Ser897 site or total GluN1 expression. *P < 0.05 v.s. VEH+VEH treated group; ##P < 0.01 v.s. VEH+D-ser treated group; n.s., no significance. n = 5–8 mice / group. (B) Pretreatment with CHE suppressed the increase in NMDA-induced nociceptive behaviors induced by D-serine administration, whereas PKI had no effect on the facilitatory effect of D-serine. **P < 0.01 v.s. VEH+NMDA treated group; ##P < 0.01 v.s. D-ser+NMDA treated group; n.s., no significance. n = 6–11 mice / group.

4. Effect of i.t. administration of LSOS or DAAO on neuropathic pain and the expression of spinal pGluN1 and GluN1 in CCI mice

To further confirm the potential role of D-serine on the development of neuropathic pain and increased NMDA receptor function, the Srr inhibitor, LSOS or the D-serine degrading enzyme, DAAO was intrathecally injected twice a day on post-operative days 0-3 (during the induction phase) in CCI mice. Repeated daily administration of LSOS (10 nmol) or DAAO (0.1 U) over this three-day period significantly attenuated the CCI-induced development of MA as compared with that of vehicle-treated mice (Fig. 2-4A; ***P < 0.001 v.s. VEH treated group on day 0, ###P < 0.001 v.s. VEH treated group on day 3). On the other hand repeated administration of DAAO or LSOS had no effect on TH (Fig. 2-4B; ***P < 0.001 v.s. VEH treated group on day 0) as previously reported (Moon et al., 2015). In addition, repeated daily administration of LSOS or DAAO significantly reduced the CCI-induced increase in expression of PKC-dependent pGluN1, but not the increase in GluN1 expression as compared to vehicle-treated CCI mice (Fig. 2-4C; *P < 0.05, **P < 0.01 v.s. Sham group, ##P < 0.01 v.s. VEH treated group). These results demonstrate that spinal D-serine modulates both CCI-induced MA and the CCI-induced increase in spinal PKC-dependent pGluN1 expression, but not CCI-induced TH or the overall increase in GluN1 expression.

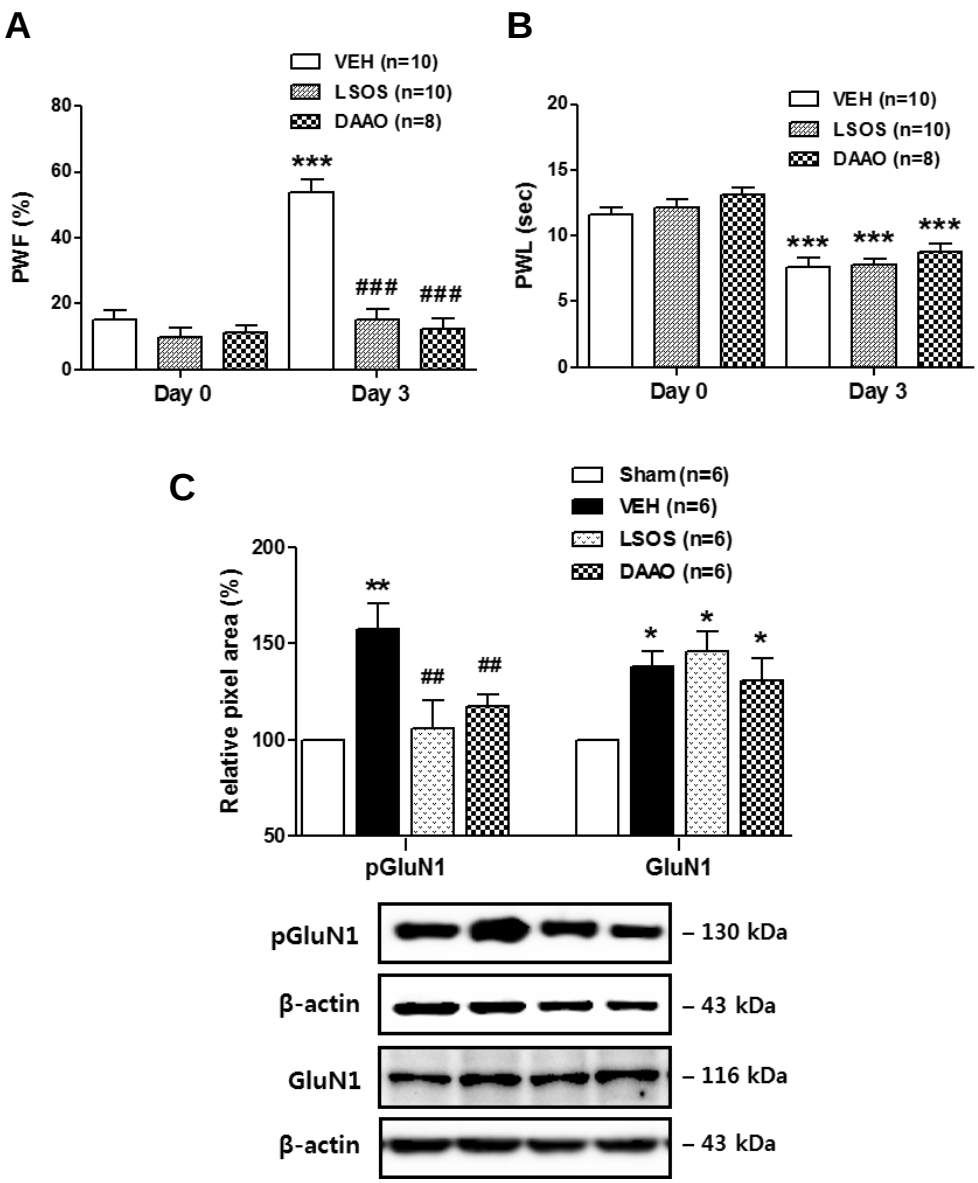
A
VEH (n=10)
LSOS (n=10)
DAAO (n=8)
PWF (%)
80
60
40
20
0
***
###
###
Day 0
Day 3
B
VEH (n=10)
LSOS (n=10)
DAAO (n=8)
PWL (sec)
20
15
10
5
0
***
***
***
Day 0
Day 3
C
Sham (n=6)
VEH (n=6)
LSOS (n=6)
DAAO (n=6)
Relative pixel area (%)
200
150
100
50
**
##
##
*
*
*
pGluN1
GluN1
pGluN1
– 130 kDa
β-actin
– 43 kDa
GluN1
– 116 kDa
β-actin
– 43 kDa

Figure 2-4. Graphs illustrating the effect of i.t. administration of the Srr inhibitor, LSOS (10 nmol) or the D-serine degrading enzyme, DAAO (0.1 U) on the development of CCI-induced MA (A) and TH (B) and the expression of PKC-dependent (Ser896) pGluN1 and GluN1 (C) in mice with neuropathic pain. (A) Repeated daily administration of LSOS or DAAO on postoperative days 0-3 blocked the increase in paw withdrawal frequency (PWF, %) that occurred in vehicle-treated CCI mice (VEH). ***P < 0.001 v.s. VEH treated group on day 0; ###P < 0.001 v.s. VEH treated group on day 3. n = 8–10 mice / group. (B) Conversely, the decrease in paw withdrawal latency (PWL, sec) to heat stimuli was unaffected by repeated i.t. injection with LSOS or DAAO. ***P < 0.001 v.s. the same group on day 0. n = 8–10 mice / group. (C) Western blot analysis illustrating the effect of i.t. administration of LSOS or DAAO on pGluN1 and GluN1 expression in the lumbar spinal cord dorsal horn. A graph depicting the changes in the pGluN1 and GluN1 is shown in the upper portion, and representative Western blot bands for pGluN1 and GluN1 expression are presented in the lower portion. I.t. administration of either LSOS or DAAO significantly decreased the level of CCI-induced PKC-dependent pGluN1 expression as compared with the vehicle-treated group (VEH). However, the CCI-induced increase in GluN1 expression was unaffected by repeated i.t. injection of LSOS or DAAO. *P < 0.05, **P < 0.01 v.s. Sham group; ##P < 0.01 v.s. VEH treated group. n = 6 mice / group.

5. Effect of coadministration of D-serine and BD1047 on neuropathic pain and the expression of spinal pGluN1 and GluN1 in CCI mice

To test the hypothesis that D-serine is a downstream effector of Sig-1R activation and contributes to increased NMDA receptor function and the development of neuropathic pain, spinal Sig-1Rs were blocked with a Sig-1R antagonist, while coadministering the putative downstream effector, D-serine to determine if the effect of Sig-1R stimulation could be reproduced. To do this exogenous D-serine was intrathecally injected in combination with, BD1047 on post-operative days 0-3 (b.i.d., during the induction phase) in CCI mice. BD1047 (100 nmol) administration significantly attenuated both the CCI-induced development of MA (Fig. 2-5A; ***P < 0.001 v.s. VEH treated group on day 0, ###P < 0.001 v.s. VEH treated group on day 3) and the increases in PKC-dependent pGluN1 and GluN1 expression (Fig. 2-5C; *P < 0.05, **P < 0.01 v.s. Sham group, #P < 0.05, ##P < 0.01 v.s. VEH treated group). Treatment with exogenous D-serine (500 nmol in combination with BD1047) reproduced the effect of Sig-1R activation in CCI mice by inducing MA (Fig. 2-5A; ‡‡‡P < 0.001 v.s. BD1047 treated group on day 3) and increasing PKC-dependent pGluN1 expression (Fig. 2-5C; ‡P < 0.05 v.s. BD1047 treated group). However, D-serine administration did not reproduce the effect of Sig-1R activation on the CCI-induced increase in GluN1 expression (Fig. 2-5C; #P < 0.05 v.s. VEH treated group). Conversely administration of BD1047 alone or in combination with D-serine did not affect the development of CCI-induced TH (Fig. 2-5B; **P < 0.01, ***P < 0.001 v.s. the same group on day 0). These results suggest that spinal D-serine is a downstream effector of Sig-1R activation and mediates Sig-1Rs' effects on both CCI-induced MA and CCI-induced PKC-dependent pGluN1 expression.

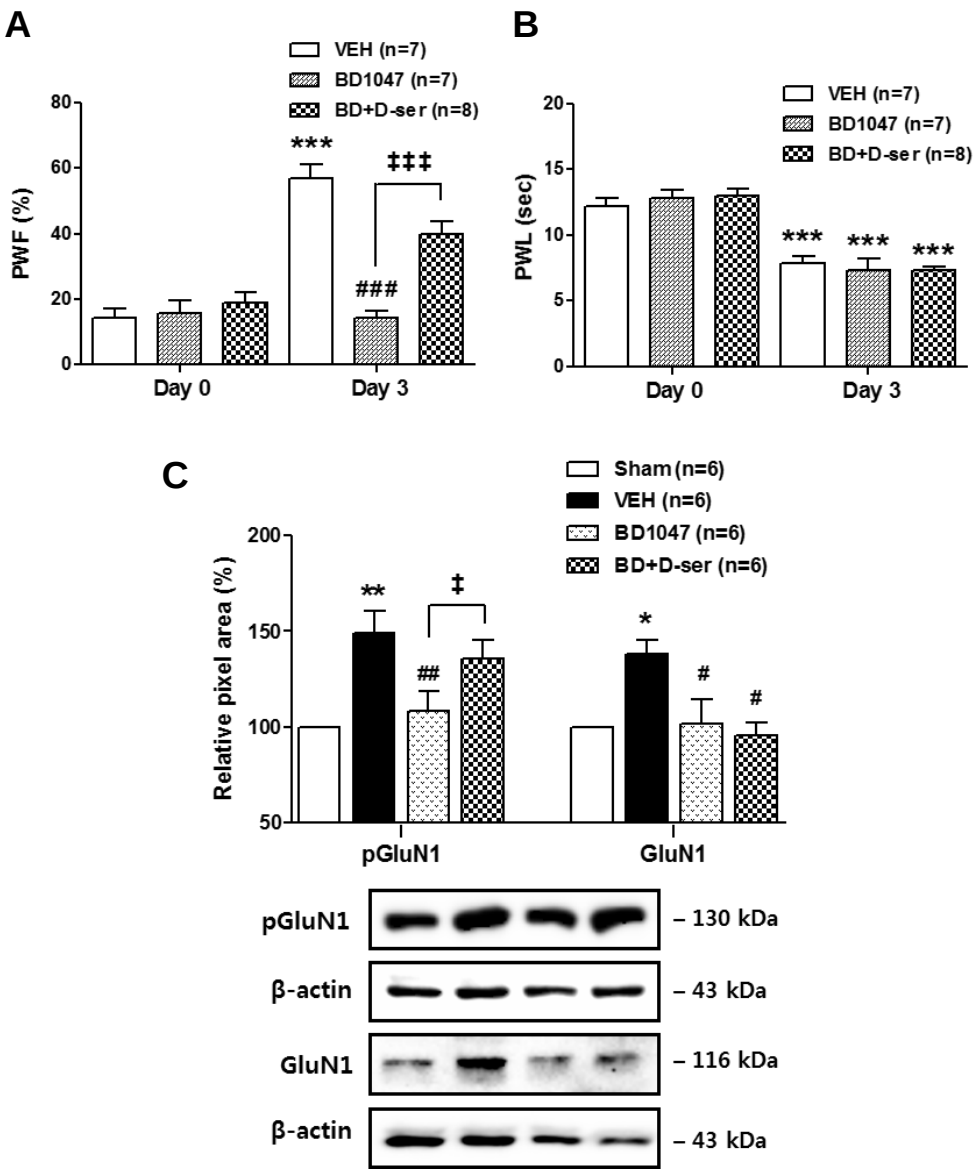
A
VEH (n=7)
BD1047 (n=7)
BD+D-ser (n=8)
PWF (%)
80
60
40
20
0
***
‡‡‡
###
Day 0
Day 3
B
VEH (n=7)
BD1047 (n=7)
BD+D-ser (n=8)
PWL (sec)
20
15
10
5
0
***
***
***
Day 0
Day 3
C
Sham (n=6)
VEH (n=6)
BD1047 (n=6)
BD+D-ser (n=6)
Relative pixel area (%)
200
150
100
50
**
‡
##
*
#
#
pGluN1
GluN1
pGluN1
– 130 kDa
β-actin
– 43 kDa
GluN1
– 116 kDa
β-actin
– 43 kDa

Figure 2-5. Graphs illustrating the effect of i.t. administration of exogenous D-serine (D-ser, 500 nmol) in combination of the Sig-1R antagonist, BD1047 (BD, 100 nmol) on the development of CCI-induced MA (A) and TH (B) and the expression of PKC-dependent (Ser896) pGluN1 and GluN1 (C) in mice with neuropathic pain. (A) Repeated daily administration with BD1047 on postoperative days 0-3 blocked the increase in paw withdrawal frequency (PWF, %) that occurred in vehicle-treated CCI mice (VEH). Treatment with exogenous D-serine in combination with BD1047 (BD+D-ser) restored the CCI-induced MA that was blocked by BD1047. ***P < 0.001 v.s. VEH treated group on day 0; ###P < 0.001 v.s. VEH treated group on day 3; ‡‡‡P < 0.001 v.s. BD1047 treated group on day 3. n = 7–8 mice / group. (B) Conversely, the decrease in paw withdrawal latency (PWL, sec) to heat stimuli was unaffected by repeated i.t. injection of BD1047 alone or in combination with D-serine. ***P < 0.001 v.s. the same group on day 0. n = 7–8 mice / group. (C) A graph depicting the changes in the pGluN1 and GluN1 is shown in the upper portion, and representative Western blot bands illustrating pGluN1 and GluN1 expression are presented in the lower portion. I.t. BD1047 administration significantly reduced the CCI-induced increase in PKC-dependent pGluN1 and GluN1 expression as compared with the vehicle-treated group (VEH). Treatment with exogenous D-serine in combination with BD1047 (BD+D-ser) restored the CCI-induced increase in pGluN1 expression that was originally blocked by BD1047 alone, while the decrease in GluN1 expression in the BD1047-treated group was unaffected by repeated i.t. injection with concomitant BD1047 and D-serine treatment. *P < 0.05, **P < 0.01 v.s. Sham group; #P < 0.05, ##P < 0.01 v.s. VEH treated group; ‡P < 0.05 v.s. BD1047 treated group. n = 6 mice / group.

6. Effect of i.t. administration of LSOS or DAAO on nNOS activation in CCI mice

To determine whether D-serine contributes to the activation of nNOS in CCI mice, LSOS or DAAO was intrathecally injected on post-operative days 0-3 (b.i.d., during the induction phase) in CCI mice and examined the ratio of phosphorylated nNOS to nNOS. Phosphorylation of nNOS (pnNOS) at serine 847 (Ser847) inhibits nNOS activity (Rameau et al., 2004; Roh et al., 2011). Because the total protein expression of nNOS does not change following sciatic nerve injury, a decrease in the ratio of pnNOS to nNOS is considered to reflect an increase in the active forms of nNOS. CCI-induced sciatic nerve injury significantly decreased the ratio of pnNOS to nNOS, and this decrease was restored by i.t. treatment with LSOS or DAAO (Fig. 2-6A; $*P < 0.05$ v.s. Sham group, $\#P < 0.05$ v.s. VEH treated group). Changes in spinal NOS activity and NO production were further confirmed by examining changes in NADPH-diaphorase staining (Morris et al., 1997) and nitrate concentration, respectively. CCI-induced sciatic nerve injury significantly increased the number of NADPH-diaphorase-positive cells in the superficial dorsal horn, and this increase was attenuated by both LSOS and DAAO treatment (Fig. 2-6B and C; $***P < 0.001$ v.s. Sham group, $\#\#\#P < 0.001$ v.s. VEH treated group). NADPH-diaphorase-positive cells were colocalized with both Fos- and NeuN-immunoreactivity, while there was no colocalization of NADPH-diaphorase staining with GFAP or Iba-1 immunostaining. CCI-induced sciatic nerve injury significantly increased total NO levels (measured as nitrate) as compared with that of the Sham group, and this increase was suppressed by treatment with LSOS or DAAO (Fig. 2-6E; $*P < 0.05$ v.s. Sham group, $\#P < 0.05$, $\#\#P < 0.01$ v.s. VEH treated group). These results indicate that D-serine modulates nNOS activity and NO concentrations in the spinal cord dorsal horn of CCI mice.

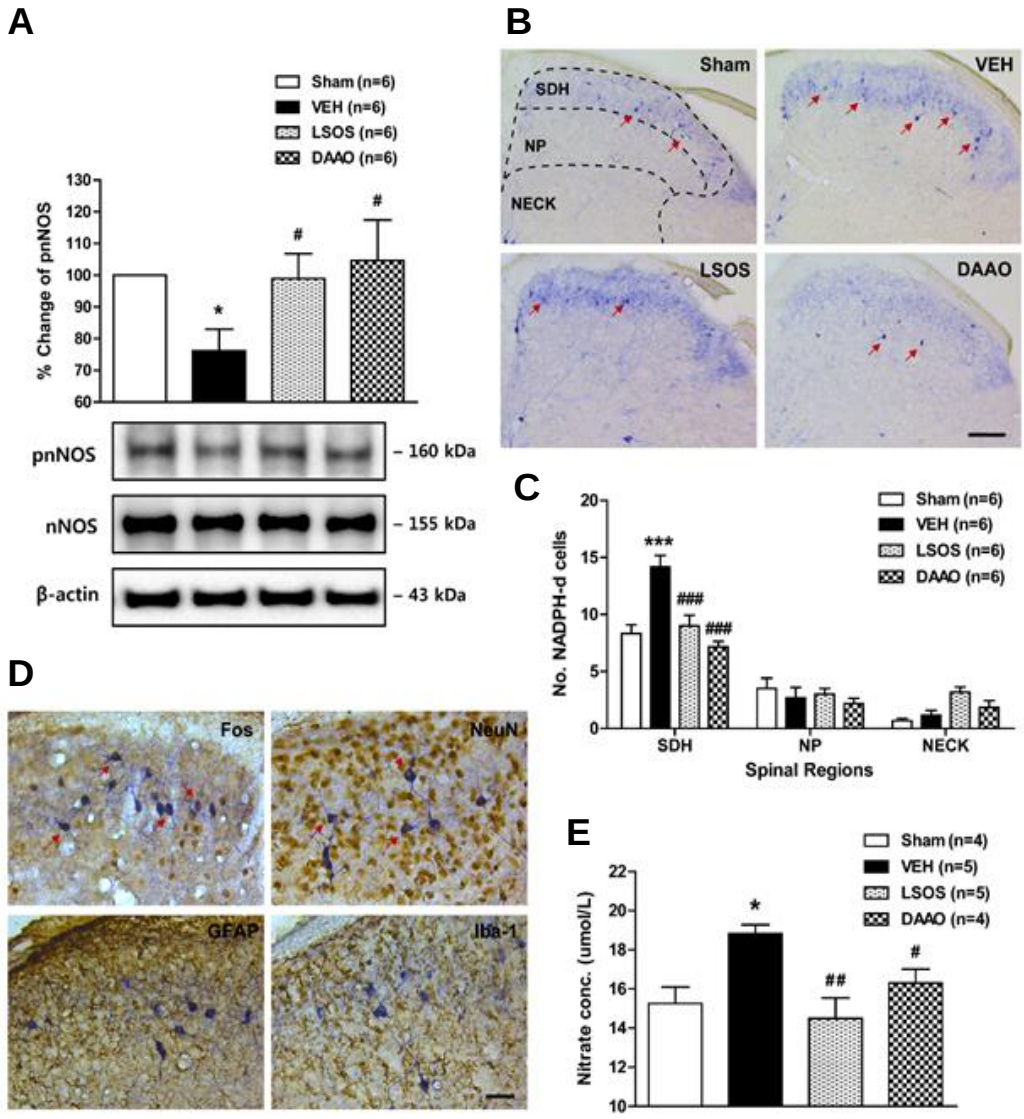
A
Sham (n=6)
VEH (n=6)
LSOS (n=6)
DAAO (n=6)
% Change of pnNOS
130
120
110
100
90
80
70
60
*
#
#
pnNOS
– 160 kDa
nNOS
– 155 kDa
β-actin
– 43 kDa
B
Sham
VEH
SDH
NP
NECK
LSOS
DAAO
C
Sham (n=6)
VEH (n=6)
LSOS (n=6)
DAAO (n=6)
No. NADPH-d cells
20
15
10
5
0
***
###
###
SDH
NP
NECK
Spinal Regions
D
Fos
NeuN
GFAP
Iba-1
E
Sham (n=4)
VEH (n=5)
LSOS (n=5)
DAAO (n=4)
Nitrate conc. (umol/L)
22
20
18
16
14
12
10
*
##
#

Figure 2-6. Western blot analysis (A), NADPH-diaphorase staining (B, C and D), and a graph of nitrate concentration (C) illustrating the effect of i.t. administration of the Srr inhibitor, LSOS (10 nmol) or the D-serine degrading enzyme, DAAO (0.1 U) on nNOS activation and total NO concentration in the lumbar spinal cord dorsal horn in mice with chronic constriction injury (CCI)-induced neuropathic pain. (A) A graph depicting the % change in the ratio of pnNOS/nNOS is shown in the upper portion, and representative Western blot bands for pnNOS and nNOS expression are illustrated in the lower portion. **P* < 0.05 v.s. Sham group; #*P* < 0.05 v.s. VEH treated group. n = 6 mice / group. (B and C) The black dotted lines in the first panel depict the location of each of the three regions analysed in the spinal cord dorsal horn: the superficial dorsal horn (SDH, lamina I-II), the nucleus proprius (NP, lamina III-IV) and the neck region (NECK, lamina V-VI). Arrows indicate representative NADPH-diaphorase-positive cells. ****P* < 0.001 v.s. Sham group; ###*P* < 0.001 v.s. VEH treated group. n = 6 mice / group. Scale bar = 100 μm. (D) Photomicrographs show the colocalization of c-Fos (brown) or NeuN (a marker of neuron, brown) with NADPH-diaphorase positive staining (purple) in the spinal cord dorsal horn. There was no colocalization of NADPH-diaphorase staining with GFAP (a marker of astrocyte, brown) or Iba-1 (a marker of microglia, brown). Scale bar = 25 μm. (E) The CCI-induced increase in total NO concentration (measured indirectly as the concentration of its stable decomposition product nitrate) in the ipsilateral spinal cord dorsal horns was significantly reduced by treatment with LSOS or DAAO. **P* < 0.05 v.s. Sham group; #*P* < 0.05, ##*P* < 0.01 v.s. VEH treated group. n = 4–5 mice / group.

7. Effect of coadministration of D-serine and fluorocitrate on neuropathic pain in CCI mice

To test the hypothesis that D-serine released from astrocytes contributes to the development of neuropathic pain, spinal astrocytes were inhibited by administration of an astrocyte metabolic inhibitor, while coadministering the putative downstream effector, D-serine. To accomplish this exogenous D-serine was intrathecally injected in combination with, fluorocitrate (FC) on post-operative days 0-3 (b.i.d., during the induction phase) in CCI mice. FC (0.03 nmol) administration alone significantly attenuated the CCI-induced development of MA (Fig. 2-7A; ***P < 0.001 v.s. VEH treated group on day 0, ###P < 0.001 v.s. VEH treated group on day 3). Treatment with exogenous D-serine (500 nmol in combination with FC) reversed the effect of FC alone and reproduced the effect of astrocyte activation in CCI mice by inducing MA (Fig. 2-7A; ‡‡P < 0.01 v.s. FC treated group on day 3). Conversely administration of FC alone or in combination with D-serine had no effect on the development of CCI-induced TH (Fig. 2-7B; ***P < 0.001 v.s. the same group on day 0). Next, in order to determine whether nNOS activation and the concomitant NO signaling cascade contribute to this D-serine-induced restoration of MA in FC treated mice, 7-NI or ODQ was intrathecally injected on post-operative day 3 in FC and D-serine co-treated mice. Intrathecal administration of 7-NI (200 nmol) or ODQ (300 pmol) at day 3 post-surgery significantly attenuated CCI-induced MA as compared with vehicle-treated mice (Fig. 2-7C; *P < 0.05, **P < 0.01 v.s. VEH treated group). These results suggest that activated spinal astrocytes release D-serine, which in turn mediates CCI-induced MA via an nNOS/sGC signaling pathway.

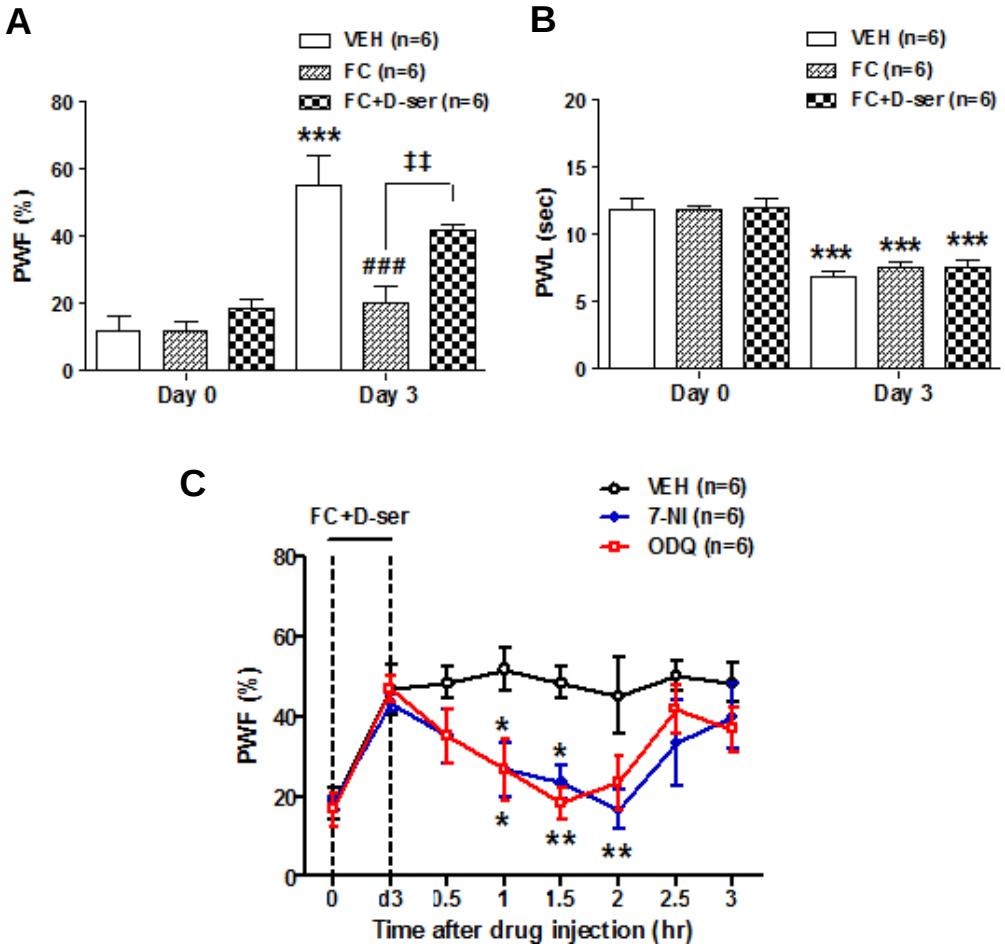
A
VEH (n=6)
FC (n=6)
FC+D-ser (n=6)
PWF (%)
80
60
40
20
0
***
‡‡
###
Day 0
Day 3
B
VEH (n=6)
FC (n=6)
FC+D-ser (n=6)
PWL (sec)
20
15
10
5
0
***
***
***
Day 0
Day 3
C
VEH (n=6)
7-NI (n=6)
ODQ (n=6)
FC+D-ser
PWF (%)
80
60
40
20
0
*
*
*
**
**
0
d3
0.5
1
1.5
2
2.5
3
Time after drug injection (hr)

Figure 2-7. Graphs illustrating the effect of i.t. administration of exogenous D-serine (D-ser, 500 nmol) in combination with the astrocyte metabolic inhibitor, fluorocitrate (FC, 0.03 nmol) on the development of CCI-induced MA (A) and TH (B) and the effect of nNOS or sGC inhibition on CCI-induced MA in FC and D-serine co-treated mice (C). (A) Repeated daily administration with FC on postoperative days 0-3 blocked the CCI-induced increase in paw withdrawal frequency (PWF, %) that occurred in vehicle-treated CCI mice (VEH). Treatment with exogenous D-serine in combination with FC (FC+D-ser) restored this CCI-induced MA that was blocked by FC indicating that D-serine is a downstream effector of astrocyte activation in CCI mice. ***P < 0.001 v.s. VEH treated group on day 0; ###P < 0.001 v.s. VEH treated group on day 3; ‡‡P < 0.01 v.s. FC treated group on day 3. n = 6 mice / group. (B) Conversely, the decrease in paw withdrawal latency (PWL, sec) to heat stimuli was unaffected by repeated i.t. injection of FC alone or in combination with D-serine. ***P < 0.001 v.s. the same group on day 0. n = 6 mice / group. (C) Intrathecal administration with 7-NI (200 nmol) or ODQ (300 pmol) at day 3 post-surgery attenuated CCI-induced MA in FC and D-serine co-treated mice. *P < 0.05, **P < 0.01 v.s. VEH treated group. n = 6 mice / group.

8. Effect of i.t. administration of 7-NI or ODQ or chelerythrine on neuropathic pain and the expression of spinal pGluN1 and GluN1 in CCI mice

To further determine whether nNOS, soluble guanylyl cyclase (sGC, a primary biological target for NO) and PKC activation contribute to the development of neuropathic pain, 7-NI, ODQ or chelerythrine (CHE) was intrathecally injected on post-operative days 0-3 (b.i.d., during the induction phase) in CCI mice. Administration of 7-NI (200 nmol), ODQ (300 pmol) or CHE (1 nmol) significantly reduced the development of MA as compared to vehicle-treated CCI mice (Fig. 2-8A; ***P < 0.001 v.s. VEH treated group on day 0, ###P < 0.001 v.s. VEH treated group on day 3). Conversely 7-NI, ODQ or CHE treatment had no effect on the development of TH in CCI mice (Fig. 2-8B; ***P < 0.001 v.s. the same group on day 0). In addition, administration of 7-NI, ODQ or CHE significantly reduced the CCI-induced increase in PKC-dependent pGluN1 expression, but not the increase in GluN1 expression as compared with the vehicle-treated group (Fig. 2-8C; *P < 0.05 v.s. Sham group, #P < 0.05 v.s. VEH treated group). These results strongly suggest that spinal nNOS/sGC signaling and PKC activation mediate the development of CCI-induced MA and the potentiation of NMDAR function via increases in PKC-dependent pGluN1 expression. On the other hand the nNOS/sGC pathway and PKC activation do not appear to be involved with CCI-induced TH and the associated increase in GluN1 expression.

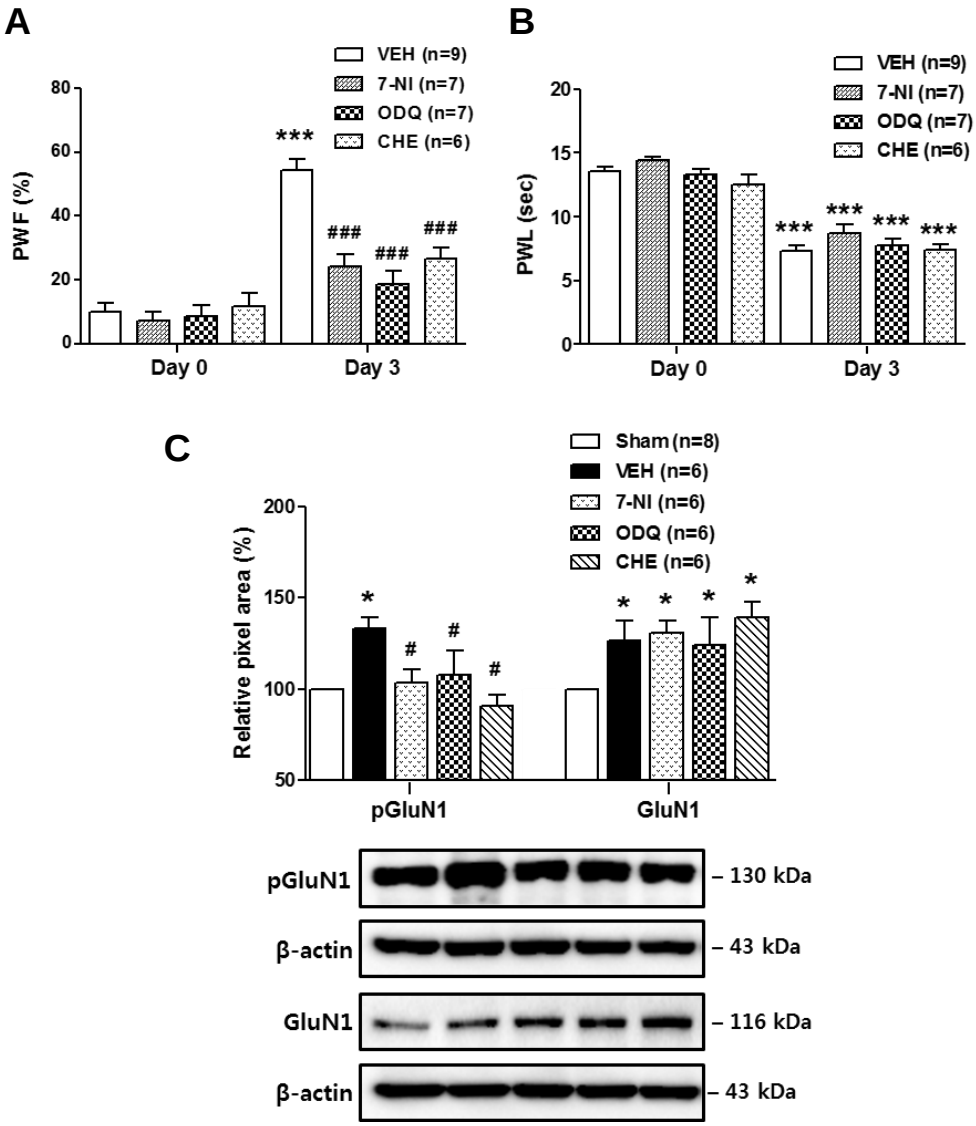
A
VEH (n=9)
7-NI (n=7)
ODQ (n=7)
CHE (n=6)
PWF (%)
80
60
40
20
0
***
###
###
###
Day 0
Day 3
B
VEH (n=9)
7-NI (n=7)
ODQ (n=7)
CHE (n=6)
PWL (sec)
20
15
10
5
0
***
***
***
***
Day 0
Day 3
C
Sham (n=8)
VEH (n=6)
7-NI (n=6)
ODQ (n=6)
CHE (n=6)
Relative pixel area (%)
200
150
100
50
*
#
#
#
*
*
*
*
pGluN1
GluN1
pGluN1
– 130 kDa
β-actin
– 43 kDa
GluN1
– 116 kDa
β-actin
– 43 kDa

Figure 2-8. Graphs illustrating the effect of i.t. administration of the selective nNOS inhibitor, 7-NI (200 nmol), the sGC inhibitor, ODQ (300 pmol) or the PKC inhibitor, CHE (1 nmol) on the development of CCI-induced MA (A) and TH (B) and expression of PKC-dependent (Ser896) pGluN1 and GluN1 (C) in mice with neuropathic pain. (A) Repeated daily 7-NI, ODQ or CHE administration on postoperative days 0-3 blocked the increase in paw withdrawal frequency (PWF, %) that occurred in vehicle-treated CCI mice (VEH). ***$P < 0.001$ v.s. the same group on day 0; ###$P < 0.001$ v.s. VEH treated group on day 3. n = 6–9 mice / group. (B) However, the decrease in paw withdrawal latency (PWL, sec) to heat stimuli was unaffected by repeated i.t. 7-NI, ODQ or CHE injection. ***$P < 0.001$ v.s. the same group on day 0. n = 6–9 mice / group. (C) Western blot analysis illustrating the effect of i.t. 7-NI, ODQ or CHE administration on pGluN1 and GluN1 expression in the lumbar spinal cord dorsal horn. A graph depicting the changes in the pGluN1 and GluN1 is shown in the upper portion, and representative Western blot bands illustrating pGluN1 and GluN1 expression are presented in the lower portion. I.t. 7-NI, ODQ or CHE administration significantly decreased the level of CCI-induced PKC-dependent pGluN1 expression as compared with the vehicle-treated group (VEH). However, the CCI-induced increase in GluN1 expression was unaffected by repeated i.t. 7-NI, ODQ or CHE injection. *$P < 0.05$ v.s. Sham group; #$P < 0.05$ v.s. VEH treated group. n = 6–8 mice / group.

DISCUSSION

D-serine is an endogenous co-agonist for the glycine site on the GluN1 subunit of the NMDA receptor (NMDAR) and is now thought to be closely involved in controlling NMDAR activation. NMDAR activation is known to be an essential contributor to the process of 'central sensitization', particularly to the early phosphorylation-dependent phase of central sensitization (Mothet *et al.*, 2000; Ultenius *et al.*, 2006). The present study is the first to demonstrate that intrathecal (i.t.) administration of exogenous D-serine facilitates NMDA-induced nociceptive behaviors. Our results further suggest that this occurs via an increase in PKC-dependent phosphorylation of the GluN1 subunit (pGluN1) at serine 896 site, which results in potentiation of NMDAR function and trafficking to the cell membrane (Raymond *et al.*, 1994; Ultenius *et al.*, 2006). Furthermore, repeated daily i.t. treatment with the serine racemase inhibitor, LSOS or the D-serine degrading enzyme, DAAO significantly reduced not only the development of CCI-induced MA, but also the CCI-induced increase in PKC-dependent pGluN1 expression in the dorsal horn. Collectively these results demonstrate that D-serine plays an important role in modulating the phosphorylation of the NMDAR GluN1 subunit, resulting in potentiation of NMDARs and ultimately contributing to the development of MA in neuropathic pain.

It has been suggested that direct activation of spinal Sig-1Rs increases the response to peripheral mechanical stimuli and potentiates NMDAR function via an increase in the phosphorylation of GluN1 in naïve mice (Kim *et al.*, 2008). Yoon et al. has further demonstrated that i.t. administration of the neurosteroid

dehydroepiandrosterone sulfate (DHEAS), an endogenous agonist of Sig-1Rs, facilitates NMDA-induced nociceptive behaviors via an increase in pGluN1 expression (Yoon *et al.*, 2010). In the present study, i.t. administration of the Sig-1R agonist, PRE084 increased NMDA-induced nociceptive behaviors, which were significantly reduced by pretreatment with DAAO or the astrocyte metabolic inhibitor, fluorocitrate. Based on these results, there is a possibility that the acute activation of spinal Sig-1Rs induced by either a Sig-1R agonist or an endogenous neurosteroid can enhance the release of D-serine from astrocytes and contribute to the increase in spinal pGluN1 and ultimately to the development of MA. In the present study, the inhibitory effect of the Sig-1R antagonist, BD1047 on pGluN1 expression in CCI mice is reversed by i.t. coadministration of exogenous D-serine. These results are consistent with our previous data demonstrating that Sig-1R activation significantly modulates spinal D-serine production in astrocytes via modulation of Srr expression (Moon *et al.*, 2015). Collectively these data provide strong evidence to support the hypothesis that D-serine is an important spinal mediator of the Sig-1R-induced facilitation of the NMDAR response.

The Sig-1R has been identified as a unique ligand-regulated molecular chaperone in the endoplasmic reticulum (ER) of cells. Sig-1Rs translocate from the ER to the plasma membrane where they modulate ligand-gated ion channels including the NMDAR (Su *et al*., 2010; Su *et al*., 2009). Pabba et al. reported that Sig-1R activation leads to an increased in the expression of GluN2 subunits, as well as trafficking of NMDARs to the cell surface in the rat hippocampus (Pabba *et al*., 2014). In addition, it has also been reported that high concentrations of Sig-1R ligands potentiate NMDAR responses by down-regulating small conductance calcium-activated K^+ (SK)

channels (Martina *et al*., 2007). Even though it has been reported that increased expression of Sig-1R occurs exclusively in astrocytes in the spinal cord of CCI mice in a previous study (Moon *et al*., 2014), the possibility exists that Sig-1Rs are not exclusively localized to astrocytes or that their distribution might change depending on a number of factors including the animal model, the type of pathophysiology, or the nervous system location being examined. Therefore, depending on a situation, Sig-1Rs could modulate NMDAR activation directly as a chaperone or they could interfere with the conformation or the availability of the D-serine binding site as it relates to the NMDAR.

Nitric oxide, which is synthesized by nNOS and iNOS in the spinal cord also plays an important role in central sensitization. The activity of nNOS is modulated by a number of diverse factors, but phosphorylation at the serine 847 site of nNOS significantly decreases the activity of this enzyme (Alderton *et al.*, 2001; Rameau *et al.*, 2004), since phosphorylation at this site interrupts the binding of the Ca^{2+}/calmodulin to nNOS, which is a critical step in the initiation of nNOS activation (Roman and Masters, 2006). In this regard, a decrease in the phosphorylated forms of nNOS at serine 847 is considered to represent an increase in the active forms of nNOS enzymes. Since the total amount of nNOS protein is not changed in the spinal cord dorsal horn of CCI mice at 3 days post-injury, the potential decrease in the ratio of pnNOS to nNOS expression was evaluated as an indicator of an increase in nNOS activation. Changes in NADPH-diaphorase staining in the spinal cord dorsal horn was further evaluated as an indirect measure of NOS activity as previously reported (Morris *et al.*, 1997). In the present study, peripheral nerve injury significantly decreased the ratio of pnNOS to nNOS expression and also increased both the number

of NADPH-diaphorase-positive neurons and total NO concentration in the spinal cord dorsal horn. Since these CCI-induced changes were totally blocked by the repeated daily administration of LSOS or DAAO, this suggests that D-serine is involved in this NO-mediated process. In this regard NMDAR activation increases Ca^{2+} influx, which is an important factor in the activation of calcineurin, a phosphatase that catalyzes the dephosphorylation of nNOS and thus, D-serine-induced NMDAR activation could be linked to the modulation of nNOS activity. Activation of guanylyl cyclase appears to be the critical step in NO's role in the induction of central sensitization through increases in neuronal excitability (Bogdan, 2001) and D-serine may be one of several molecular switches that affect nNOS/NO signaling cascades that ultimately regulate NMDAR activation in the spinal cord dorsal horn.

In the present study, NO-sGC signaling was shown to modulate PKC-dependent pGluN1 expression in the spinal cord dorsal horn of CCI mice. Several reports have suggested that NO donors selectively activate the PKCα isoform in kidney cells and the PKCε isoform in the heart (Liang and Knox, 1999; Ping *et al.*, 1999). PKCα is a conventional subtype, which is Ca^{2+}- and diacylglycerol (DAG)-dependent, while PKCε is a novel subtype, which is Ca^{2+}-independent and DAG-dependent (Way *et al.*, 2000). Wright and coworkers (Wright *et al.*, 1996) reported that NO can modulate the activation of phospholipase C (PLC), an enzyme that synthesizes both DAG and IP_3, in response to external oxidant stress, and thus, it is plausible that PKCα and/or PKCε may be regulated by NO indirectly. In our previous study, both PKCα and PKCε isoforms are activated by Sig-1Rs activation and play critical roles in the Sig-1R-induced increases in pGluN1 and nociception (Roh *et al.*, 2008a; Roh *et al.*, 2010). Furthermore, there is converging evidence from several laboratories that the PKCγ

isoform is primarily associated with the production of MA after peripheral nerve injury (Malmberg AB *et al.*, 1997; Zou *et al.*, 2011). Since PKCγ immunoreactivity is confined to interneurons of the inner part of lamina II, where the positive NADPH-diaphorase staining exists, it is plausible that nNOS-induced NO modulates the PKCγ isoform regulating the integration process of noxious and non-noxious inputs to dorsal horn neurons, which contributes to the development of MA (Malmberg AB *et al.*, 1997). Based on these data, further research is needed to investigate the underlying mechanisms of NO-induced PKC activation. Moreover, i.t. administration of D-serine increased PKC-dependent pGluN1 expression via nNOS activation, while PKA-dependent pGluN1 was not affected by D-serine. These results imply that phosphorylation of NMDARs is regulated by the activation of PKC and/or PKA through different mechanisms.

Results of this study show that the CCI-induced increase in the total protein expression of the NMDAR GluN1 subunit is modulated by Sig-1Rs activation, but neither D-serine nor nNOS alters this increase in GluN1 expression. Based on work with primary cortical cultures, Lau and coworkers suggested that the transcription of GluN1 is regulated by PKA signaling via binding of the cAMP response element binding protein (CREB) to the endogenous GluN1 gene (Lau *et al.*, 2004). A recent study by Zhang and colleagues provided evidence that the translocation of CREB into nucleus (and thus activation of the CREB pathway) can be induced by methamphetamine activation of Sig-1Rs in primary rat astrocytes (Zhang *et al.*, 2015). Moreover, to generate functional NMDAR ion channel complexes, the NMDAR subunits must first be assembled in the ER and then released from the ER before trafficking to the cell surface. Sig-1Rs have been suggested to perform a chaperoning

function in the ER and to bind directly to the GluN1 subunit, likely modulating NMDAR trafficking and function (Balasuriya *et al.*, 2013; Su *et al.*, 2010). It has been shown that the activation of Sig-1Rs increase both PKC- and PKA-dependent pGluN1 expression in the spinal cord dorsal horn (Roh *et al.*, 2011), which has been suggested to serve as a novel control mechanism to suppress ER retention and facilitate surface expression of GluN1 (Scott *et al.*, 2003). Thus, it could be possible that the Sig-1Rs activation modulates GluN1 expression not only at the transcriptional level, but also at the post-translational level, through mechanisms that involve CREB and/or protein kinase pathways. However, the precise mechanisms involved will require further investigation.

It was found that inhibition of Sig-1Rs, D-serine or nNOS significantly suppressed the development of MA in neuropathic mice, but had no effect on CCI-induced TH in these animals. These results suggest that Sig-1R-induced D-serine and nNOS signaling in the spinal cord are more important factors in the development of CCI-induced MA but not TH. This is consistent with several reports suggesting that different mechanisms are associated with the development of MA versus TH (Bian *et al.*, 1998; Roh *et al.*, 2008b). In contrast, several studies have demonstrated that inhibition of NO signaling significantly attenuates TH in animal models of pain (Ferreira *et al.*, 1999; Handy and Moore, 1998), but this did not occur in our study. This discrepancy may be due to the difference in the animal models being examined and the different time course of nociception in each model, to the different behavioral assays used to evaluate nociception and/or to the nervous system location being examined. These differences require further investigation to clarify the role that NO plays in the development and maintenance of MA and TH in different models of pain.

The present study demonstrates that both D-serine and NO are downstream effectors of CCI-induced Sig-1R activation in the spinal cord and mediate Sig-1R effects on both CCI-induced PKC-dependent phosphorylation of the NMDAR GluN1 subunit and the development of CCI-induced MA. In this regard D-serine induces an increase in the nNOS/NO signaling cascade, which contributes to the enhancement of NMDA-induced nociceptive behaviors and the development of CCI-induced MA. Because spinal NMDARs play an important role in nociceptive processing and are implicated in central sensitization, this study opens interesting possibilities for further investigations into the mechanisms underlying Sig-1R-induced spinal pain transmission mediated by D-serine and more importantly for potential therapeutic use of both Sig-1R and D-serine antagonists to treat neuropathic pain conditions.

CHAPTER 3

The role of sigma-1 receptor-induced Nox2 activation in the development of neuropathic pain

Manuscript published in Pharmacol Res. 2013 Aug;74:56-67.

ABSTRACT

It has been demonstrated that spinal sigma-1 receptors (Sig-1Rs) mediate pain hypersensitivity in mice and neuropathic pain in rats. In this study, the role of NADPH oxidase 2 (Nox2)-induced reactive oxygen species (ROS) on Sig-1R-induced pain hypersensitivity and the induction of chronic neuropathic pain is examined. Neuropathic pain was produced by chronic constriction injury (CCI) of the right sciatic nerve in rats. Mechanical allodynia and thermal hyperalgesia were evaluated in mice and CCI-rats. Western blotting and dihydroethidium (DHE) staining were performed to assess the changes in Nox2 activation and ROS production in spinal cord, respectively. Direct activation of spinal Sig-1Rs with the Sig-1R agonist, PRE084 induced mechanical allodynia and thermal hyperalgesia, which were dose-dependently attenuated by pretreatment with the ROS scavenger, NAC or the Nox inhibitor, apocynin. PRE084 also induced an increase in Nox2 activation and ROS production, which were attenuated by pretreatment with the Sig-1R antagonist, BD1047 or apocynin. CCI-induced nerve injury produced an increase in Nox2 activation and ROS production in the spinal cord, all of which were attenuated by intrathecal administration with BD1047 during the induction phase of neuropathic pain. Furthermore, administration with BD1047 or apocynin reversed CCI-induced mechanical allodynia during the induction phase, but not the maintenance phase. These findings demonstrate that spinal Sig-1Rs modulate Nox2 activation and ROS production in the spinal cord, and ultimately contribute to the Sig-1R-induced pain hypersensitivity and the peripheral nerve injury-induced induction of chronic neuropathic pain.

INTRODUCTION

The sigma-1 receptors (Sig-1Rs) have been recognized as a unique ligand-operated receptor predominantly localized to the endoplasmic reticulum in cells of the nervous system and Sig-1Rs have been shown to play an important role in pain sensitization (Alonso et al., 2000; Maurice and Su, 2009; Su and Hayashi, 2003). It has been previously reported that intrathecal administration of a Sig-1R antagonist, BD1047 attenuates formalin-induced pain and chronic constriction injury (CCI)-induced induction of neuropathic pain (Kim et al., 2006; Roh et al., 2008b). This is consistent with data showing that Sig-1Rs are essential for capsaicin-induced and partial sciatic nerve injury-induced pain hypersensitivity using Sig-1R knockout mice (de la Puente et al., 2009; Entrena et al., 2009). Recently, it has been suggested that systemic administration of a new selective Sig-1R antagonist, S1RA also inhibits formalin-, capsaicin-, and sciatic nerve injury-induced pain hypersensitivity (Romero et al., 2012). In addition, it has been shown that direct activation of the spinal Sig-1R induces pain hypersensitivity, which involves calcium (Ca^{2+})-dependent second messenger cascades, including protein kinase C (PKC) activation, and PKC-dependent phosphorylation of the NMDA receptor GluN1 subunit (pGluN1) in spinal cord (Roh et al., 2011; Roh et al., 2008).

Reactive oxygen species (ROS) are molecules and ions of oxygen that have an unpaired electron, rendering them extremely reactive. Thus, they interact with a large number of molecules leading to alterations in the function of the target molecules (Bedard and Krause, 2007). ROS have been suggested as important modulators of persistent pain, including neuropathic and capsaicin-induced inflammatory pain, and they have also been implicated in NMDA receptor activation via enhancement of spinal pGluN1s, which is an essential step in central sensitization (Gao et al., 2007;

Kim et al., 2004; Schwartz et al., 2008). Recent studies suggest that NADPH oxidase (Nox) is the first identified enzyme system that generates ROS as its primary function and is also important during pain sensitization (Bedard and Krause, 2007; Kallenborn-Gerhardt et al., 2012). In mice lacking Nox1, nociceptive behavior induced by intraplantar injection of the carrageenan is significantly attenuated (Ibi et al., 2008). Nox2 expression in spinal microglia or Nox4 expression in peripheral nerves is increased after peripheral nerve injury, which contributes to the initiation or maintenance of the neuropathic pain, respectively (Kallenborn-Gerhardt et al., 2012; Kim et al., 2010).

Among several homologs of Nox identified so far, Nox2 activation can be induced by elevated intracellular Ca^{2+} concentration and the activation of Ca^{2+}-activated protein kinases, particularly PKC, which plays a critical role in Nox2 activation (Raad et al., 2009). As previously described, spinal Sig-1R activation modulates intracellular Ca^{2+} signaling by promoting the efflux of Ca^{2+} into the cytoplasm, leading to an increase in PKC activity, which results in potentiation of NMDA receptor function (Monnet, 2005; Roh et al., 2011; Roh et al., 2008). Although it has been documented that Sig-1R activation in the spinal cord mediates induction of the chronic neuropathic pain after peripheral nerve injury, there is limited understanding of the cellular mechanisms relating to Sig-1R-mediated pain facilitation. Moreover, it has been suggested that Nox2 activation is related to pain sensitization, but the receptor or upstream signaling involved in the modulation of spinal Nox2 activation is poorly understood, particularly in the case of nociceptive signaling. In this respect, the present study was focused on the potential role of spinal Nox2 activation in Sig-1R mediated pain facilitation.

The main purpose of this study was to investigate whether spinal Sig-1Rs

modulate Nox2 activation and the concomitant ROS production, ultimately leading to the induction of pain hypersensitivity in mice and chronic pain in a rat model of neuropathic pain. In this regard, it was examined whether: (1) direct activation of the spinal Sig-1R using the agonist, PRE084 in naïve mice induces Nox2 activation and ROS production; (2) pretreatment with the ROS scavenger, NAC or with the Nox inhibitor, apocynin reduces Sig-1R-induced pain hypersensitivity; (3) CCI in sciatic nerve induces spinal cord Nox2 activation and accompanying ROS production, which contributes to the CCI-induced increase in GluN1 phosphorylation and induction of the neuropathic pain in rats; and finally (4) these CCI-induced changes are inhibited by time-dependent administration of the Sig-1R antagonist, BD1047.

MATERIALS AND METHODS

Experimental animals

Male ICR mice (20-25 g) and Sprague-Dawley rats (180-200 g) were purchased from the Laboratory Animal Center of Seoul National University (Seoul, Republic of Korea). Maintaining condition is identical with those of Chapter 1.

Peripheral nerve injury model

Chronic constriction injury (CCI) of the right sciatic nerve in rats based on the method described by Bennett and Xie (1988). The right sciatic nerve of anesthetized rat was exposed at the mid-thigh level and four loose ligatures of 4-0 chromic gut were tied around the nerve and spaced apart from each other by 1.0- to 1.5-mm separations. In the sham group the sciatic nerve was exposed in the same manner, but without ligation of the nerve.

Drugs and i.t. administration

The following drugs were used: 2-(4-morpholinethyl)1-phenylcyclohexanecarboxylate (PRE084; 3 nmol), a sigma-1 receptor agonist; N-[2-(3,4-dichlorophenyl)ethyl]-N-methyl-2-(dimethylamino) ethylamine dihydro-bromide (BD1047; 100 nmol), a sigma-1 receptor antagonist; N-Acetyl-L-cysteine (NAC; 30, 100, 300 nmol), a ROS scavenger; 4′ -Hydroxy-3′ -methoxyacetophenone (apocynin; 10, 30, 100 nmol), a NADPH oxidase inhibitor; 7-nitroindazole (7-NI; 200 nmol), a specific nNOS inhibitor. PRE084 and BD1047 were supplied from Tocris Cookson Ltd. (Bristol, UK), and NAC, apocynin and 7-NI from Sigma–Aldrich (St. Louis, MO). The doses of PRE084, BD1047 and 7-NI were based on our previous

studies showing that these doses produce maximal effects with no detectable side-effects (Roh et al., 2011; Roh et al., 2008). The doses of NAC and apocynin were selected based on doses previously used in the literature (Doyle et al., 2010; MacFarlane et al., 2011). Apocynin was dissolved in 5% DMSO in physiological saline and 7-NI was dissolved in 5% DMSO in Corn oil. All drugs except apocynin and 7-NI were dissolved in physiological saline.

The procedure of i.t. drug administration was performed in unanesthetized naïve mice and CCI rats that were anesthetized with 3% isoflurane in a mixture of N_2O/O_2 gas according to the method described in Chapter 1. A 26-gauge needle was used in neuropathic rats. All drugs injected into mice were dissolved in 5 μl of vehicle and were administered 10 minutes before PRE084 injection. All drugs for rats were dissolved in 15 μl of vehicle and were administered twice a day on postoperative days 0-5 (the induction phase of neuropathic pain) or postoperative days 15-20 (the maintenance phase of neuropathic pain). The control groups received only vehicle injection.

Behavioral assessments

Experimental method for mechanical allodynia assay was identical with that of Chapter 1. The 0.16 g or 2.0 g von Frey filament was used for mice or rats, respectively. Thermal hyperalgesia was examined using a hot-plate apparatus in naive mice and a plantar analgesia meter in neuropathic rats as described in Chapter 1 and Chapter 2, respectively. Behavioral assessments in mice were performed before and at 30, 60, and 120 min after PRE084 (or vehicle) administration. Behavioral assessments in rats were performed before and at 1, 3, 4, and 5 days (induction phase) after CCI

surgery in one set of rats or before and at 5, 10, 15, 18, and 20 days (maintenance phase) after surgery in a second set of CCI rats.

Western blot assay

Animals were euthanized before or at 30, 60, or 120 min after PRE084 administration in mice and at 5 or 20 days after surgery in rats. Experimental procedures for collection of spinal cord are identical with those of Chapter 1. For preparation of Nox2 subunit p47phox membrane fraction, the right and left spinal dorsal horns in mice or ipsilateral spinal dorsal horn in rats were homogenized in lysis buffer (20mM Tris-HCl, 10mM EGTA, 2mM EDTA, pH 7.4, and proteinase inhibitors). Homogenates were centrifuged at 15,000 rpm for 40 min at 4℃ and, then, the pellet was re-suspended in lysis buffer containing 1% Triton X-100. For preparation of total proteins, the spinal dorsal horns were homogenized first in lysis buffer containing 1% Triton X-100. Homogenates were subsequently centrifuged using the same method as described above and the supernatant was used for Western blot analysis.

Spinal cord homogenates (25 - 35 μg protein) were separated and transferred to nitrocellulose membrane. The membranes were blocked with 5% skimmed milk for 1 h at RT and incubated at 4℃ overnight with a primary antibody specific for pan-cadherin (rabbit polyclonal anti-pan-cadherin antibody, 1:1k, cat# 10733, Santa Cruz Biotechnology Inc.), p47phox (rabbit polyclonal anti-p47phox antibody, 1:1k, cat# 14015, Santa Cruz Biotechnology Inc.), pGluN1 Ser896 (rabbit polyclonal anti-pGluN1 Ser896 antibody, 1:1k, cat# 06–640, Upstate Biotechnology.; this antibody is specific for rabbit GluN1 phosphorylated on serine 896), or β-actin (mouse

monoclonal anti-β-actin antibody, 1:2k, cat# 47778, Santa Cruz Biotechnology Inc.). After washing with TBST, membranes were incubated for 4 h with horseradish peroxidase (HRP)-conjugated anti-rabbit or anti-mouse antibody (1:10k, Santa Cruz Biotechnology Inc.).

Detection of in situ generation of ROS

To detect in situ generation of ROS in the spinal cord, dihydroethidium (DHE) staining was performed as previously described (Aoyama et al., 2008). Animals were euthanized before or at 30, 60, or 120 min after PRE084 injection in mice or at 5 days post-CCI surgery in rats. The lumbar spinal cord was collected and embedded in Tissue-Tek O.C.T. compound (Sakura Finetechnical Co.) and then frozen immediately in liquid nitrogen. Spinal cord segments were cut into 40 μm thick transverse sections and placed on a glass slide. DHE (1 nM, cat# D-1168; Invitrogen) was topically applied to each section and cover-slipped. Slides were incubated in a dark, humidified chamber at 37℃ for 30 min. DHE is oxidized by superoxide to ethidium bromide, which binds to the DNA and emits red fluorescence (Aoyama et al., 2008). The red fluorescence was detected through a 580 nm long-pass filter, using a fluorescence microscope (Zeiss Axioscope, Hallbergmoos, Germany) and digitally recorded with a cooled CCD camera (Micromax Kodak 1317; Princeton Instruments, AZ). For quantitative analysis of red fluorescence, spinal cord sections were analyzed according to the method described in Chapter 1.

Statistical analysis

The statistical analyzing methods are identical with those of Chapter 1.

RESULTS

1. Intrathecal PRE084 administration in mice induces mechanical allodynia, thermal hyperalgesia, and ROS production

The intrathecal administration of the Sig-1R agonist, PRE084 (PRE, 1, 3, or 10 nmol) dose-dependently increased the paw withdrawal frequency (PWF) to innocuous mechanical stimuli (mechanical allodynia) and decreased the paw withdrawal latency (PWL) to noxious heat stimuli (thermal hyperalgesia) at both the 30 and 60 min time points post-injection (Fig. 3-1A and B; $*P < 0.05$, $**P < 0.01$, $***P < 0.001$ vs. VEH treated group). In addition, dihydroethidium (DHE)-derived fluorescence was increased in the superficial dorsal horn (SDH, laminae I–II) at the 30 and 60 min time points after PRE084 (3 nmol, a dose selected because of its maximal effect on pain) administration (Fig. 3-1C and D; $*P < 0.05$, $***P < 0.001$ vs. 0min).

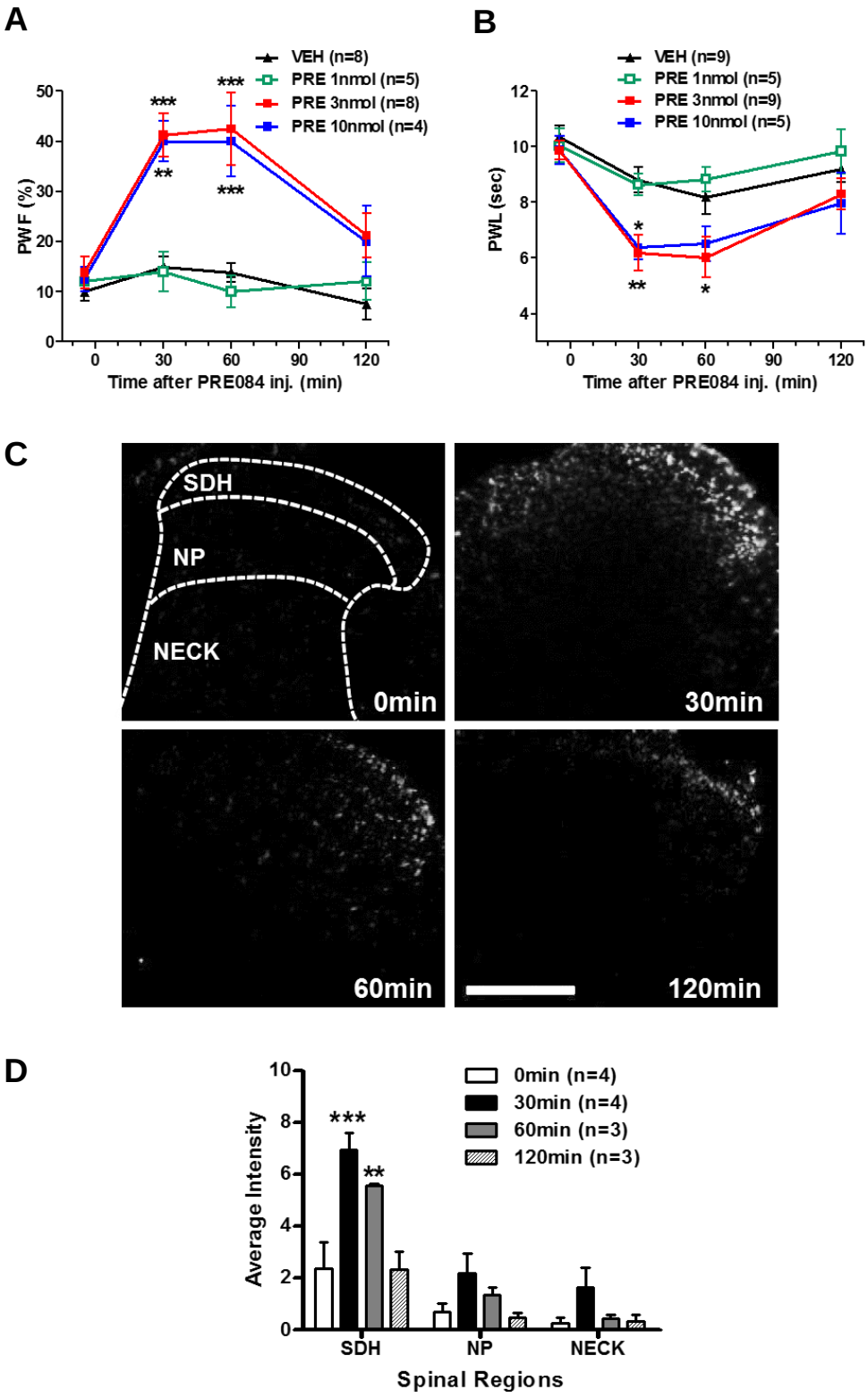
A
VEH (n=8)
PRE 1nmol (n=5)
PRE 3nmol (n=8)
PRE 10nmol (n=4)
PWF (%)
Time after PRE084 inj. (min)
B
VEH (n=9)
PRE 1nmol (n=5)
PRE 3nmol (n=9)
PRE 10nmol (n=5)
PWL (sec)
Time after PRE084 inj. (min)
C
SDH
NP
NECK
0min
30min
60min
120min
D
0min (n=4)
30min (n=4)
60min (n=3)
120min (n=3)
Average Intensity
SDH
NP
NECK
Spinal Regions

Figure 3-1. The effects of i.t. administration of the sigma-1 receptor agonist, PRE084 (PRE) on the induction of pain hypersensitivity (A and B) and ROS production (C and D) in mice. (A and B) Paw withdrawal frequency (PWF, %) and paw withdrawal latency (PWL, sec) were measured at 0, 30, 60, and 120 min after PRE (1, 3, or 10 nmol) injection using a von-Frey filament (0.16 g) and hot plate test (55±0.5℃), respectively. n = 4–9 mice / group. (C) Time course of ROS production in the lumbar spinal cord dorsal horn of the PRE (3 nmol)-treated mice was detected with dihydroethidium (DHE) staining. (D) Fluorescence intensity of DHE in the superficial dorsal horn (SDH, lamina I–II), nucleus proprius (NP, lamina III–IV), and neck region (NECK, lamina V–VI) of mice was quantitated using an image analysis system. The lumbar dorsal horn was sampled at 0, 30, 60, and 120 min after PRE injection. Scale bar = 200 μm. $*P < 0.05$, $**P < 0.01$, $***P < 0.001$ vs. VEH or 0min. n = 3–4 mice / group.

2. Intrathecal NAC or apocynin attenuates PRE084-induced mechanical allodynia and thermal hyperalgesia in mice

To determine whether the increased ROS production is involved in Sig-1Rs-induced pain hypersensitivity and the ROS are produced by NADPH oxidase (Nox) activation, the effects of the pretreatment with the ROS scavenger, NAC or the Nox inhibitor, apocynin on the PRE084-induced pain hypersensitivity were examined. Intrathecal pretreatment with NAC (30, 100, and 300 nmol) or apocynin (APO, 10, 30, and 100 nmol) dose-dependently suppressed PRE084 (3 nmol)-induced mechanical allodynia (Fig. 3-2A and B; ***P < 0.001 vs. VEH+VEH, #P < 0.05, ##P < 0.01, ###P < 0.001 vs. VEH+PRE). PRE084-induced thermal hyperalgesia was also ameliorated by pretreatment with NAC (300 nmol) or apocynin (100 nmol) (Fig. 3-2C and D; *P < 0.05, **P < 0.01 vs. VEH+VEH, #P < 0.05, ##P < 0.01 vs. VEH+PRE). The intrathecal injection of these inhibitors alone (NAC+VEH or APO+VEH), in the absence of PRE084, had no effect on PWF and PWL as compared with the VEH+VEH group.

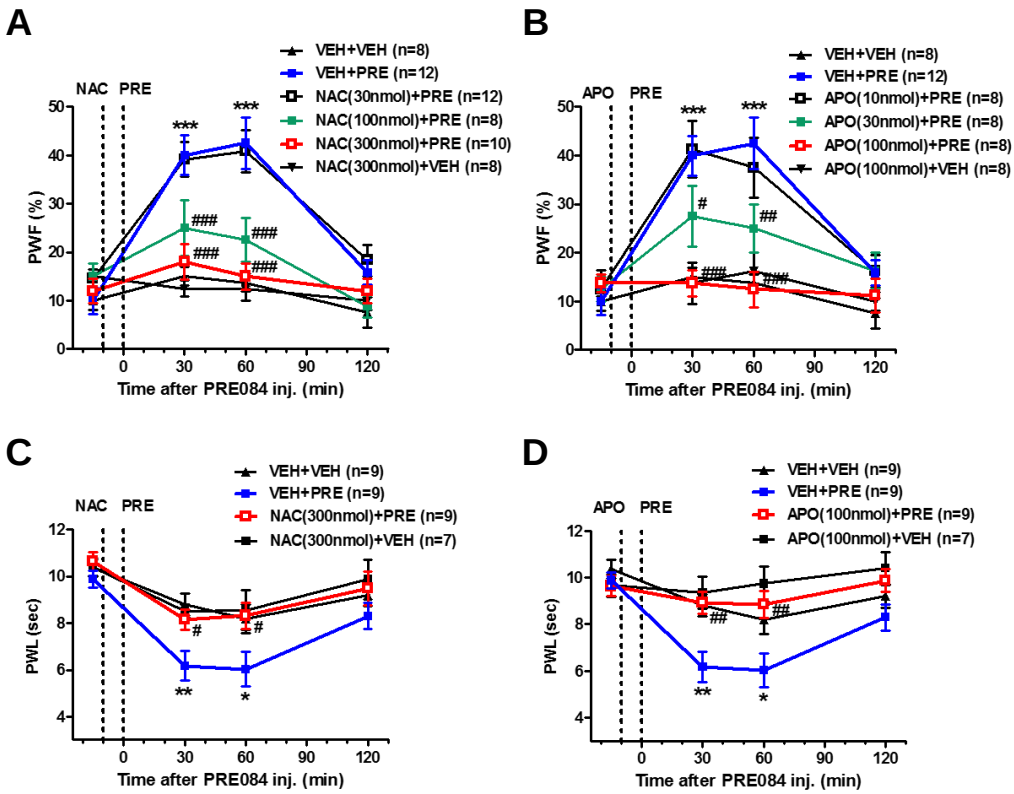

Figure 3-2. The time course of the inhibitory effect of intrathecal pretreatment with the ROS scavenger, NAC or the Nox inhibitor, apocynin (APO) on PRE084 (PRE)-induced mechanical allodynia (A and B) and thermal hyperalgesia (C and D) in mice. (A and B) Paw withdrawal frequency (PWF, %) and (C and D) paw withdrawal latency (PWL, sec) were measured at 0, 30, 60, and 120 min after PRE injection using a von-Frey filament (0.16 g) and hot plate test (55±0.5℃), respectively. NAC or APO was administered 10 min before PRE injection. **P* < 0.05, ***P* < 0.01, ****P* < 0.001 vs. VEH+VEH; #*P* < 0.05, ##*P* < 0.01, ###*P* < 0.001 vs. VEH+PRE. n = 7–12 mice / group.

3. Intrathecal pretreatment with BD1047, apocynin or 7-NI suppresses PRE084-induced Nox2 activation

To further investigate whether direct sig-1Rs activation can modulate the spinal NADPH oxidase 2 (Nox2) activation, the time course of PRE084-induced changes in Nox2 activity was examined by measuring the membrane fraction of spinal Nox2 subunit p47phox using a Western blot assay. Intrathecal administration of PRE084 (3 nmol) significantly increased the ratio of membrane (M) to total (T) protein expression of Nox2 subunit p47phox, which indicates an increase in the active form of Nox2, at the 30 min time point after injection as compared with that of the non-treatment group (0 min) (Fig. 3-3A; $*P < 0.05$ vs. 0 min). To further investigate whether the changes illustrated in Fig. 3-3A resulted from direct activation of Sig-1Rs, the effect of intrathecal pretreatment with the Sig-1R antagonist, BD1047 on the PRE084-induced increase in Nox activity was examined. Intrathecal pretreatment with BD1047 (100 nmol, BD+PRE) significantly suppressed the PRE084-induced increase in the ratio of membrane (M) to total (T) protein expression of p47phox 30 min post-PRE084 injection (Fig. 3-3B; $*P < 0.05$ vs. VEH+VEH, $\#P < 0.05$ vs. VEH+PRE). In addition, i.t. pretreatment with apocynin (100 nmol, APO+PRE) or 7-nitroindazole (200 nmol, 7-NI+PRE) significantly suppressed the PRE084-induced increase in the ratio of membrane (M) to total (T) protein expression of p47phox 30 min post-PRE084 injection (Fig. 3-3C and D; $*P < 0.05$ vs. VEH+VEH, $\#P < 0.05$ vs. VEH+PRE). No significant changes were detected in total fraction of p47phox in each group.

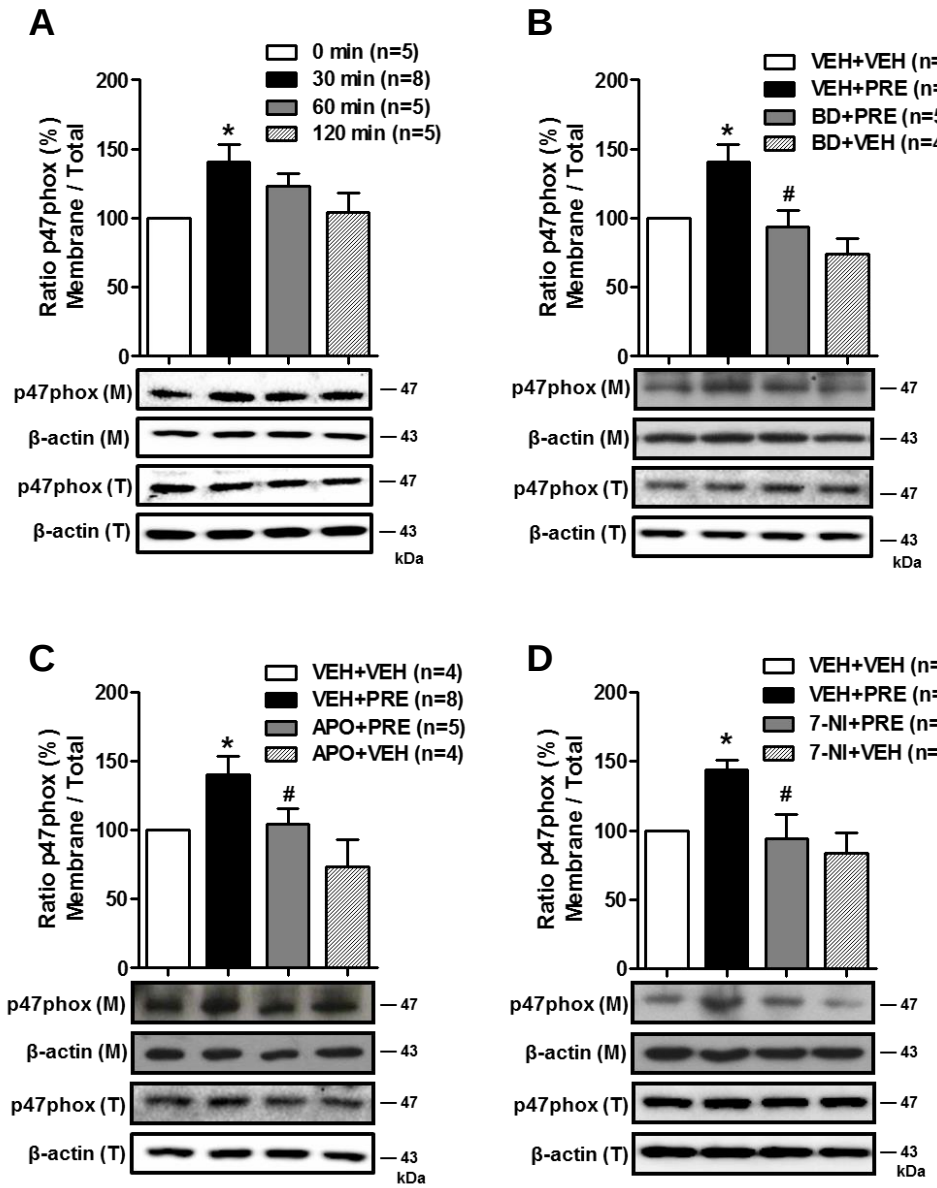
A
0 min (n=5)
30 min (n=8)
60 min (n=5)
120 min (n=5)
Ratio p47phox (%)
Membrane / Total
200
150
100
50
0
*
p47phox (M)
β-actin (M)
p47phox (T)
β-actin (T)
47
43
47
43
kDa
B
VEH+VEH (n=4)
VEH+PRE (n=8)
BD+PRE (n=5)
BD+VEH (n=4)
Ratio p47phox (%)
Membrane / Total
200
150
100
50
0
*
#
p47phox (M)
β-actin (M)
p47phox (T)
β-actin (T)
47
43
47
43
kDa
C
VEH+VEH (n=4)
VEH+PRE (n=8)
APO+PRE (n=5)
APO+VEH (n=4)
Ratio p47phox (%)
Membrane / Total
200
150
100
50
0
*
#
p47phox (M)
β-actin (M)
p47phox (T)
β-actin (T)
47
43
47
43
kDa
D
VEH+VEH (n=6)
VEH+PRE (n=6)
7-NI+PRE (n=6)
7-NI+VEH (n=6)
Ratio p47phox (%)
Membrane / Total
200
150
100
50
0
*
#
p47phox (M)
β-actin (M)
p47phox (T)
β-actin (T)
47
43
47
43
kDa

Figure 3-3. The time-dependent effect of i.t. administration of the sigma-1 receptor agonist, PRE084 (PRE) on the Nox2 subunit p47phox expression (A) and the effect of i.t. pretreatment with the sigma-1 receptor antagonist, BD1047 (BD), the Nox inhibitor, apocynin (APO) or the nNOS inhibitor, 7-nitroindazole (7-NI) on the PRE-induced changes in Nox2 subunit p47phox expression (B–D) in mice. (A–D) Nox2 subunit p47phox expression in the lumbar spinal cord dorsal horn was measured by Western blot analysis. The graphs depicting the changes in the ratio of membrane (M) to total (T) protein expression of p47phox are shown in the upper portion, while representative immunoblots of p47phox and β-actin expression are presented in the lower portion. The lumbar dorsal horn was sampled at 0, 30, 60, or 120 min (A) and at 30 min (B–D) after PRE injection. **P* < 0.05 vs. VEH+VEH; #*P* < 0.05 vs. VEH+PRE. n = 4–8 mice / group.

4. Intrathecal pretreatment with BD1047, apocynin or 7-NI suppresses PRE084-induced ROS production

Dihydroethidium (DHE)-derived fluorescence in the superficial dorsal horn (SDH, lamina I–II) was significantly increased by administration with PRE084 (VEH+PRE, 3 nmol; Fig. 3-4A), which was decreased by pretreatment with BD1047 (BD+PRE, 100 nmol; Fig. 3-4B), apocynin (APO+PRE, 100 nmol; Fig. 3-4C) or 7-NI (7-NI+PRE, 200 nmol; Fig.3-4D) (Fig. 3-4E; ***$P < 0.001$ vs. VEH+VEH, #$P < 0.05$, ##$P < 0.01$ vs. VEH+PRE). Importantly the intrathecal injection of these inhibitors alone (BD+VEH or APO+VEH), in the absence of PRE084, had no effect on p47phox or ROS production in comparison to the VEH+VEH group.

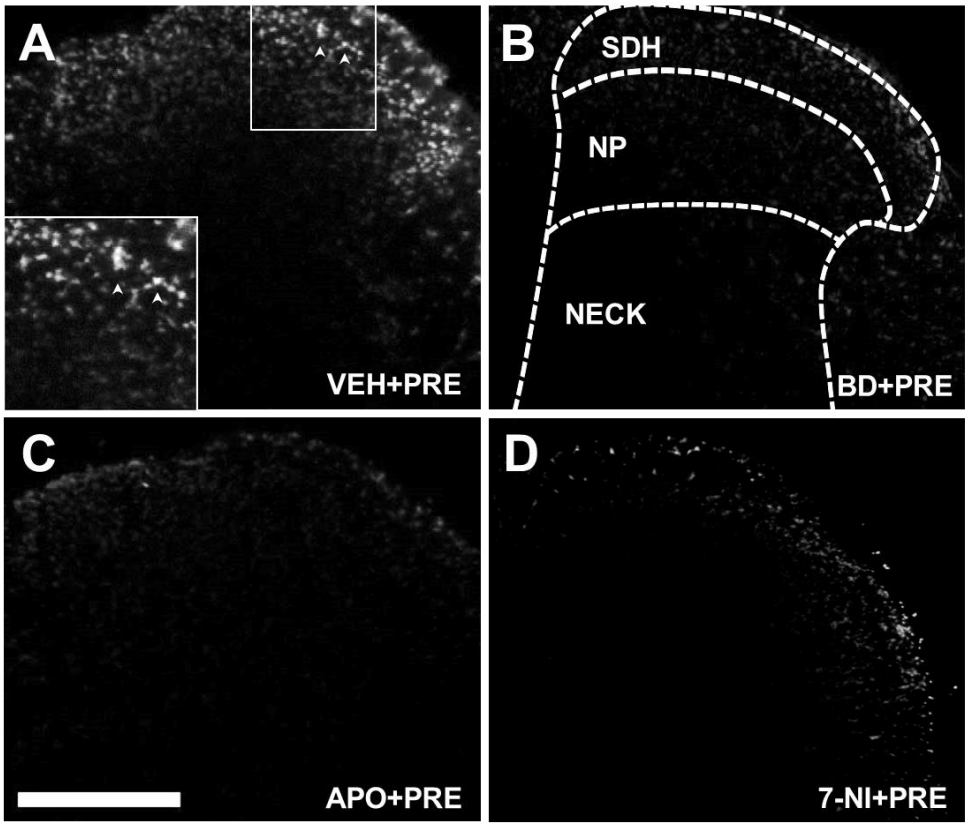
A
VEH+PRE
B
SDH
NP
NECK
BD+PRE
C
APO+PRE
D
7-NI+PRE

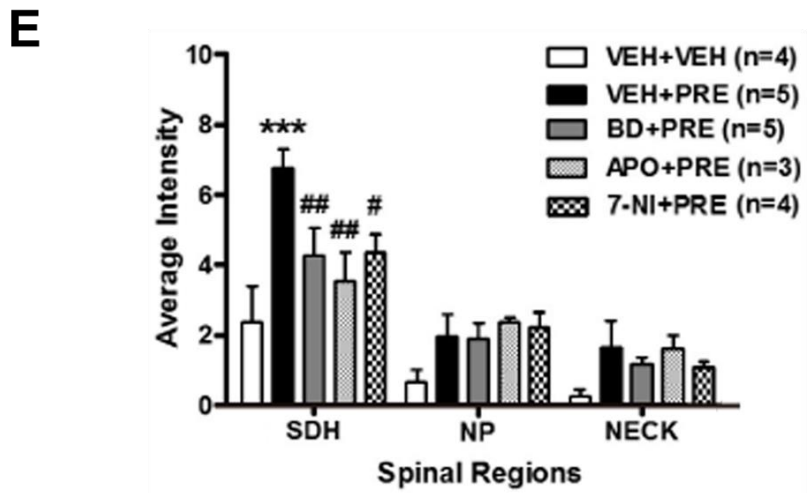
E
Average Intensity
10
8
6
4
2
0
***
##
##
#
SDH
NP
NECK
Spinal Regions
VEH+VEH (n=4)
VEH+PRE (n=5)
BD+PRE (n=5)
APO+PRE (n=3)
7-NI+PRE (n=4)

Figure 3-4. The effect of i.t. pretreatment with the sigma-1 receptor antagonist, BD1047 (BD), the Nox inhibitor, apocynin (APO) or the nNOS inhibitor, 7-nitroindazole (7-NI) on the PRE084 (PRE)-induced changes in ROS production in mice. (A–D) ROS production in the lumbar spinal cord dorsal horn was detected with dihydroethidium (DHE) staining. Representative fluorescence marked with arrowhead in A. Magnified image is shown in rectangles. (E) Fluorescence intensity of DHE in the superficial dorsal horn (SDH, lamina I–II), nucleus proprius (NP, lamina III–IV), and neck region (NECK, lamina V–VI) of mice was quantitated using an image analysis system. The lumbar dorsal horn was sampled at 30 min after PRE injection. Scale bar = 200 μm. ***P < 0.001 vs. VEH+VEH; #P < 0.05, ##P < 0.01 vs. VEH+PRE. n = 3–5 mice / group.

5. Intrathecal BD1047 or apocynin given during the induction phase inhibits mechanical allodynia, but not thermal hyperalgesia in CCI rats

CCI-induced sciatic nerve injury significantly increased paw withdrawal frequency (PWF, %) to innocuous mechanical stimuli (mechanical allodynia) and decreased paw withdrawal latency (PWL, sec) to noxious heat stimuli (thermal hyperalgesia) as compared with that of the sham group (Fig. 3-5A and B; $^{**}P < 0.01$, $^{***}P < 0.001$ vs. sham). Repeated daily administration with BD1047 (BD, 100 nmol) or apocynin (APO, 100 nmol) from days 0 to 5 (during the induction phase, twice a day) after CCI-surgery (CCI+BD or CCI+APO) significantly attenuated the induction of the mechanical allodynia (Fig. 3-5A), but not the thermal hyperalgesia (Fig. 3-5B) as compared to vehicle-treated CCI rats (CCI+VEH) ($\#P < 0.05$, $\#\#\#P < 0.001$ vs. CCI+VEH).

To investigate the potential mechanism underlying the Sig-1R-associated mechanical allodynia in CCI rats, spinal Nox2 activity was examined by measuring the Nox2 subunit p47phox expression in both the membrane (M) and total (T) fraction of the spinal dorsal horn using a Western blot assay. CCI-induced sciatic nerve injury caused an increase in p47phox expression in the membrane fraction as well as the total fraction at day 5 after surgery (Fig. 3-5C; $^{*}P < 0.05$ vs. sham). Repeated BD1047 treatment suppressed this increase in both the membrane and the total fraction (Fig. 3-5C; $\#P < 0.05$, $\#\#P < 0.01$ vs. CCI+VEH). The pan-cadherin expression was used as a marker of protein expression in the membrane fraction. In addition, repeated daily administration of apocynin significantly reduced the CCI-induced increase in expression of PKC-dependent pGluN1 expression as compared to vehicle-treated CCI rats (Fig. 3-5D; $^{***}P < 0.001$ v.s. sham, $\#\#P < 0.01$ v.s. CCI+VEH).

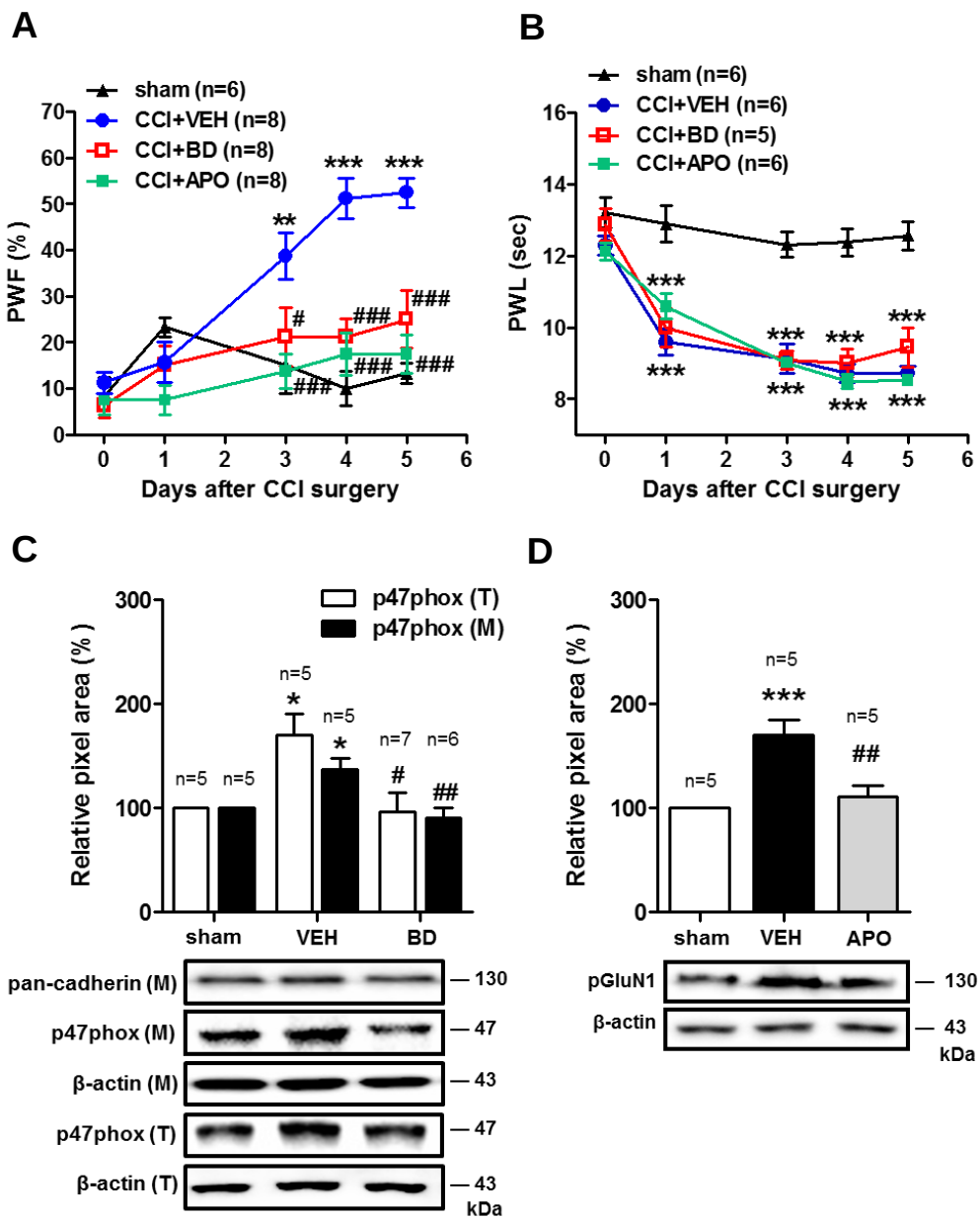
A
sham (n=6)
CCI+VEH (n=8)
CCI+BD (n=8)
CCI+APO (n=8)
PWF (%)
Days after CCI surgery
B
sham (n=6)
CCI+VEH (n=6)
CCI+BD (n=5)
CCI+APO (n=6)
PWL (sec)
Days after CCI surgery
C
p47phox (T)
p47phox (M)
Relative pixel area (%)
sham
VEH
BD
pan-cadherin (M)
p47phox (M)
β-actin (M)
p47phox (T)
β-actin (T)
kDa
D
Relative pixel area (%)
sham
VEH
APO
pGluN1
β-actin
kDa

Figure 3-5. The effect of repeated i.t. administration of the sigma-1 receptor antagonist BD1047 (BD) or the Nox inhibitor apocynin (APO) on the induction phase (days 0-5 after surgery) of mechanical allodynia (A), thermal hyperalgesia (B), Nox2 subunit p47phox expression (C), or PKC-dependent pGluN1 expression (D) in CCI rats. (A and B) Paw withdrawal frequency (PWF, %) and paw withdrawal latency (PWL, sec) were measured at 0, 1, 3, 4, and 5 days after surgery using a von-Frey filament (2.0 g) and plantar paw-flick latency test, respectively. n = 5–8 rats / group. (C) Nox2 subunit p47phox expression in the ipsilateral dorsal horn was measured by Western blot analysis. A graph depicting the change in p47phox expression is shown in the upper portion, while representative immunoblots of pan-cadherin in the membrane (M) fraction, p47phox in the membrane (M) and total (T) fraction, and β-actin expression are presented in the lower portion. The lumbar dorsal horn was sampled at day 5 post-surgery. $*P < 0.05$, $**P < 0.01$, $***P < 0.001$ vs. sham; $\#P < 0.05$, $\#\#P < 0.01$ $\#\#\#P < 0.001$ vs. CCI+VEH. n = 5–7 rats / group. (D) PKC-dependent pGluN1 expression in the ipsilateral dorsal horn was measured by Western blot analysis. A graph depicting the change in pGluN1 expression is shown in the upper portion, while representative immunoblots of pGluN1 and β-actin expression are presented in the lower portion. $***P < 0.001$ vs. sham; $\#\#P < 0.01$ vs. CCI+VEH. n = 5 rats / group.

6. Intrathecal BD1047 given during the induction phase inhibits spinal ROS production in CCI rats

I next examined the effects of the BD1047 treatment on ROS production in the lumbar dorsal horn of CCI rats. The effect of BD1047 (100 nmol) administration on CCI-induced ROS production is shown in Fig. 3-6. DHE-derived fluorescence was significantly increased in the superficial dorsal horn (SDH, lamina I–II) and nucleus proprius (NP, lamina III–IV) region in the spinal dorsal horn of CCI rats (CCI+VEH; Fig. 3-6B) at day 5 after surgery. This increase was significantly decreased by repeated BD1047 treatment (CCI+BD; Fig. 3-6C) (Fig. 3-6D; $^{**}P < 0.01$, $^{***}P < 0.001$ vs. sham, $\#P < 0.05$, $\#\#\#P < 0.001$ vs. CCI+VEH).

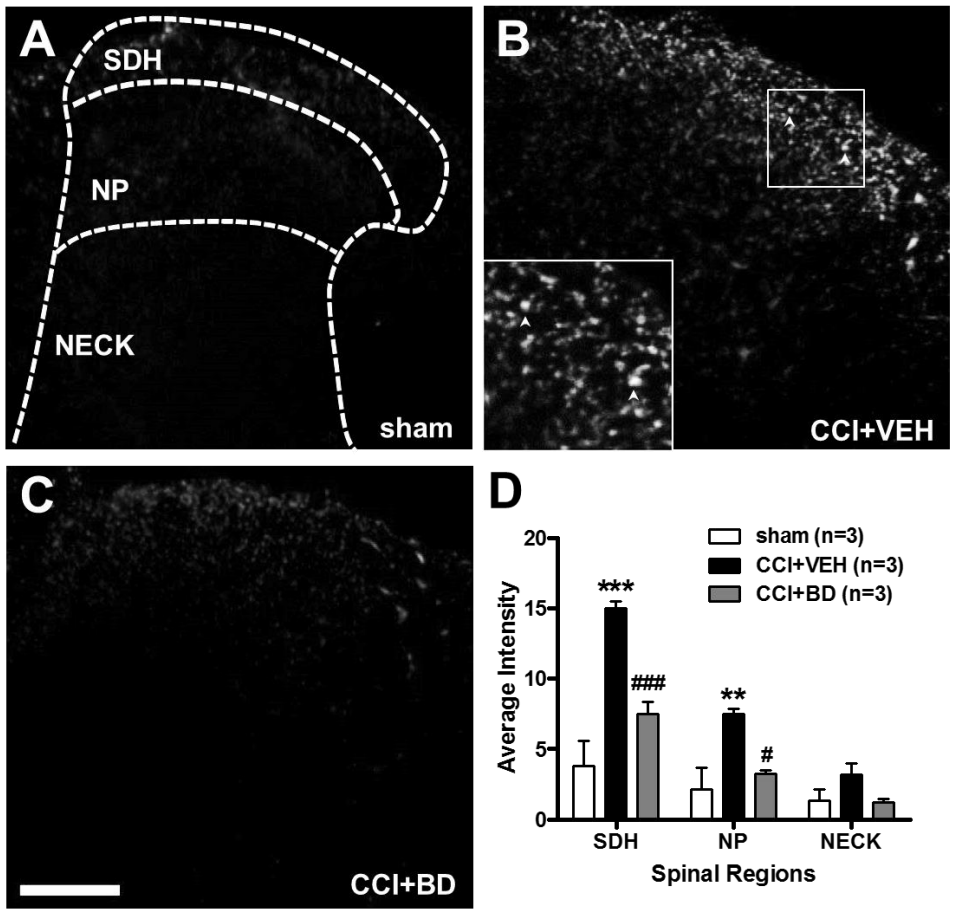

Figure 3-6. The effects of repeated i.t. administration of the sigma-1 receptor antagonist, BD1047 (BD) on ROS production during the induction phase of neuropathic pain (days 0-5 after surgery) in CCI rats. (A–C) ROS production in the ipsilateral dorsal horn was detected with dihydroethidium (DHE) staining. Representative fluorescence marked with arrowhead in B. Magnified image is shown in rectangles. (D) Fluorescence intensity of DHE in the superficial dorsal horn (SDH, lamina I–II), nucleus proprius (NP, lamina III–IV), and neck region (NECK, lamina V–VI) of rats was quantitated using an image analysis system. The lumbar dorsal horn was sampled at day 5 post-surgery. Scale bar = 200 μm. $^{**}P < 0.01$, $^{***}P < 0.001$ vs. sham; $^{\#}P < 0.05$, $^{\#\#\#}P < 0.001$ vs. CCI+VEH. n = 3 rats / group.

7. Intrathecal BD1047 administration during the maintenance phase has no effect on CCI-induced mechanical allodynia, thermal hyperalgesia, and Nox2 activation

In order to determine if the activation of Sig-1Rs also contributes to the maintenance of the chronic neuropathic pain and Nox2 activation, the analgesic and inhibitory effect of Sig-1R antagonist was examined during the maintenance phase of neuropathic pain in CCI rats. Repeated daily administration of BD1047 (BD, 100 nmol; twice a day) from days 15 to 20 (during the maintenance phase) following CCI surgery (CCI+BD) had no analgesic effects on CCI-induced mechanical allodynia (Fig. 3-7A) or thermal hyperalgesia (Fig. 3-7B) as compared to vehicle-treated CCI rats (CCI+VEH) (**P* < 0.05, ***P* < 0.01, ****P* < 0.001 vs. sham). In addition, Nox2 subunit p47phox expression in both the membrane (M) and total (T) fractions was significantly increased in vehicle-treated CCI rats at day 20 after surgery (VEH) (Fig. 3-7C; ***P* < 0.01 vs. sham), however, repeated administration of BD1047 from days 15 to 20 following surgery had no effect on these increases (**P* < 0.05, ***P* < 0.01 vs. sham). Pan-cadherin expression was used as a general marker of protein expression in the membrane fraction. In addition, PKC-dependent pGluN1 expression was significantly increased in vehicle-treated CCI rats at day 20 after surgery (VEH) (Fig. 3-7D; **P* < 0.05 vs. sham), however, repeated administration of apocynin from days 15 to 20 following surgery had no effect on these increases (**P* < 0.05 vs. sham).

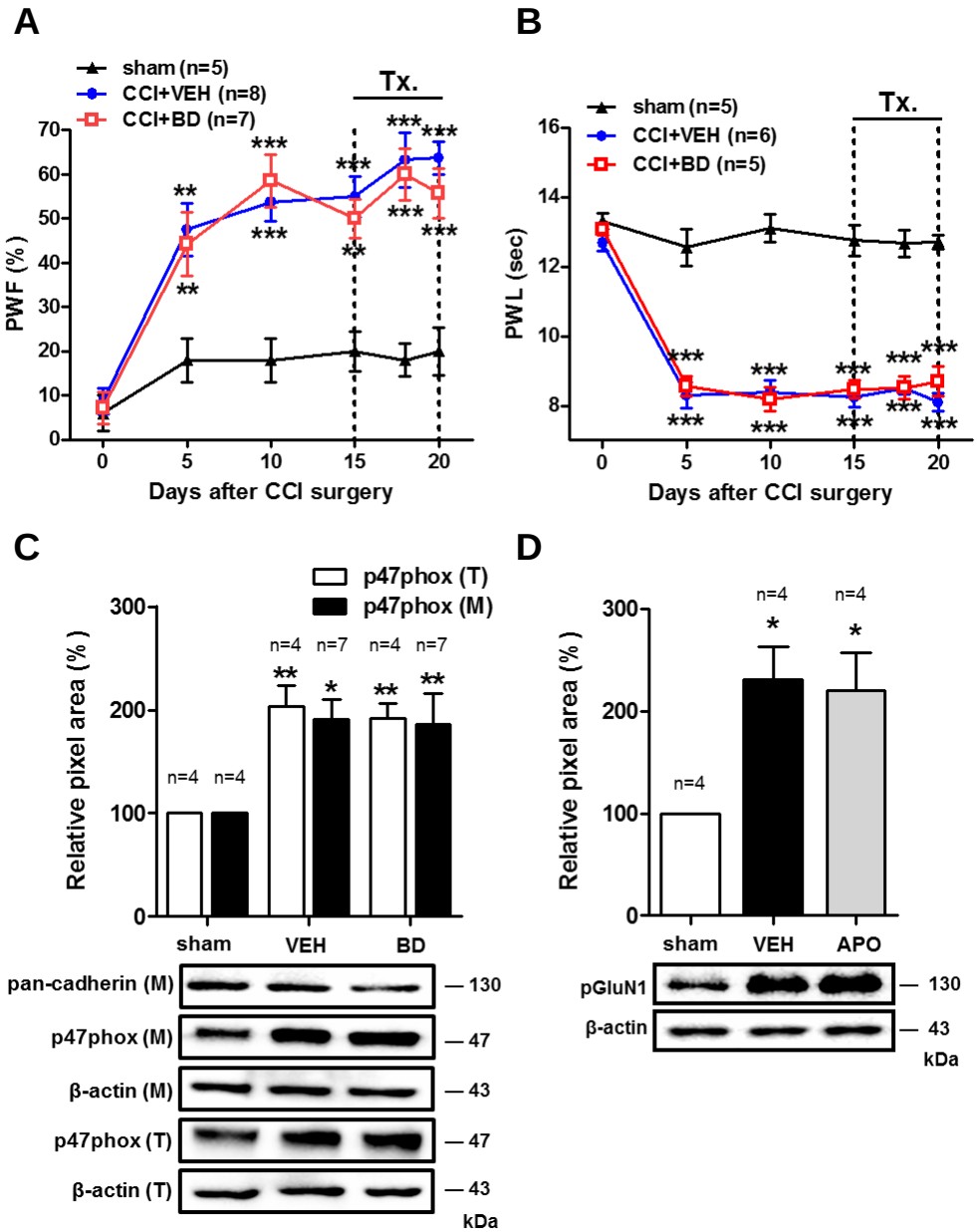
A
sham (n=5)
CCI+VEH (n=8)
CCI+BD (n=7)
Tx.
PWF (%)
Days after CCI surgery
B
sham (n=5)
CCI+VEH (n=6)
CCI+BD (n=5)
Tx.
PWL (sec)
Days after CCI surgery
C
p47phox (T)
p47phox (M)
Relative pixel area (%)
sham
VEH
BD
pan-cadherin (M)
p47phox (M)
β-actin (M)
p47phox (T)
β-actin (T)
kDa
D
Relative pixel area (%)
sham
VEH
APO
pGluN1
β-actin
kDa

Figure 3-7. The effect of repeated i.t. administration of the sigma-1 receptor antagonist BD1047 (BD) or the Nox inhibitor apocynin (APO) on the maintenance phase (days 0-5 after surgery) of mechanical allodynia (A), thermal hyperalgesia (B), Nox2 subunit p47phox expression (C), or PKC-dependent pGluN1 expression (D) in CCI rats. (A and B) Paw withdrawal frequency (PWF, %) and paw withdrawal latency (PWL, sec) were measured at 0, 5, 10, 15, 18 and 20 days after surgery using a von-Frey filament (2.0 g) and plantar paw-flick latency test, respectively. n = 5–8 rats / group. (C) Nox2 subunit p47phox expression in the ipsilateral dorsal horn was measured by Western blot analysis. A graph depicting the change in p47phox expression is shown in the upper portion, while representative immunoblots of pan-cadherin in the membrane (M) fraction, p47phox in the membrane (M) and total (T) fraction, and β-actin expression are presented in the lower portion. The lumbar dorsal horn was sampled at day 20 post-surgery. $*P < 0.05$, $**P < 0.01$, $***P < 0.001$ vs. sham. n = 4–7 rats / group. (D) PKC-dependent pGluN1 expression in the ipsilateral dorsal horn was measured by Western blot analysis. A graph depicting the change in pGluN1 expression is shown in the upper portion, while representative immunoblots of pGluN1 and β-actin expression are presented in the lower portion. $*P < 0.05$ vs. sham vs. sham. n = 4 rats / group.

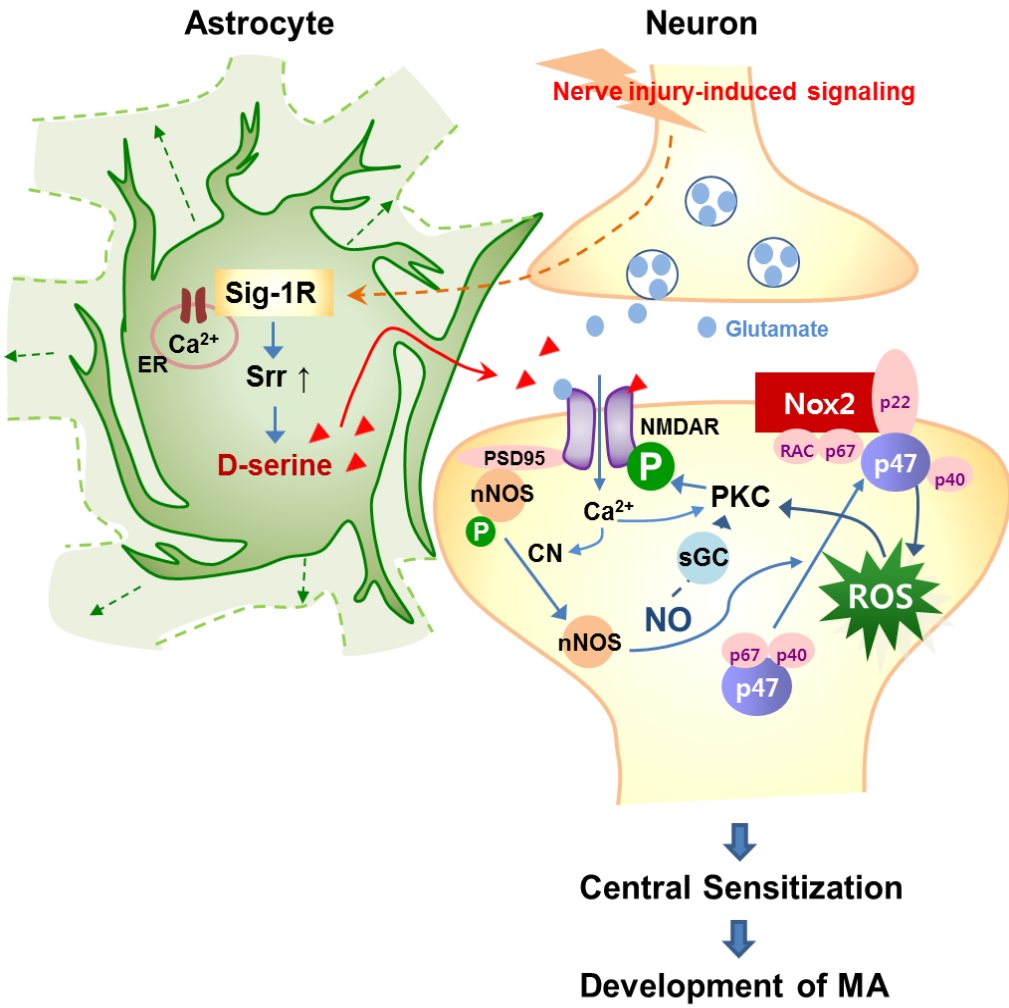

Figure 3-8. Schematic diagram summarizing the proposed biochemical pathway underlying CCI-induced central sensitization and the development of mechanical allodynia (MA).

DISCUSSION

This study demonstrates two important novel findings. First, intrathecal administration of a Sig-1R agonist, PRE084 in naïve mice time-dependently increased spinal Nox2 activation and ROS production in the lumbar spinal cord dorsal horn, which in turn contributed to mechanical allodynia and thermal hyperalgesia in these animals. Secondly, CCI-induced sciatic nerve injury also increased spinal Nox2 activation and ROS production in the lumbar spinal cord dorsal horn, which contributes to the induction of the mechanical allodynia. These CCI-induced increases in Nox2 activation and ROS production were significantly reduced by intrathecal administration of a Sig-1R antagonist, BD1047 in CCI rats. Collectively these findings demonstrate that spinal Sig-1Rs activation modulates Nox2 activation and accompanying ROS production in the spinal cord dorsal horn, ultimately contributing to pain hypersensitivity in mice and to peripheral nerve injury-induced chronic neuropathic pain in CCI rats.

Nox2 is a highly regulated membrane bound enzyme complex that is composed of membrane-bound subunits p22phox, gp91phox, and cytosolic subunits p40phox, p47phox, p67phox as well as the small GTPase RAC (Demaurex and Scorrano, 2009). In resting cells, Nox2 is segregated into cytosolic and membrane compartments. During activation of the Nox2, the cytosolic components translocate to the membrane to form a functional active enzyme complex (DeLeo and Quinn, 1996; Lambeth, 2004). Of all cytosolic subunits, p47phox plays an important role in translocation as well as in the assembly, which are both critical steps in the initiation of Nox2 activation (Groemping and Rittinger, 2005; Qian et al., 2008; Touyz et al., 2003). In this regard, an increase in the membrane fraction of the p47phox has been considered

to represent an increase in the active form of the Nox2 enzyme (Brennan et al., 2009). Based on this, p47phox expression in membrane fraction was assessed as a specific indicator of the Nox2 activation and pan-cadherin as a general marker of proteins in membrane fraction. In the present study, direct Sig-1R activation by single injection of a Sig-1R agonist increased p47phox expression in the membrane fraction, but not in the total fraction in mice. It is likely that the time window associated with a single injection is too short to affect the level of protein expression. On the other hand, repeated injection of the Sig-1R antagonist, BD1047 during the induction phase of neuropathic pain in CCI rats suppressed the CCI-induced increase in p47phox expression, not only in the membrane fraction, but also in the total fraction. These results indicate that Sig-1Rs can modulate the total protein expression of p47phox at gene transcription level as well as Nox2 activation at the post-translational level during the induction phase of neuropathic pain in CCI rats.

ROS generated from the activation of the Nox2 enzyme oxidizes the DHE dye to ethidium bromide, which in turn binds to the DNA and emits red fluorescence (Aoyama et al., 2008). In this study, Nox2-induced ROS production was assessed by using this DHE staining procedure. Peripheral nerve injury as well as direct Sig-1R activation induced ROS production in both the superficial dorsal horn (SDH, laminae I–II) and the underlying nucleus proprius (NP, laminae III–IV). In this regard Sig-1Rs are rich in small- and medium-sized neurons within the superficial dorsal horn of the spinal cord, where sensory information, particularly nociceptive information, is conveyed from the periphery to higher levels of the central nervous system (Alonso et al., 2000). Furthermore, the expression of the cytochrome P450 side-chain cleavage (P450scc), a key enzyme that produces endogenous ligands of Sig-1Rs, have been shown to increase in the SDH region and to spread into the NP region following

sciatic nerve ligation (Patte-Mensah et al., 2006). While neurons in the spinal cord dorsal horn appear to express Sig-1Rs (Alonso et al., 2000), it has recently been suggested that L_5 spinal nerve transection induces Nox2 expression and ROS production mainly in spinal cord microglia, which are located in the SDH and NP (Kim et al., 2010). In addition, there are several recent reports that further suggest that Nox2 can be expressed in non-phagocytic cells, such as neurons and astrocytes in central nervous system (CNS) (Sorce and Krause, 2009). NMDA injections into the hippocampus showed a robust increase of superoxide production by Nox2 activation in hippocampal neurons (Brennan et al., 2009). Furthermore, increased Nox2 expression is found in reactive astrocytes, which is likely to play important roles in CNS physiology and pathology (Abramov et al., 2005). Because the role of the each cell type in spinal nociceptive processing may depend in part on the type of pain stimuli, modality, and duration, it is possible that the specific Nox2 expressing cell type can differ depending on the type of pain, the animal model used and/or the time-dependency following the initiation of the pain. It is likely that Sig-1R activation in dorsal horn neurons triggers a pathway that activates ROS in microglia within this region. Collectively, these results suggest the possibility that spinal Sig-1Rs play an important role in conveying nerve injury-induced nociceptive information from the periphery to the central nervous system via production of the ROS in the SDH and NP regions, which is closely regulated by its ligands synthesized in the vicinity of the Sig-1Rs.

There are two possibilities to modulate Nox2 activation and ROS production by spinal Sig-1Rs activation; intracellular or intercellular mechanism. First, spinal Sig-1Rs could activate Nox2 enzyme localized in the same cell via Ca^{2+} and protein kinase activation. Sig-1Rs are predominantly localized to the endoplasmic reticulum in cells

of the nervous system, which modulate intracellular Ca^{2+} levels to promote the efflux of Ca^{2+} to the cytoplasm (Monnet, 2005). Increased cytosolic Ca^{2+} then influences Ca^{2+}-dependent activation of the protein kinase C (PKC), leading to phosphorylation of the Nox2 subunit p47phox and activation of this enzyme at the plasma membrane or within the endoplasmic reticulum (Raad et al., 2009). It has been suggested that intrathecal administration of a Sig-1R agonist, PRE084 significantly activates pan-PKC, especially the PKC α, ε, and ζ isoforms in the spinal cord dorsal horn (Roh et al., 2008). Furthermore, PKCα is known as a conventional PKC isoform having diacylglycerol- and Ca^{2+}-sensitivity and it has also been reported that this isoform plays an important role in Nox2 activation through increases in phosphorylation of p47phox (Raad et al., 2009). Secondly, spinal Sig-1Rs could activate Nox2 enzyme localized in neighboring cells via nitric oxide (NO) signaling-mediated cell to cell communication. It has been demonstrated that Sig-1Rs can modulate NO signaling induced by neuronal nitric oxide synthase activation (Roh et al., 2011). NO is a diffusible gas, thus it can diffuse from its site of production to act on other cells. It has been suggested that NO may mediate the increase in Nox2 activation and ROS production in cortical neuronal cultures via its downstream signaling, cGMP and protein kinase G (Girouard et al., 2009). Thus, Sig-1Rs can modulate Nox2 activation through both intracellular and intercellular mechanisms, which are thought to be involved in Ca^{2+} and protein kinase dependent- or NO signaling dependent-cascades. However, the precise mechanisms involved need to be further investigated.

This study was focused on Sig-1R-induced positive modulation of Nox2-ROS signaling in the spinal cord as a potential nociceptive mechanism that underlies the development of neuropathic pain as well as the Sig-1R-induced nociceptive hypersensitivity in mice. In contrast, Sig-1Rs in the brain have been reported to exert

robust cellular protective actions in vivo by preventing oxidative stress in cerebral ischemic stroke, diabetes-induced retinal neurodegeneration, and amyloid β-induced toxicity (Meunier et al., 2006; Schetz et al., 2007; Smith et al., 2008; Su et al., 2010). These actions are supported by in vitro studies showing that Sig-1Rs regulate dendritic spine formation and promote cellular survival by regulating Bcl-2 expression via a reduction in ROS signaling (Meunier and Hayashi, 2010; Tsai et al., 2009). While this type of association between Sig-1Rs and oxidative stress has been well documented in several brain diseases, it has not been examined with regard to the process of nociception at the level of the spinal cord. Sig-1Rs have been localized to diverse regions of the central nervous system, which are related to a number of different disease states (i.e., addiction, amnesia, depression, stroke, cancer, pain, etc.) with different pathophysiologic mechanisms (Alonso et al., 2000; Maurice and Su, 2009). Unlike the more positive effects that occur with Sig-1R activation in brain, both Sig-1R activation and ROS signaling in spinal cord appear to contribute to central sensitization, which plays a critical role in acute and chronic nociception (Chung, 2004; Gao et al., 2007; Kim et al., 2008). In this regard, it is likely that Sig-1Rs modulate ROS signaling in the spinal cord in association with pain in different ways than those associated with other Sig-1R-related diseases that occur at higher levels of the neuroaxis.

Results of this study show that spinal Sig-1R activation induced mechanical allodynia and thermal hyperalgesia in mice, which were ameliorated by pretreatment with the ROS scavenger, NAC or the Nox inhibitor, apocynin. These results demonstrate that spinal Sig-1Rs appear to mediate two different abnormal pain sensations, mechanical allodynia and thermal hyperalgesia, via modulation of the Nox-ROS signaling in the level of spinal cord. On the other hand, inhibition of spinal

Sig-1Rs or Nox attenuates peripheral nerve injury-induced mechanical allodynia, but not thermal hyperalgesia. Similarly partial sciatic nerve ligation-induced mechanical and cold allodynia are attenuated in Sig-1R knockout mice, however, nerve injury-induced heat hyperalgesia is not affected in knockout mice with respect to wild-type mice (de la Puente et al., 2009). These results suggest that Sig-1Rs are more important for the development of peripheral nerve injury-induced mechanical allodynia rather than thermal hyperalgesia. This is consistent with previous work suggesting that mechanical allodynia and thermal hyperalgesia are caused by different mechanisms (Ossipov et al., 1999; Tal and Bennett, 1994). Peripheral nerve injury induces changes in primary afferent neurons, nociceptive C-fibers and non-nociceptive myelinated A-fibers, leading to peripheral sensitization. The injury triggers the expression of the sodium channels and transient receptor potential vanilloid 1 (TRPV1) receptors on uninjured fibers that enhance the pain response to noxious stimuli. In this regard peripheral TRPV1 receptors are known to be important contributors to the development of thermal hyperalgesia in neuropathic pain (Jhaveri et al., 2005). Spontaneous activity in C-fibers leads to hyperexcitability of second-order neurons in the spinal cord, leading to central sensitization. This causes non-noxious stimuli from mechanoreceptive A-fibers to be perceived as pain, which is known as mechanical allodynia. Dysfunction of the inhibitory interneurons and descending modulatory control systems as well as activation of the spinal glial cells also leads to central sensitization (Baron, 2006). In previous study from our laboratories, CCI-induced peripheral nerve injury increased the phosphorylation of the NMDA receptor GluN1 subunit (pGluN1) in the spinal cord, which can potentiate NMDA receptor function resulting in central sensitization, and this increase is significantly attenuated by the inhibition of spinal Sig-1Rs (Kim et al., 2008; Woolf, 1983). In addition, the systemic

injection of a ROS scavenger dramatically attenuates L_5 spinal nerve ligation-induced mechanical allodynia by reducing pGluN1 expression and restoring GABA inhibitory transmission in spinal dorsal horn (Gao et al., 2007; Yowtak et al., 2011). Therefore, spinal Sig-1Rs and ROS may be closely related to peripheral nerve injury-induced development of the mechanical allodynia by contributing to the central sensitization rather than to thermal hyperalgesia which is associated with peripheral TRPV1 receptors.

In the present study, the Sig-1R antagonist, BD1047-induced analgesic effect and suppression of Nox2 activation occurred during the induction phase, but not during the maintenance phase of chronic neuropathic pain. Based on our previous study, Sig-1R expression in the ipsilateral spinal cord dorsal horn of CCI rats was significantly increased between days 1 to 3 days post-surgery, peaked at day 3 and then returned to sham values by day 7 post-surgery (Roh et al., 2008b). Since Sig-1Rs returned to sham levels by day 7, it is likely that the failure of late spinal Sig-1R inhibition to attenuate the CCI-induced chronic neuropathic pain or to modulate Nox2 activation is due to a return to basal levels of Sig-1R expression during the maintenance phase of neuropathic pain. Therefore, it could be possible that the role of Sig-1Rs in neuropathic pain may be more important during the induction phase. In this regard, it has been shown that early inhibition of the Sig-1Rs during the induction phase of CCI-induced neuropathic pain has a significant analgesic effect that is sustained over the 30 day experimental period following CCI surgery (Roh et al., 2008b). It has been demonstrated that spinal Sig-1Rs are potently activated by the binding of endogenous neurosteroid ligands, that include pregnenolone and allopregnanolone, which increase markedly in the spinal cord dorsal horn of neuropathic rats 2 days after sciatic nerve ligation (Patte-Mensah et al., 2004). These endogenous neurosteroids peak at day 6

and then slowly decline by day 10 post-ligation. Furthermore, the mRNA, protein expression, and bioactivity of P450scc, the rate-limiting step in the biosynthesis of all classes of neurosteroids, increases in the spinal cord dorsal horn following nerve ligation in rats (Patte-Mensah et al., 2006). Collectively, these results demonstrate that the early expression and activation of spinal Sig-1Rs plays a critical role in the induction of the nerve injury-induced neuropathic pain in CCI rats. The therapeutic potential of Sig-1R ligands has been recognized for many years and the present results suggest that Sig-1Rs may also be a potential therapeutic target in the clinical management of neuropathic pain particularly during the induction phase.

The present study demonstrates that activation of the spinal Sig-1Rs increases the Nox2 activation, as demonstrated by the significant increase in the expression of the membrane fraction of the Nox2 subunit p47phox, and ROS production in the lumbar spinal cord dorsal horn. Moreover, Sig-1R-induced Nox2 activation and ROS production contribute to Sig-1R-induced pain hypersensitivity and peripheral nerve injury-induced induction, but not the maintenance, of the chronic neuropathic pain. Collectively, these findings suggest that spinal Sig-1Rs play an important role in the modulation of the Nox2 activation and accompanying ROS production in the spinal cord, and ultimately contribute to the induction of the neuropathic pain.

CONCLUSION

Damage to the peripheral nerves can lead to the development of neuropathic pain, which causes considerable suffering and distress to these patients and is associated with several diagnostic symptoms including mechanical allodynia (MA, sensation of pain to non-noxious mechanical stimuli) and thermal hyperalgesia (TH, increased pain response to noxious thermal stimuli). The development of peripheral neuropathic pain involves a variety of pathophysiological mechanisms in both the peripheral and central nervous systems. In this regard spinal NMDA receptors have been shown to play a key role in the development of 'central sensitization', a phenomenon in which nociceptive inputs to the dorsal horn increase the excitability and synaptic efficacy of neurons in spinal pain pathways. In our previous study, activation of spinal sigma-1 receptors (Sig-1Rs) contributes to the functional potentiation of NMDA receptors via increases in phosphorylation of GluN1 subunit. However, the precise cellular mechanisms underlying Sig-1Rs-related neuropathic pain are not investigated.

In the first study, i.t. injection of Sig-1R agonist, PRE084 significantly evoked mechanical and thermal hypersensitivity, and increased the number of PKC and PKA-dependent pGluN1-ir cells in spinal cord. The PRE084-induced hypersensitivity and increase in PKC-dependent pGluN1 expression were significantly blocked by pretreatment with L-NAME or 7-nitroindazole. I.t. PRE084 time-dependently decreased the ratio of phosphorylated nNOS (pnNOS) to nNOS expression and the number of spinal pnNOS-ir cells. This decrease in the pnNOS form was prevented by BD1047, a Sig-1R antagonist and cyclosporin A, a calcineurin inhibitor, but not by a sGC inhibitor.

In the second study, i.t. administration of the D-serine degrading enzyme, DAAO

attenuated the facilitation of NMDA-induced pain behaviors induced by the Sig-1R agonist, PRE084. Exogenous D-serine facilitates NMDA-induced nociception and increases PKC-dependent pGluN1 expression, which was attenuated by preteatment with the nNOS inhibitor, 7-nitroindazole. In CCI mice, i.t. administration of exogenous D-serine during the induction phase of neuropathic pain restored MA and PKC-dependent pGluN1 suppressed by BD1047. Furthermore, administration of the serine racemase inhibitor, LSOS or DAAO suppressed CCI-induced MA, pGluN1, nNOS activation and NO production. Intrathecal administration of 7-nitroindazole or the sGC inhibitor, ODQ also attenuated CCI-induced MA and pGluN1. By contrast, D-serine and nNOS signaling had no effect on CCI-induced TH or GluN1 expression.

In the third study, Sig-1R-induced pain hypersensitivity was dose-dependently attenuated by pretreatment with the ROS scavenger, NAC or the Nox inhibitor, apocynin. PRE084 also induced an increase in Nox2 activation and ROS production, which were attenuated by pretreatment with BD1047, apocynin, or 7-nitroindazole. CCI-induced nerve injury produced an increase in Nox2 activation and ROS production in the spinal cord, all of which were attenuated by i.t. administration with BD1047 during the induction phase of neuropathic pain. Furthermore, administration with BD1047 or apocynin reversed CCI-induced increase in pGluN1 expression and MA during the induction phase, but not the maintenance phase.

Collectively, these findings demonstrate that spinal Sig-1R activation plays an important role in the development of neuropathic pain induced by peripheral nerve injury, and Sig-1Rs could be a useful therapeutic target for alleviating mechanical allodynia under the neuropathic pain conditions.

REFERENCES

Abramov AY, Jacobson J, Wientjes F, Hothersall J, Canevari L, Duchen MR (2005). Expression and modulation of an NADPH oxidase in mammalian astrocytes. J Neurosci 25: 9176–9184.

Alderton WK, Cooper CE, Knowles RG (2001). Nitric oxide synthases : structure, function and inhibition. Biochem J 357: 593–615.

Alonso G, Phan V, Guillemain I, Saunier M, Legrand A, Anoal M, et al. (2000). Immunocytochemical localization of the sigma1 receptor in the adult rat central nervous system. Neuroscience 97: 155–170.

Aoyama T, Hida K, Kuroda S, Seki T, Yano S, Shichinohe H, et al. (2008). Edaravone (MCI-186) scavenges reactive oxygen species and ameliorates tissue damage in the murine spinal cord injury model. Neurol Med Chir (Tokyo) 48: 539–545.

Balasuriya D, Stewart AP, Edwardson JM (2013). The σ-1 receptor interacts directly with GluN1 but not GluN2A in the GluN1/GluN2A NMDA receptor. J Neurosci 33: 18219–18224.

Baron R (2006). Mechanisms of disease: neuropathic pain—a clinical perspective. Nat Clin Pract Neurol 2: 95–106.

Bedard K, Krause KH (2007). The NOX family of ROS-generating NADPH oxidases: physiology and pathophysiology. Physiol Rev 87: 245–313.

Bennett GJ, Xie YK (1988). A peripheral mononeuropathy in rat that produces disorders of pain sensation like those seen in man. Pain 33: 87–107.

Bian D, Ossipov MH, Zhong C, Malan TP Jr, Porreca F (1998). Tactile allodynia, but not thermal hyperalgesia, of the hindlimbs is blocked by spinal transection in rats with nerve injury. Neurosci Lett 241: 79–82.

Bogdan C (2001). Nitric oxide and the regulation of gene expression. Trends Cell Biol 11: 66–75.

Brenman JE, Chao DS, Gee SH, McGee AW, Craven SE, Santillano DR, et al. (1996). Interaction of nitric oxide synthase with the postsynaptic density protein PSD-95 and alpha1-syntrophin mediated by PDZ domains. Cell 84: 757–767.

Brennan AM, Suh SW, Won SJ, Narasimhan P, Kauppinen TM, Lee H, et al. (2009). NADPH oxidase is the primary source of superoxide induced by NMDA receptor activation. Nat Neurosci 12: 857–863.

Chen L, Huang LY (1992). Protein kinase C reduces Mg^{2+} block of NMDA-receptor channels as a mechanism of modulation. Nature 356: 521–523.

Choi SR, Roh DH, Yoon SY, Kang SY, Moon JY, Kwon SG et al. (2013). Spinal sigma-1 receptors activate NADPH oxidase 2 leading to the induction of pain hypersensitivity in mice and mechanical allodynia in neuropathic rats. Pharmacological research : the official journal of the Italian Pharmacological Society 74: 56–67.

Christopherson KS, Hillier BJ, Lim WA, Bredt DS (1999). PSD-95 assembles a ternary complex with the N-methyl-D-aspartic acid receptor and a bivalent neuronal NO synthase PDZ domain. J Biol Chem 274: 27467–27473.

Chu YC, Guan Y, Skinner J, Raja SN, Johns RA, Tao YX (2005). Effect of genetic knockout or pharmacologic inhibition of neuronal nitric oxide synthase on complete Freund's adjuvant-induced persistent pain. Pain 119: 113–123.

Chung JM (2004). The role of reactive oxygen species (ROS) in Persistent Pain. Molecular Interventions 4: 248–250.

Collier TL, Waterhouse RN, Kassiou M (2007). Imaging sigma receptors: applications in drug development. Curr Pharm Des 13: 51–72.

Cury Y, Picolo G, Gutierrez VP, Ferreira SH (2011). Pain and analgesia: The dual effect of nitric oxide in the nociceptive system. Nitric Oxide 25: 343–354.

de la Puente B, Nadal X, Portillo-Salido E, Sanchez-Arroyos R, Ovalle S, Palacios G, et al. (2009). Sigma-1 receptors regulate activity-induced spinal sensitization and neuropathic pain after peripheral nerve injury. Pain 145: 294–303.

DeLeo FR, Quinn MT (1996). Assembly of the phagocyte NADPH oxidase: molecular interaction of oxidase proteins. J Leukoc Biol 60: 677–691.

Demaurex N, Scorrano L (2009). Reactive oxygen species are NOXious for neurons. Nat Neurosci 12: 819–820.

Doyle T, Bryant L, Muscoli C, Cuzzocrea S, Esposito E, Chen Z, et al. (2010). Spinal NADPH oxidase is a source of superoxide in the development of morphine-induced hyperalgesia and antinociceptive tolerance. Neurosci Lett 483: 85–89.

Duman EN, Kesim M, Kadioglu M, Ulku C, Kalyoncu NI, Yaris E (2006). Effect of gender on antinociceptive effect of paroxetine in hot plate test in mice. Prog Neuropsychopharmacol Biol Psychiatry 30: 292–296.

Ferreira J, Santos AR, Calixto JB (1999). The role of systemic, spinal and supraspinal L-arginine-nitric oxide-cGMP pathway in thermal hyperalgesia caused by intrathecal injection of glutamate in mice. Neuropharmacology 38: 835–842.

Gabra BH, Kessler FK, Ritter JK, Dewey WL, Smith FL (2007). Decrease in N-methyl-D-aspartic acid receptor-NR2B subunit levels by intrathecal short-hairpin RNA blocks group I metabotropic glutamate receptor-mediated hyperalgesia. J Pharmacol Exp Ther

322: 186–194.

Gao X, Kim HK, Chung JM, Chung K (2007). Reactive oxygen species (ROS) are involved in enhancement of NMDA-receptor phosphorylation in animal models of pain. Pain 131: 262–271.

Garthwaite J (2008). Concepts of neural nitric oxide-mediated transmission. Eur J Neurosci 27: 2783–2802.

Girouard H, Wang G, Gallo EF, Anrather J, Zhou P, Pickel VM, et al. (2009). NMDA receptor activation increases free radical production through nitric oxide and NOX2. J Neurosci 29: 2545–2552.

Groemping Y, Rittinger K (2005). Activation and assembly of the NADPH oxidase: a structural perspective. Biochem J 386: 401–416.

Guggilam A, Patel KP, Haque M, Ebenezer PJ, Kapusta DR, Francis J (2008). Cytokine blockade attenuates sympathoexcitation in heart failure: cross-talk between nNOS, AT-1R and cytokines in the hypothalamic paraventricular nucleus. Eur J Heart Fail 10: 625–634.

Handy RL, Moore PK (1998). Effects of selective inhibitors of neuronal nitric oxide synthase on carrageenan-induced mechanical and thermal hyperalgesia. Neuropharmacology 37: 37–43.

Hargreaves K, Dubner R, Brown F, Flores C, Joris J (1988). A new and sensitive method for measuring thermal nociception in cutaneous hyperalgesia. Pain 32: 77–88.

Hess DT, Matsumoto A, Kim SO, Marshall HE, Stamler JS (2005). Protein S-nitrosylation: purview and parameters. Nat Rev Mol Cell Biol 6: 150–166.

Hylden JL, Wilcox GL (1980). Intrathecal morphine in mice: a new technique. Eur J Pharmacol 67: 313–316.

Ibi M, Matsuno K, Shiba D, Katsuyama M, Iwata K, Kakehi T, et al. (2008). Reactive oxygen species derived from NOX1/NADPH oxidase enhance inflammatory pain. J Neurosci 28: 9486–9494.

Jhaveri MD, Elmes SJ, Kendall DA, Chapman V (2005). Inhibition of peripheral vanilloid TRPV1 receptors reduces noxious heat-evoked responses of dorsal horn neurons in naive, carrageenan-inflamed and neuropathic rats. Eur J Neurosci 22: 361–370.

Kallenborn-Gerhardt W, Schröder K, Del Turco D, Lu R, Kynast K, Kosowski J, et al. (2012). NADPH oxidase-4 maintains neuropathic pain after peripheral nerve injury. J Neurosci 32: 10136–10145.

Karlsson J, Fong KS, Hansson MJ, Elmer E, Csiszar K, Keep MF (2004). Life span extension and reduced neuronal death after weekly intraventricular cyclosporin injections in the

G93A transgenic mouse model of amyotrophic lateral sclerosis. J Neurosurg 101: 128–137.

Kawamata T, Omote K (1999). Activation of spinal N-methyl-D-aspartate receptors stimulates a nitric oxide/cyclic guanosine 3,5-monophosphate/glutamate release cascade in nociceptive signaling. Anesthesiology 91: 1415–1424.

Kim HW, Kwon YB, Roh DH, Yoon SY, Han HJ, Kim KW et al. (2006). Intrathecal treatment with sigma1 receptor antagonists reduces formalin-induced phosphorylation of NMDA receptor subunit 1 and the second phase of formalin test in mice. British journal of pharmacology 148: 490–498.

Kim HK, Park SK, Zhou JL, Taglialatela G, Chung K, Coggeshall RE, et al. (2004). Reactive oxygen species (ROS) play an important role in a rat model of neuropathic pain. Pain 111: 116–124.

Kim HW, Roh DH, Yoon SY, Seo HS, Kwon YB, Han HJ et al. (2008). Activation of the spinal sigma-1 receptor enhances NMDA-induced pain via PKC- and PKA-dependent phosphorylation of the NR1 subunit in mice. British journal of pharmacology 154: 1125–1134.

Kim D, You B, Jo EK, Han SK, Simon MI, Lee SJ (2010). NADPH oxidase 2-derived reactive oxygen species in spinal cord microglia contribute to peripheral nerve injury-induced neuropathic pain. Proc Nat Acad Sci 107: 14851–14856.

Koesling D, Russwurm M, Mergia E, Mullershausen F, Friebe A (2004). Nitric oxide-sensitive guanylyl cyclase: structure and regulation. Neurochem Int 45: 813–819.

Kwon YB, Lee JD, Lee HJ, Han HJ, Mar WC, Kang SK, et al. (2001). Bee venom injection into an acupuncture point reduces arthritis associated edema and nociceptive responses. Pain 90: 271–280.

Lambeth JD (2004). NOX enzymes and the biology of reactive oxygen. Nat Rev Immunol 4: 181–189.

Lau GC, Saha S, Faris R, Russek SJ (2004). Up-regulation of NMDAR1 subunit gene expression in cortical neurons via a PKA-dependent pathway. Journal of Neurochemistry 88: 564–575.

Lee JH, Wilcox GL, Beitz AJ (1992). Nitric oxide mediates Fos expression in the spinal cord induced by mechanical noxious stimulation. Neuroreport 3: 841–844.

Lefèvre Y, Amadio A, Vincent P, Descheemaeker A, Oliet SH, Dallel R et al. (2015). Neuropathic pain depends upon D-serine co-activation of spinal NMDA receptors in rats. Neurosci Lett 603: 42–47.

Levy D, Zochodne DW (2004). NO pain: potential roles of nitric oxide in neuropathic pain.

Pain Pract 4: 11–18.

Liang M, Knox FG (1999). Nitric oxide activates PKCalpha and inhibits Na^+-K^+-ATPase in opossum kidney cells. Am J Physiol 277: F859–865.

MacFarlane PM, Vinit S, Mitchell GS (2011). Serotonin 2A and 2B receptor-induced phrenic motor facilitation: differential requirement for spinal NADPH oxidase activity. Neuroscience 178: 45–55.

Malmberg AB, Chen C, Tonegawa S, Basbaum AI (1997). Preserved acute pain and reduced neuropathic pain in mice lacking PKCgamma. Science 278: 279–283.

Martina M, Turcotte ME, Halman S, Bergeron R (2007). The sigma-1 receptor modulates NMDA receptor synaptic transmission and plasticity via SK channels in rat hippocampus. J Physiol 578(Pt 1): 143–157.

Maurice T, Su TP (2009). The pharmacology of sigma-1 receptors. Pharmacol Ther 124: 195–206.

Meller ST, Gebhart GF (1993). Nitric oxide (NO) and nociceptive processing in the spinal cord. Pain 52: 127–136.

Meunier J, Hayashi T (2010). Sigma-1 receptors regulate Bcl-2 expression by reactive oxygen species-dependent transcriptional regulation of nuclear factor kappaB. J Pharmacol Exp Ther 332: 388–397.

Meunier J, Ieni J, Maurice T (2006). The anti-amnesic and neuroprotective effects of donepezil against amyloid beta25-35 peptide-induced toxicity in mice involve an interaction with the sigma1 receptor. Br J Pharmacol 149: 998–1012.

Milano J, Oliveira SM, Rossato MF, Sauzem PD, Machado P, Beck P, et al. (2008). Antinociceptive effect of novel trihalomethyl-substituted pyrazoline methyl esters in formalin and hot-plate tests in mice. Eur J Pharmacol 581: 86–96.

Miraucourt LS, Peirs C, Dallel R, Voisin DL (2011). Glycine inhibitory dysfunction turns touch into pain through astrocyte-derived D-serine. Pain 152: 1340–1348.

Miyamoto T, Dubin AE, Petrus MJ, Patapoutian A (2009). TRPV1 and TRPA1 mediate peripheral nitric oxide-induced nociception in mice. PLoS One 4: e7596.

Moon JY, Choi SR, Roh DH, Yoon SY, Kwon SG, Choi HS et al. (2015). Spinal sigma-1 receptor activation increases the production of D-serine in astrocytes which contributes to the development of mechanical allodynia in a mouse model of neuropathic pain. Pharmacological research : the official journal of the Italian Pharmacological Society 100: 353–364.

Moon JY, Roh DH, Yoon SY, Choi SR, Kwon SG, Choi HS et al. (2014). σ1 receptors activate astrocytes via p38 MAPK phosphorylation leading to the development of mechanical

allodynia in a mouse model of neuropathic pain. Br J Pharmacol 171: 5881–5897.

Moon JY, Roh DH, Yoon SY, Kang SY, Choi SR, Kwon SG et al. (2013). Sigma-1 receptor-mediated increase in spinal p38 MAPK phosphorylation leads to the induction of mechanical allodynia in mice and neuropathic rats. Experimental neurology 247: 383–391.

Morita K, Kitayama T, Morioka N, Dohi T (2008). Glycinergic mediation of tactile allodynia induced by platelet-activating factor (PAF) through glutamate-NO-cyclic GMP signalling in spinal cord in mice. Pain 138: 525–536.

Morris BJ, Simpson CS, Mundell S, Maceachern K, Johnston HM, Nolan AM (1997). Dynamic changes in NADPH-diaphorase staining reflect activity of nitric oxide synthase: Evidence for a dopaminergic regulation of striatal nitric oxide release. Neuropharmacology 36: 1589–1599.

Mothet JP, Parent AT, Wolosker H, Brady RO Jr, Linden DJ, Ferris CD et al. (2000). D-serine is an endogenous ligand for the glycine site of the N-methyl-D-aspartate receptor. Proc Natl Acad Sci U S A 97: 4926–4931.

National Institute of Health. Guide for the Care and Use of Laboratory Animals, DHEW Publication (NIH), 2nd revised edn, Office of Science and Health Reports. Bethesda, MD: DRR/NIH, 1985.

Ossipov MH, Bian D, Malan TP Jr, Lai J, Porreca F (1999). Lack of involvement of capsaicin-sensitive primary afferents in nerve-ligation injury induced tactile allodynia in rats. Pain 79: 127–133.

Osuka K, Watanabe Y, Usuda N, Atsuzawa K, Aoshima C, Yamauchi K, et al. (2007). Phosphorylation of neuronal nitric oxide synthase at Ser847 in the nucleus intermediolateralis after spinal cord injury in mice. Neuroscience 145: 241–247.

Osuka K, Watanabe Y, Usuda N, Nakazawa A, Fukunaga K, Miyamoto E, et al. (2002). Phosphorylation of neuronal nitric oxide synthase at Ser847 by CaM-KII in the hippocampus of rat brain after transient forebrain ischemia. J Cereb Blood Flow Metab 22: 1098–1106.

Pabba M, Wong AY, Ahlskog N, Hristova E, Biscaro D, Nassrallah W et al. (2014). NMDA receptors are upregulated and trafficked to the plasma membrane after sigma-1 receptor activation in the rat hippocampus. J Neurosci 34: 11325–11338.

Palmer RM, Ashton DS, Moncada S (1988). Vascular endothelial cells synthesize nitric oxide from L-arginine. Nature 333: 664–666.

Patte-Mensah C, Kibaly C, Boudard D, Schaeffer V, Béglé A, Saredi S, et al. (2006). Neurogenic pain and steroid synthesis in the spinal cord. J Mol Neurosci 28: 17–31.

Patte-Mensah C, Li S, Mensah-Nyagan AG (2004). Impact of neuropathic pain on the gene expression and activity of cytochrome P450side-chain-cleavage in sensory neural networks. Cell Mol Life Sci 61: 2274–2284.

Ping P, Takano H, Zhang J, Tang XL, Qiu Y, Li RC et al. (1999). Isoform-selective activation of protein kinase C by nitric oxide in the heart of conscious rabbits: a signaling mechanism for both nitric oxide-induced and ischemia-induced preconditioning. Circ Res 84: 587–604.

Qian L, Wei SJ, Zhang D, Hu X, Xu Z, Wilson B, et al. (2008). Potent anti-inflammatory and neuroprotective effects of TGF-1b are mediated through the inhibition of ERK and p47phox-ser345 phosphorylation and translocation in microglia. J Immunol 181: 660–668.

Raad H, Paclet MH, Boussetta T, Kroviarski Y, Morel F, Quinn MT, et al. (2009). Regulation of the phagocyte NADPH oxidase activity: phosphorylation of gp91phox/NOX2 by protein kinase C enhances its diaphorase activity and binding to Rac2, p67phox, and p47phox. FASEB J 23: 1011–1022.

Rameau GA, Chiu LY, Ziff EB (2004). Bidirectional regulation of neuronal nitric-oxide synthase phosphorylation at serine 847 by the N-methyl-D-aspartate receptor. J Biol Chem 279: 14307–14314.

Raymond LA, Tingley WG, Blackstone CD, Roche KW, Huganir RL (1994). Glutamate receptor modulation by protein phosphorylation. J Physiol Paris 88: 181–192.

Roh DH, Choi SR, Yoon SY, Kang SY, Moon JY, Kwon SG et al. (2011). Spinal neuronal NOS activation mediates sigma-1 receptor-induced mechanical and thermal hypersensitivity in mice: involvement of PKC-dependent GluN1 phosphorylation. British journal of pharmacology 163: 1707–1720.

Roh DH, Kim HW, Yoon SY, Seo HS, Kwon YB, Kim KW et al. (2008a). Intrathecal administration of sigma-1 receptor agonists facilitates nociception: involvement of a protein kinase C-dependent pathway. Journal of neuroscience research 86: 3644–3654.

Roh DH, Kim HW, Yoon SY, Seo HS, Kwon YB, Kim KW et al. (2008b). Intrathecal injection of the sigma(1) receptor antagonist BD1047 blocks both mechanical allodynia and increases in spinal NR1 expression during the induction phase of rodent neuropathic pain. Anesthesiology 109: 879–889.

Roh DH, Yoon SY, Seo HS, Kang SY, Moon JY, Song S et al. (2010). Sigma-1 receptor-induced increase in murine spinal NR1 phosphorylation is mediated by the PKCalpha and epsilon, but not the PKCzeta, isoforms. Neurosci Lett 477: 95–99.

Roman LJ, Masters BS (2006). Electron transfer by neuronal nitric-oxide synthase is regulated

by concerted interaction of calmodulin and two intrinsic regulatory elements. J Biol Chem 281: 23111–23118.

Romero L, Zamanillo D, Nadal X, Sánchez-Arroyos R, Rivera-Arconada I, Dordal A, et al. (2012). Pharmacological properties of S1RA, a new sigma-1 receptor antagonist that inhibits neuropathic pain and activity-induced spinal sensitization. Br J Pharmacol 166: 2289–2306.

Schetz JA, Perez E, Liu R, Chen S, Lee I, Simpkins JW (2007). A prototypical Sigma-1 receptor antagonist protects against brain ischemia. Brain Res 1181: 1–9.

Schmidtko A, Gao W, Konig P, Heine S, Motterlini R, Ruth P, et al. (2008). cGMP produced by NO-sensitive guanylyl cyclase essentially contributes to inflammatory and neuropathic pain by using targets different from cGMP-dependent protein kinase I. J Neurosci 28: 8568–8576.

Schmidtko A, Tegeder I, Geisslinger G (2009). No NO, no pain? The role of nitric oxide and cGMP in spinal pain processing. Trends Neurosci 32: 339–346.

Schwartz ES, Lee I, Chung K, Chung JM (2008). Oxidative stress in the spinal cord is an important contributor in capsaicin-induced mechanical secondary hyperalgesia in mice. Pain 138: 514–524.

Scott DB, Blanpied TA, Ehlers MD (2003). Coordinated PKA and PKC phosphorylation suppresses RXR-mediated ER retention and regulates the surface delivery of NMDA receptors. Neuropharmacology 45: 755–767.

Smith SB, Duplantier J, Dun Y, Mysona B, Roon P, Martin PM, et al. (2008). In vivo protection against retinal neurodegeneration by sigma receptor 1 ligand (+)-pentazocine. Invest Ophthalmol Vis Sci 49: 4154–4161.

Sorce S, Krause KH (2009). NOX enxymes in the central nervous system: from signaling to disease. Antioxid Redox Signal 11: 2481–2504.

Su TP, Hayashi T (2003). Understanding the molecular mechanism of sigma-1 receptors: towards a hypothesis that sigma-1 receptors are intracellular amplifiers for signal transduction. Curr Med Chem 10: 2073–2080.

Su TP, Hayashi T, Maurice T, Buch S, Ruoho AE (2010). The sigma-1 receptor chaperone as an inter-organelle signaling modulator. Trends Pharmacol Sci 31: 557–566.

Su TP, Hayashi T, Vaupel DB (2009).When the endogenous hallucinogenic trace amine N,N-dimethyltryptamine meets the sigma-1 receptor. Sci Signal 2: pe12.

Tal M, Bennett GJ (1994). Neuropathic pain sensations are differentially sensitive to dextrorphan. Neuroreport 5: 1438–1440.

Tanabe M, Nagatani Y, Saitoh K, Takasu K, Ono H (2009). Pharmacological assessments of

nitric oxide synthase isoforms and downstream diversity of NO signaling in the maintenance of thermal and mechanical hypersensitivity after peripheral nerve injury in mice. Neuropharmacology 56: 702–708.

Tao YX, Johns RA (2002). Activation and up-regulation of spinal cord nitric oxide receptor, soluble guanylate cyclase, after formalin injection into the rat hind paw. Neuroscience 112(2): 439–446.

Touyz RM, Yao G, Schiffrin EL (2003). c-Src induces phosphorylation and translocation of p47phox: Role in superoxide generation by angiotensin II in human vascular smooth muscle cells. Arterioscler Thromb Vasc Biol 23: 981–987.

Tsai SY, Hayashi T, Harvey BK, Wang Y, Wu WW, Shen RF, et al. (2009). Sigma-1 receptors regulate hippocampal dendritic spine formation via a free radical-sensitive mechanism involving Rac1xGTP pathway. Proc Natl Acad Sci U S A 106: 22468–22473.

Ultenius C, Linderoth B, Meyerson BA, Wallin J (2006). Spinal NMDA receptor phosphorylation correlates with the presence of neuropathic signs following peripheral nerve injury in the rat. Neurosci Lett 399: 85–90.

Way KJ, Chou E, King GL (2000). Identification of PKC-isoform-specific biological actions using pharmacological approaches. Trends Pharmacol Sci 21: 181–187.

Wolosker H, Blackshaw S, Snyder SH (1999). Serine racemase: a glial enzyme synthesizing D-serine to regulate glutamate-N-methyl-D-aspartate neurotransmission. Proc Natl Acad Sci U S A 96: 13409–13414.

Woolf CJ (1983). Evidence for a central component of post-injury pain hypersensitivity. Nature 306: 686–688.

Woolf CJ, Mannion RJ (1999). Neuropathic pain: aetiology, symptoms, mechanisms, and management. Lancet 353: 1959–1964.

Wright DT, Fischer BM, Li C, Rochelle LG, Akley NJ, Adler KB (1996). Oxidant stress stimulates mucin secretion and PLC in airway epithelium via a nitric oxide-dependent mechanism. Am J Physiol 271: L854–861.

Xu L, Mabuchi T, Katano T, Matsumura S, Okuda-Ashitaka E, Sakimura K, et al. (2007). Nitric oxide (NO) serves as a retrograde messenger to activate neuronal NO synthase in the spinal cord via NMDA receptors. Nitric Oxide 17: 18–24.

Yajima Y, Narita M, Tsuda M, Imai S, Kamei J, Nagase H et al. (2000). Modulation of NMDA- and (+)TAN-67-induced nociception by GABA(B) receptors in the mouse spinal cord. Life Sci 68: 719–725.

Yonezawa T, Kurata R, Kimura M, Inoko H (2009). PKC delta and epsilon in drug targeting and therapeutics. Recent Pat DNA Gene Seq 3: 96–101.

Yoon SY, Kwon YB, Kim HW, Roh DH, Seo HS, Han HJ, et al. (2008). Bee venom injection produces a peripheral anti-inflammatory effect by activation of a nitric oxide-dependent spinocoeruleus pathway. Neurosci lett 430: 163–168.

Yoon SY, Roh DH, Seo HS, Kang SY, Moon JY, Song S et al. (2010). An increase in spinal dehydroepiandrosterone sulfate (DHEAS) enhances NMDA-induced pain via phosphorylation of the NR1 subunit in mice: involvement of the sigma-1 receptor. Neuropharmacology 59: 460–467.

Yowtak J, Lee KY, Kim HY, Wang J, Kim HK, Chung K, et al. (2011). Reactive oxygen species contribute to neuropathic pain by reducing spinal GABA release. Pain 152: 844–852.

Zhang Y, Lv X, Bai Y, Zhu X, Wu X, Chao J et al. (2015). Involvement of sigma-1 receptor in astrocyte activation induced by methamphetamine via up-regulation of its own expression. Journal of neuroinflammation 12: 29.

Zhou C, Li C, Yu HM, Zhang F, Han D, Zhang GY (2008). Neuroprotection of gamma-aminobutyric acid receptor agonists via enhancing neuronal nitric oxide synthase (Ser847) phosphorylation through increased neuronal nitric oxide synthase and PSD95 interaction and inhibited protein phosphatase activity in cerebral ischemia. J Neurosci Res 86: 2973–2983.

Zhou L, Zhu DY (2009). Neuronal nitric oxide synthase: structure, subcellular localization, regulation, and clinical implications. Nitric Oxide 20: 223–230.

Zou W, Song Z, Guo Q, Liu C, Zhang Z, Zhang Y (2011). Intrathecal lentiviral-mediated RNA interference targeting PKCγ attenuates chronic constriction injury-induced neuropathic pain in rats. Hum Gene Ther 22: 465–475.

국 문 초 록

척수 별아교세포 sigma-1 수용체를 통한 GluN1 인산화 조절이 신경병증성 통증 형성에 미치는 영향

지도교수: 이 장 헌

서울대학교 대학원
수의학과 수의생명과학 전공
최 스 란

말초 신경 손상으로 유도되는 신경병증성 통증은 환자에게 극심한 고통과 괴로움을 주며, 물리적 이질통 및 열성 통각과민증 등의 임상 증상을 일으킨다. 이러한 말초 신경병증성 통증은 말초 및 중추 신경계에서의 다양한 병태생리학적 기전에 의해 형성된다. 척수 내 *N*-methyl-D-aspartate (NMDA) 수용체는 통증 자극에 대해 척수 후각 신경의 흥분성을 증가시키는 중추성 감작 현상에 핵심적인 역할을 하는 것으로 알려져 있다. 최근 척수 내 sigma-1 수용체의 활성이 NMDA 수용체 GluN1 subunit의 인산화를 증가시켜 이 수용체의 기능 강화에 기여한다고 보고되었으나, 그와 관련된 정확한 세포 기전은 명확히 밝혀진 바가 없다.

따라서 본 연구는 (1) sigma-1 수용체 활성을 통하여 나타나는 통증

현상 및 NMDA 수용체의 인산화 증가에 nNOS 유래 NO가 관여하는지, sigma-1 수용체 활성에 의하여 척수 후각의 nNOS 활성도가 변화하는지, (2) 척수 내 NMDA 주입으로 유도되는 통증 동물 모델과 말초신경 손상으로 유도되는 신경병증성 통증 동물 모델에서, sigma-1 수용체에 의해 조절되는 별아교세포 내 D-serine이 nNOS를 활성화시켜 NMDA 수용체의 인산화 증가에 기여하는지, (3) 마지막으로 척수 내 sigma-1 수용체가 nNOS의 활성을 통하여 Nox2의 활성화 및 활성 산소종 생성을 조절하는지, Nox의 활성이 신경병증성 통증 형성에 기여하는지를 체계적으로 규명하고자 하였다.

모든 실험은 수컷 ICR 마우스와 Sprague-Dawley 랫드로 수행되었으며, 신경병증성 통증은 좌골신경의 만성 압박 손상에 의해 유도되었다. 통증 반응은 0.16 g 또는 2.0 g의 von Frey filament로 무해한 물리적 자극에 대한 발바닥 회피 반응 빈도를 측정하거나, hot-plate apparatus 또는 plantar analgesia meter의 유해한 열 자극에 대한 발바닥 회피 반응 시간을 측정하여 평가하였다. 실험에 사용된 약물은 PRE084 (sigma-1 수용체 효능제), BD1047 (sigma-1 수용체 길항제), L-NAME (비특이적 NOS 억제제), 7-nitroindazole (특이적 nNOS 억제제), ODQ (sGC 억제제), cyclosporin A (calcineurin 억제제), NMDA (NMDA 수용체 효능제), D-serine, LSOS (serine racemase 억제제), DAAO (내인성 D-serine 분해 효소), fluorocitrate (별아교세포 억제제), chelerythrine (PKC 억제제), PKI (PKA 억제제), NAC (활성 산소종 제거제), apocynin (Nox 억제제)이고, 척수 내로 주입하였다. 면역조직화학법, DHE 염색, NADPH-diaphorase 염색, NO detection, Western blot assay, co-immunoprecipitation을 실시하였으며, 이미지 분석은 컴퓨터와 연계된 이미지 분석 프로그램 (Metamorph)으로, 통계 분석은 Prism 5.0을 이용하여 수행하였다.

sigma-1 수용체 효능제인 PRE084를 척수 내로 주입하면 물리적, 열적 자극에 대한 통각과민증이 유의하게 나타나며, 척수에서 PKC-의존적인 NMDA 수용체 GluN1 subunit의 인산화가 증가한다. 이러한 통증 현상과 인산화는 L-NAME 또는 7-nitroindazole 전처치에 의해 유의적으로 감소한다. PRE084는 시간 의존적으로 nNOS에 대한 인산화된 nNOS의 발현 비율을 감소시키고 인산화된 nNOS가 염색되는 세포 수도 감소시킨다. 이러한 감소는 sigma-1 수용체 길항제인 BD1047과 calcineurin 억제제인 cyclosporin A의 전처치에 의해 억제되는 반면, sGC 억제제의 전처치에 의해서는 영향을 받지 않았다.

D-serine 분해효소인 DAAO를 척수 내로 주입하면 PRE084에 의한 NMDA 통증반응의 증폭 현상이 억제된다. 외인성 D-serine은 NMDA 통증반응을 증폭시킬 뿐 아니라, PKC-의존적인 NMDA 수용체 GluN1 subunit의 인산화를 증가시킨다. 이러한 증가는 7-nitroindazole의 전처치에 의해 억제된다. 좌골신경 만성 압박 손상 마우스 모델에서, 외인성 D-serine을 척수 내로 주입하면 BD1047에 의해 억제되었던 물리적 이질통 및 PKC-의존적인 GluN1 인산화의 증가가 반전된다. Serine racemase 억제제인 LSOS와 DAAO는 물리적 이질통, GluN1 인산화의 증가, nNOS 활성화 및 NO 생성을 억제한다. 7-nitroindazole과 ODQ 또한 물리적 이질통과 GluN1 인산화의 증가를 억제한다. 그러나 D-serine과 nNOS signaling은 열성 통각과민증과 GluN1 단백질 발현에는 영향을 미치지 않았다.

척수 내 PRE084 주입에 의해 나타나는 통증 현상은 활성 산소종 제거제인 NAC과 Nox 억제제인 apocynin의 전처치에 의해 농도 의존적으로 억제된다. 또한, PRE084는 Nox2 활성화 및 그에 따른 활성 산소종의 생성을 증가시키며, 이러한 증가는 BD1047, apocynin, 7-nitroindazole의 전처치에 의해 억제된다. 좌골신경 만성 압박 손상은 척수

내 Nox2 활성화 및 활성 산소종의 생성을 증가시키며, 이러한 증가는 통증의 형성 시기에 BD1047 반복 투여로 억제된다. BD1047과 apocynin은 PKC-의존적인 GluN1 인산화의 초기 증가 및 물리적 이질통의 형성을 억제하는 반면, 이미 형성된 통증에는 영향을 미치지 않았다.

본 연구는 sigma-1 수용체에 의한 별아교세포 내 D-serine의 조절이 PKC-의존적인 인산화를 통하여 NMDA 수용체 기능을 강화시키는 역할을 하고, 이 과정이 신경병증성 만성 통증의 형성에 기여함을 밝혔다. 이러한 D-serine의 작용은 nNOS가 매개하고, nNOS는 Nox2 활성 조절을 통하여 활성 산소종의 형성을 증가시켜 중추 신경계에서 산화 촉진제 효과를 내며, 궁극적으로 만성 통증에 기여함을 확인하였다. 따라서, 척수 내 sigma-1 수용체는 말초 신경 손상에 의해 유도되는 신경병증성 통증의 형성에 핵심적인 역할을 하며, 물리적 이질통에 대한 효과적인 치료 인자로서 고려될 수 있을 것으로 기대한다.

주요어: sigma-1 수용체, nNOS, Nox2, D-serine, 신경병증성 통증, 별아교세포, GluN1

학번: 2009-21641